Order Number 1331425

Characterization of the optical properties of some transition metal carbides and nitrides

Shimshock, Richard Paul, M.S.

The University of Arizona, 1987

U·M·I
300 N. Zeeb Rd.
Ann Arbor, MI 48106

PLEASE NOTE:

In all cases this material has been filmed in the best possible way from the available copy. Problems encountered with this document have been identified here with a check mark ✓.

1. Glossy photographs or pages ✓
2. Colored illustrations, paper or print _____
3. Photographs with dark background ✓
4. Illustrations are poor copy _____
5. Pages with black marks, not original copy ✓
6. Print shows through as there is text on both sides of page _____
7. Indistinct, broken or small print on several pages ✓
8. Print exceeds margin requirements _____
9. Tightly bound copy with print lost in spine _____
10. Computer printout pages with indistinct print _____
11. Page(s) _____ lacking when material received, and not available from school or author.
12. Page(s) _____ seem to be missing in numbering only as text follows.
13. Two pages numbered _____. Text follows.
14. Curling and wrinkled pages _____
15. Dissertation contains pages with print at a slant, filmed as received _____
16. Other _____

_____

_____

CHARACTERIZATION OF THE OPTICAL PROPERTIES OF SOME TRANSITION METAL CARBIDES AND NITRIDES

by

Richard Paul Shimshock

A Thesis Submitted to the Faculty of the

COMMITTEE ON OPTICAL SCIENCES

In Partial Fulfillment of the Requirements
For the Degree of

MASTER OF SCIENCES

In the Graduate College

THE UNIVERSITY OF ARIZONA

1 9 8 7

STATEMENT BY AUTHOR

This thesis has been submitted in partial fulfillment of the requirement for an advanced degree at The University of Arizona and is deposited in the University Library to be made available to borrowers under rules of the Library.

Brief quotations from this thesis are allowable without special permission, provided that accurate acknowledgment of source is made. Requests for permission for extended quotation from or reproduction of this manuscript in whole or in part may be granted by the head of the major department or the Dean of the Graduate College when in his or her judgment the proposed use of the material is in the interests of scholarship. In all other instances, however, permission must be obtained from the author.

SIGNED: Richard Paul Grinstead

APPROVAL BY THESIS DIRECTOR

This thesis has been approved on the date shown below:

Michael R. Rapaport 31 July 1987

ACKNOWLEDGMENTS

This work represents an effort to investigate the optical properties of a well characterized family of interstitial transition metal compounds. The motivation for this work was to support research associated with intentionally engineering the optical properties of materials. Ideally these materials could be used as spectrally selective coatings in high temperature photothermal solar energy conversion. Significant efforts were made in collecting and characterizing the samples. A core group of transition metal carbide and nitride samples were obtained by Dr. B. O. Seraphin under an international NSF grant from researchers working under the direction of Dr. Jean Spitz in Grenoble, France.

Motivated by the desire to increase the breadth of our studies, over eighty additional samples were collected from industrial, university, and government laboratories. This increase in the sample set was made possible by the generous nature of these groups whose ongoing investigations were primarily focused on characterizing aspects of these materials other than optical properties, such as hardness and corrosion resistance.

The following laboratories and groups are to be sincerely thanked for sharing some of their samples with us: Mr. H. Kalish of Adams Carbide Corp.; Mr. E. Foster, Batelle Columbus Laboratories; Dr. R. Blickensderfer, Bureau of Mines, U.S. Department of the Interior; Dr. J. Spitz, CNRS, France; Mr. E. N. Smith, Kennametal, Inc.; Dr. E. K. Storms, Los Alamos Scientific Laboratory; Dr. Frank Fonzi, Materials Technology Corp.; the research group at Sandvik Metals; Dr. J. Haygarth, Teledyne Wah Chang; Mr. M. Bagle, Ti-Coating;

Dr. R. F. Bunshah, Materials Laboratory, UCLA; and Mr. J. M. Moyer, Union Carbide Corp.

Our compositional analysis work would not have progressed without access to the facilities and guidance of the following people: Dr. Tom Teska (microprobe and SEM) at the Lunar and Planetary Laboratory, University of Arizona; Prof. Louis Demer (X-ray diffraction), Department of Metallurgy, University of Arizona; Prof. G. K. Wehner and Dr. Tilak Raj (Auger spectroscopy), Department of Electrical Engineering, University of Minnesota; and Dr. David Lynch (Kramers-Kronig analysis), Ames Laboratory, U.S. Department of Energy.

The following people are to be especially mentioned for the part they played in seeing this through: Dr. Bjorn Karlsson for his wit, leadership, and friendship; Prof. Bernie Seraphin for introducing me to the scope of the problem and for helping me understand the importance of being able to communicate effectively; Dr. Mike Jacobson for the time spent helping shape this work into a presentable form; Dr. Dave Allred for his guidance and help in compositional analysis; Prof. Angus Macleod for his comments and support; Mr. Ross Potoff for his unflagging friendship and support; Mr. Rich Lamoreaux for his help in the lab; Drs. Don Booth and Gary Carver for their friendship and cooperation in the laboratory; Dr. Jack Gaskill and Ms. Brenda Striegel, who many times had given up on me, but were willing to see this to the end; and Anna McKew, Maggie Whitney, and Mary McGoldrick who were willing to devote their time to support the various changes required in this effort.

I want to especially thank my parents and family for whose financial and emotional support and encouragement I am most grateful. Finally, I wish to thank my wife, Susan; without her this effort would never have been completed.

TABLE OF CONTENTS

TABLE OF CONTENTS—Continued

LIST OF ILLUSTRATIONS

LIST OF ILLUSTRATIONS—Continued

LIST OF ILLUSTRATIONS—Continued

LIST OF TABLES

ABSTRACT

We established measurement and analysis techniques necessary to investigate the optical properties of some transition metal compounds: specifically the carbides and nitrides of Ti, Zr, and Hf.

Two distinct techniques determined the optical constants of these films: a Nestell-Christy method to invert measurements of thickness, reflection, and transmission and a Kramers-Kronig analysis of reflection. The compositions of the samples were evaluated by X-ray diffraction, Auger spectroscopy, scanning electron microprobe analysis, and nuclear analysis.

We found it possible to correlate these materials' optical and electronic properties and relate these to compositional changes. The ability to engineer a specific optical response of materials is discussed. Additions of carbon and nitrogen change the optical properties in a specific manner; the roles of these elements as electron donors and their effect on the location and population of the d electron bands with respect to the Fermi level are postulated.

CHAPTER 1

INTRODUCTION/STATEMENT OF PROBLEM

For more than a decade the Solar Energy Group at the Optical Sciences Center has worked under the direction of Professor B. O. Seraphin to develop and fabricate high temperature spectrally selective surfaces necessary for efficient photothermal conversion of solar energy. The group met with remarkable success in depositing coatings capable of operating at temperatures above 500°C for thousands of hours with little or no degradation in performance (Seraphin and Meinel, 1976; Allred, 1979). However, these coatings are based on multiple layers of materials and the original vacuum process had costs and fabrication complexities limiting their utilization.

The group attacked these limitations by choosing a deposition process not widely used for optical applications - Chemical Vapor Deposition (CVD). This method readily lends itself to coating objects with axial symmetry, allows greater control over both the purity of the film source material and the condensing microstructure, and has potentially lower unit coating costs. After considerable effort the group reduced to practice coating methods applicable to high temperature solar energy conversion.

The decision to apply a coating to a system component is made on the basis of improving the optical performance or increasing the environmental durability. The most desirable situation occurs when the application of a single layer of material yields the desired system gain. If one is faced with meeting

system performance goals unobtainable with single layers and the costs can be justified, the decision is made to apply multiple layers of differing materials (multilayers). By applying CVD processes to optical applications, the costs associated with the use of multilayer technology might be reduced while offering equivalent or superior optical and mechanical performance. This approach has been the focus of one part of the Solar Energy Group. This group successfully developed materials and CVD processes superior to the existing technology base.

However, even if a superior or equivalent product is achieved by using a nonstandard deposition technology, the limitations associated with multilayer systems remain. Finding a set of materials and developing the process parameters which can successfully deposit a sequence of binder layers, protective layers, barrier layers, and the optical layers is a formidable problem. The set of materials to choose from is very limited. The optical and mechanical properties of materials in thin film form are not well known, since these properties tend to be strong functions of the deposition process employed. Time and effort must be expended to characterize the optical and mechanical properties of both the individual thin film components and the overall multilayer formulations; most data has been compiled on bulk materials, and thin film properties rarely mimic bulk properties. This characterization can be costly. Thus, even after optimal deposition parameters become available, the problems and costs arising from the limited choices of thin film materials remain.

Many coating development programs quickly develop a strong material science flavor, because the great majority of the coating problems today are materials problems. Coating materials may either fail to perform as desired optically or fail to maintain optical performance in the working environment.

Evidence abounds of coatings that fail to meet a spectral specification over time, fail to adhere to the substrate and/or fail to withstand environmental conditions. Clever solutions on the part of the thin film designer, utilizing the small set of materials available for multilayer solutions, partly overcome these limitations, but inevitably increase costs. A potentially more effective solution focuses on the materials themselves and works to solve the problem at this level. If only the need for multilayer coatings could be removed by the deliberate engineering of the desired optical response of a single material, then a cost and utilization breakthrough of great significance would be achieved. The problems of cost, fabrication sequence limitations, and high temperature deterioration of multilayer configurations encountered in solar energy applications could be avoided if a single material with the desired optical and chemical properties could be found or synthesized. The pursuit of this concept of the ideal single layer converter coating has been the focus of efforts within the Solar Energy Group for nearly eight years and it has proven to be a difficult task. This thesis describes one contribution towards this goal.

Manipulation of the optical response of a single material for high temperature applications is an attractive problem for the optical researcher, for it not only involves some of the more interesting problems in material science, solid state physics, and physical chemistry, but also has implications wider than the development of solar conversion technology. Optical technologists must face these problems in many different applications. Stability of coated components under considerable thermal and radiative loads is increasingly required by other demanding applications; wavelength selective coatings are needed in many new

optical systems; and finally, demands for coatings with improved environmental durability continue.

A literature survey of high temperature materials and data provided by Professor A. F. Turner interested our group in the properties of the transition metal compounds (TMC's) particularly carbides and nitrides. The field of interstitial compounds has an enormous literature chronicling fifty years of work by crystal chemists and metallurgists trying to exploit the great hardness and high temperature stability of these materials. These materials have been in industrial processes for many years: 1) tons of TMC's are produced every year for antiwear coatings on cutting and grinding tools; 2) large quantities of high temperature structural components fabricated from TMC's are utilized by the aerospace and defense industry; 3) TMC's, especially nitrides are employed extensively in the semiconductor industry because of their electrical, passivating and superconducting properties. Despite this widespread interest in the materials, relatively little is known about the basic optical properties as a function of composition.

Solid State Chemistry of Transition Metal Compounds

The term interstitial compound first appeared in Hägg's (1931) classical survey in which he developed a set of empirical rules regulating the crystal chemistry of the transition-metal carbides, nitrides, oxides, borides, and hydrides. Traditionally, the term denotes the compounds combining the large transition metal atoms of periods IV, V, and VI (see Figure 1) with the small metalloid atoms - hydrogen, boron, carbon, nitrogen and oxygen. Metalloids are nonmetal elements with some, but not all the properties of metals, and they possess the ability to fill the spaces in the lattice structure of the larger transition metal atoms (see

PERIODIC TABLE OF THE ELEMENTS

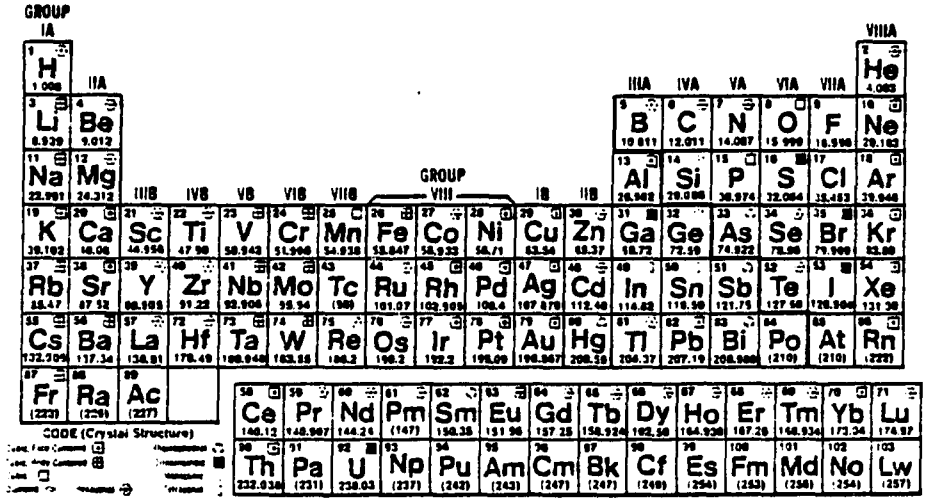

Figure 1. Long form of the periodic table.

Figure 2). These combinations form a group of materials that are among the hardest materials known and that have the highest melting points measured. Great hardness and high melting points indicate bonding of an ionic or covalent nature. However, the electronic and optical properties of these compounds demonstrate a strong metallic character. In general, these materials have the simple cubic lattice structure of sodium chloride as shown in Figure 2.

Following the treatment of Goldschmidt (1967) these materials should be considered, in the strictest sense, neither interstitial nor compounds. They are not interstitial in the sense that the structure of the compound is rarely that of the parent elemental transition metal, which has a hexagonal close-packed (hcp) structure. When C or N are introduced to the host matrix of Ti, Zr, and Hf metals, for example, the hcp structure remains until a metalloid saturation occurs. Then, a phase transformation switches the material to the NaCl (B1) structure. It is usually only after this transformation occurs that the term interstitial is applied. The materials are alloy-like rather than strict compounds since they occur over broad ranges of composition. The net metalloid solubility is conserved, and it is the sum of all these interstitial metalloids in the host matrix which must be considered. While this flexibility in composition is useful when trying to engineer specific optical properties, the wide range of the compositional spectrum becomes a burden when trying to make precise determinations of stoichiometry.

These interstitial compounds will tend to form simple or complex crystal structures depending on the ratio of the metalloid atomic radius (r_x) to that of the transition metal (r_{me}). Hägg used this ratio ($r = r_x/r_{me}$) in his investigations of these materials. He found that if the ratio is less than 0.59 the light elements are accommodated in the largest interstitial sites of the metal host structure. The

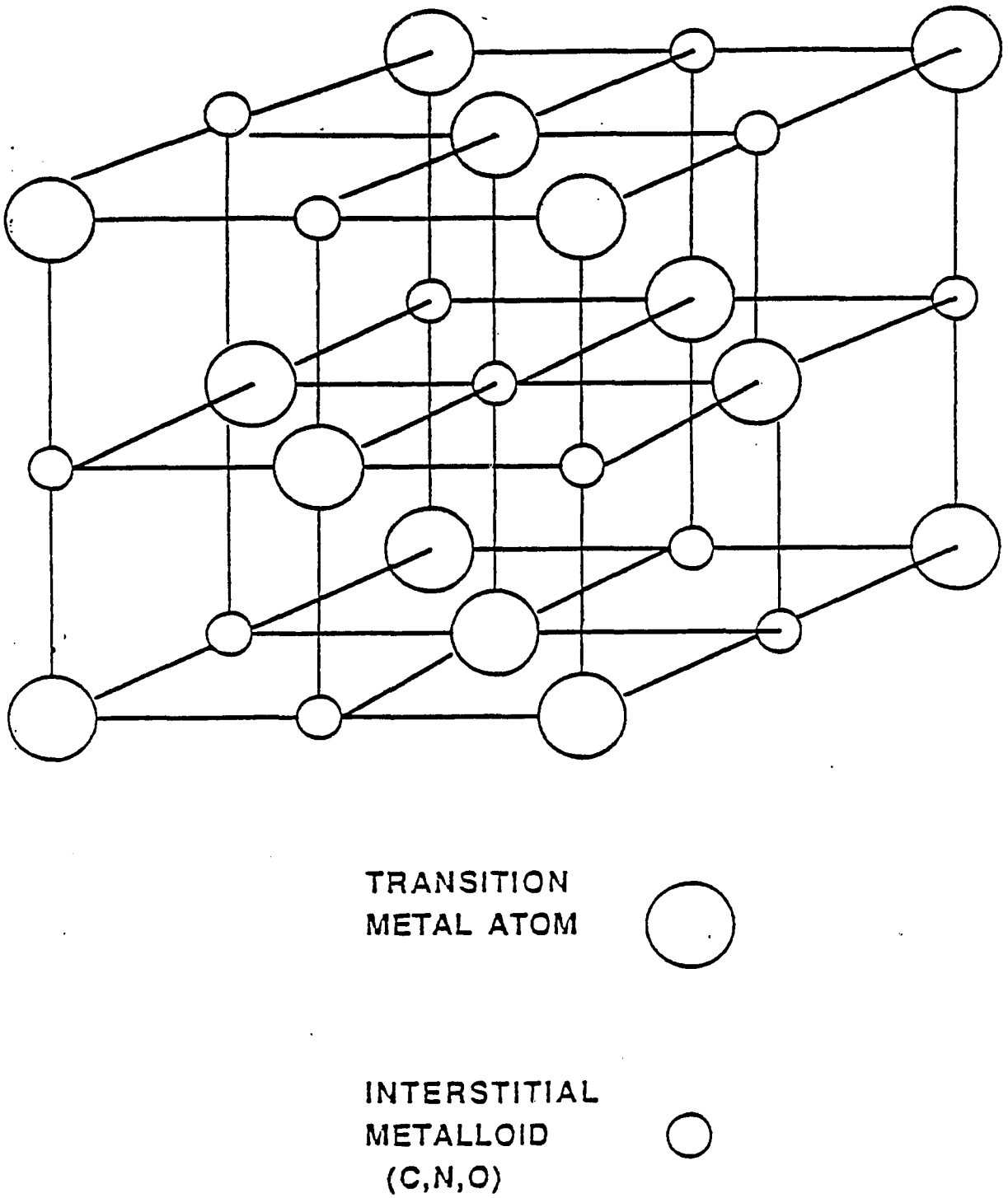

Figure 2. Structural representation of the sodium chloride type (B1) crystal of the transition metal carbides and nitrides.

structures of the compounds with Hägg ratios below 0.59 are simple: face and body centered cubic; and close packed or simple hexagonal. These Hägg compounds are conveniently described by an interstitial-site model with the octahedral sites of a face centered cubic metal array occupied by the metalloid. This ratio can be viewed as an indication of the maximum expansion which can be tolerated by the metal lattice. Ratios larger than 0.59 indicate unstable structures will form due to the insufficient bonding between the metal and metalloid; these structures are complex and prevent undue dilation of the host metal structure by the relatively large interstitial atoms.

If we begin with the elemental transition metals, which are typically characterized as poor metals (moderately shiny, moderate conductors), and introduce small concentrations of nonmetal atoms such as C or N, the compounds become more metallic (more shiny, better conductor) than the elemental metals. This effect of the interstitial atoms is attributed to their ability to donate electrons to the metal lattice and thus produce a more metallic response. This increase in electron count amounts to an effective increase in the atomic number of the metal and produces the so called "leftward shift" (in the periodic table) of properties that occurs as interstitial metalloids are introduced.

The small metalloid atoms tend to "straighten out" the framework of the host metal lattice by filling the electron orbitals of the host metal atoms. We also see this effect in the materials' properties. The room temperature resistivity of elemental Zr is 42 microhm-cm while the interstitial compound ZrN is a more metallic 7 microhm-cm. Similar effects occur in optical properties of the transition metal nitrides which we shall discuss later.

Favorable atomic size ratios are a necessary though not sufficient condition for the formation of interstitial alloys. In Figure 3 (1) we consider the atoms as rigid spheres. This representation helps us visualize the elemental combinations favoring the formation of interstitial alloys with respect to the Hägg criteria. For comparison the radii of typical holes or unoccupied lattice sites are included. These holes can occur as vacancies in the metalloid sublattice.

The solid solubilities of the interstitial atoms in the host transition metals decrease with increasing group number. Moreover, the solubility of different interstitials is conserved for a metal host. Thus, the solubility of H in zirconium decreases if the concentrations of O, N or C increase (Goldschmidt, 1967).

The solubility of O is particularly troublesome because considerable concentrations can occur as shown in Figure 4 (Murarka, 1980). What this means is that in an oxygen environment group VI and V metals can dissolve considerable amounts of O prior to the formation of an oxide. Oxygen dissolved in an interstitial compound can be nearly impossible to remove. The melting points of the transition metals and some interstitial compounds are shown in Figure 5. The melting point may be regarded as a rough measure of the affinity between the metal and metalloid and of the bonding strength. Strictly speaking, heats of formation or compressibility would be more indicative, but such data remain scarce. The melting points of both the metals and their interstitial compounds increase steadily as we pass from the 1st to the 3rd Period. The NaCl (B1) type interstitial compounds have by far the highest melting points, even higher than that of the parent metals. However, in Group VI the melting point of the metal surpasses its interstitial compounds as the B1 structures are abandoned; here, the

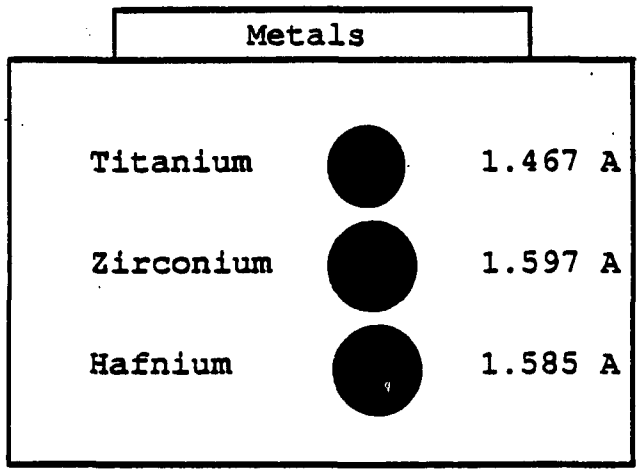

(1)

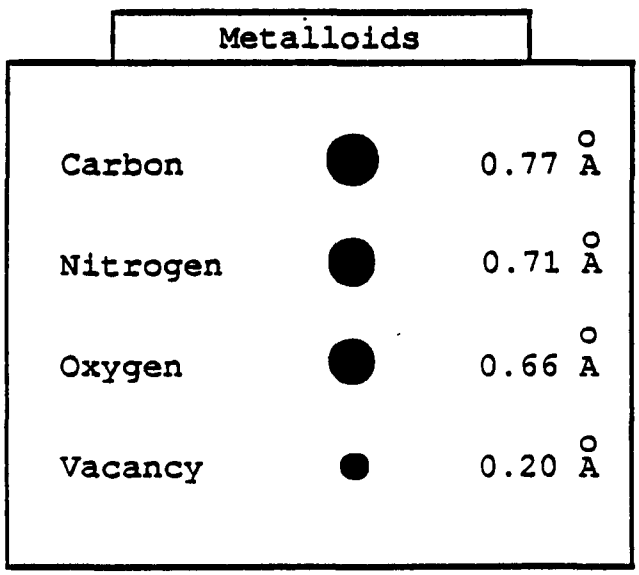

(2)

Figure 3. Rigid sphere atomic radii of the elements investigated in this study. Pauling's atomic dimensions are used.

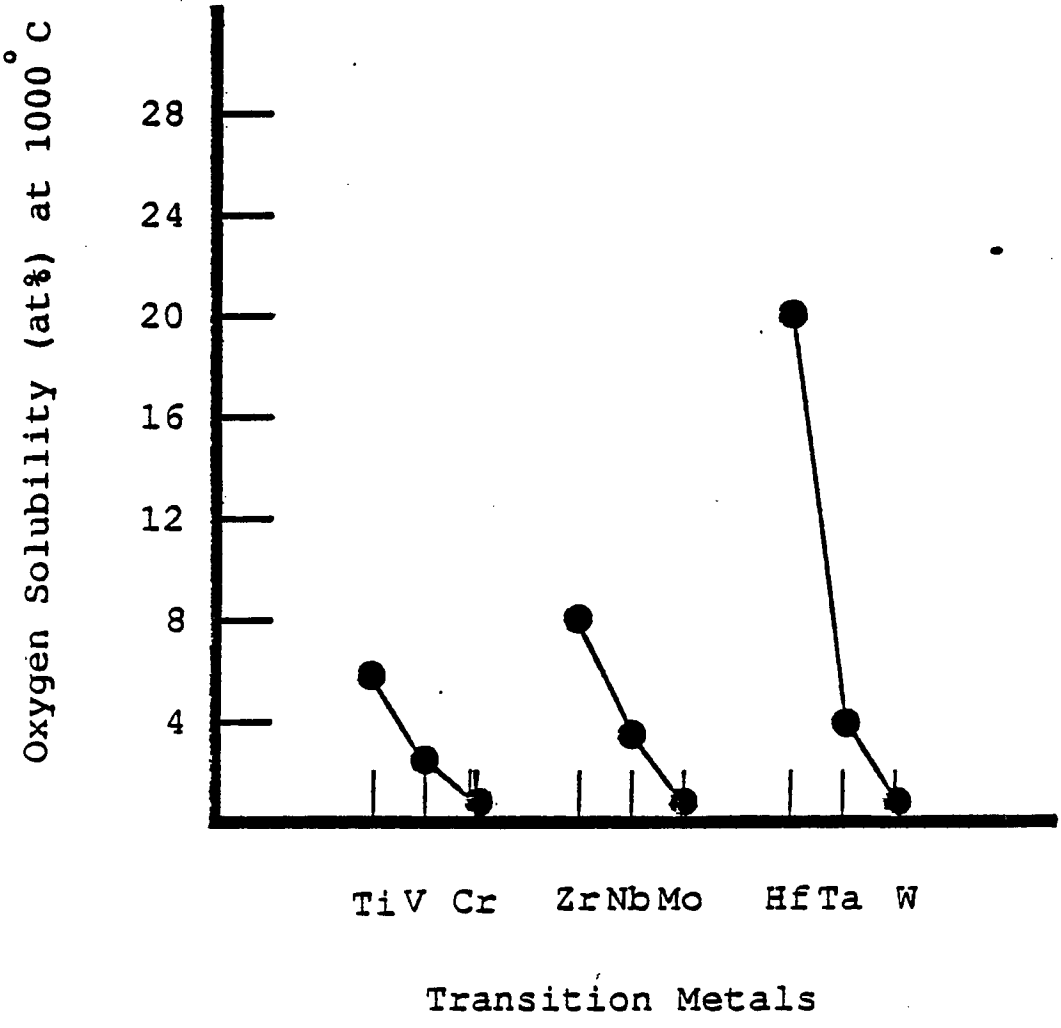

Figure 4. Oxygen solubility in metals of IV,V,VI. (After Murarka, 1980)

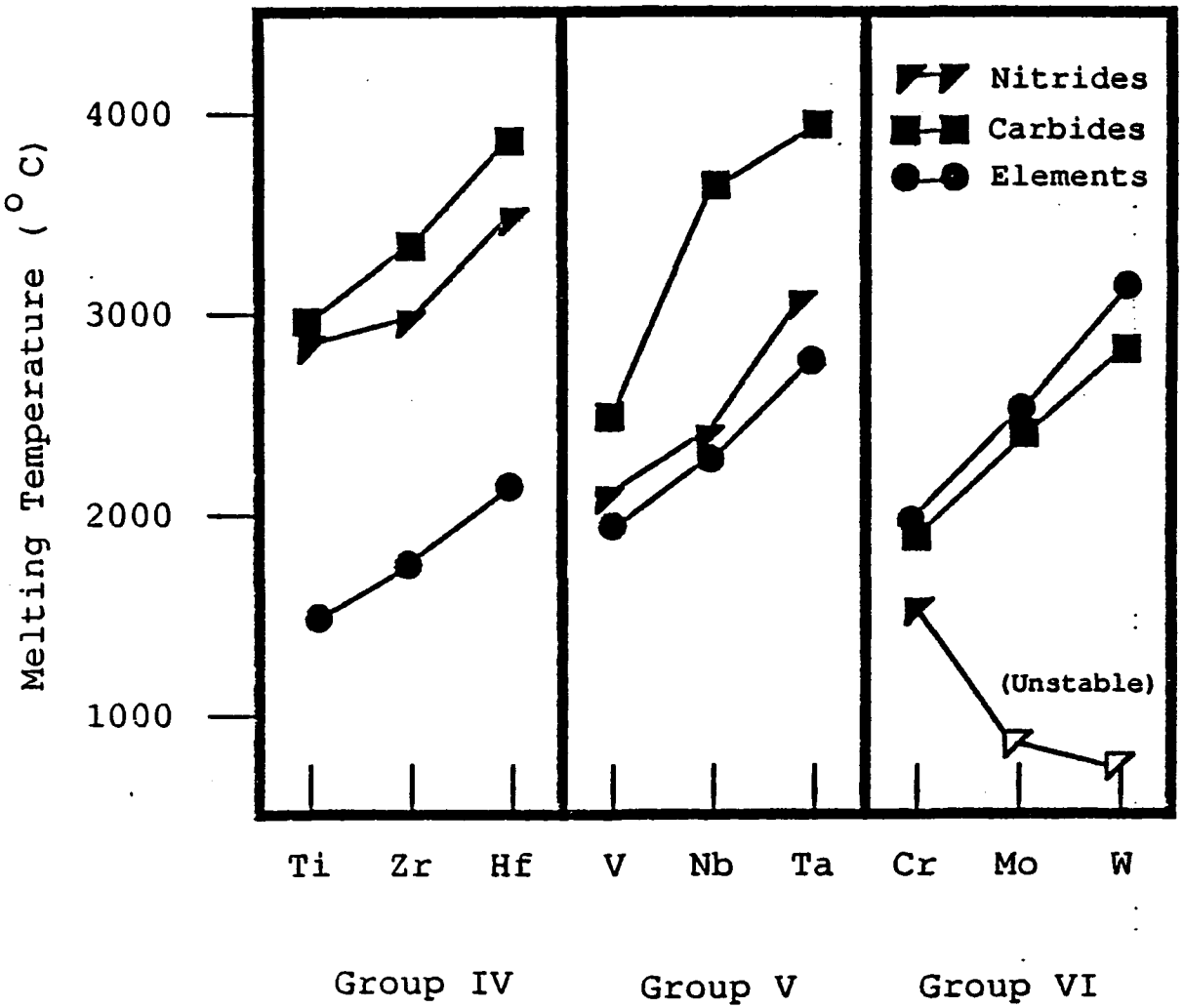

Figure 5. **Melting points of transition metals and transition metal compounds.**

structure responsible for the high melting points of the interstitial compounds of the earlier groups is now assumed by the elemental metals.

If we plot the difference in melting points between the metal carbide compounds and the corresponding elemental transition metals and normalize the difference to the latter as shown in Figure 6, we see that the second long Period (Zr, Nb, Mo) displays a marked discontinuity between the 1st and 3rd periods. This is attributed to a change in the electronic structure of the parent metal as Hf, Ta, and W fill the f electron shell and undergo the lanthinide contraction. The fact that the melting points of the nitrides are lower than the carbides and greater than the oxides can be explained by the predominance of the metal to nonmetal bond in these phases. The C, N and O atoms contribute, in that order, a decreasing number of electrons, so that the main bonds are progressively weakened and the melting point decreases (see Figure 7). A connection also exists between the atomic radii of the metals and the strength and stability of the bond. As the metal atom size decreases the metallic bond strength becomes sufficient to work against and then prevent compound formation.

This brief review of the physical and chemical properties of these compounds has emphasized the ability of the interstitial metalloid atoms C, N and O to control and facilitate structural and electronic transformations as they alloy and bond with the transition metals. The broad compositional range of interstitial structures produces a wide range of properties. Thus, a thorough material characterization is an essential requirement for meaningful comparison between materials and properties. Since the physical properties are sensitive to so many parameters one immediately becomes aware of the importance of thorough characterization. The researcher must begin by accurately determining the

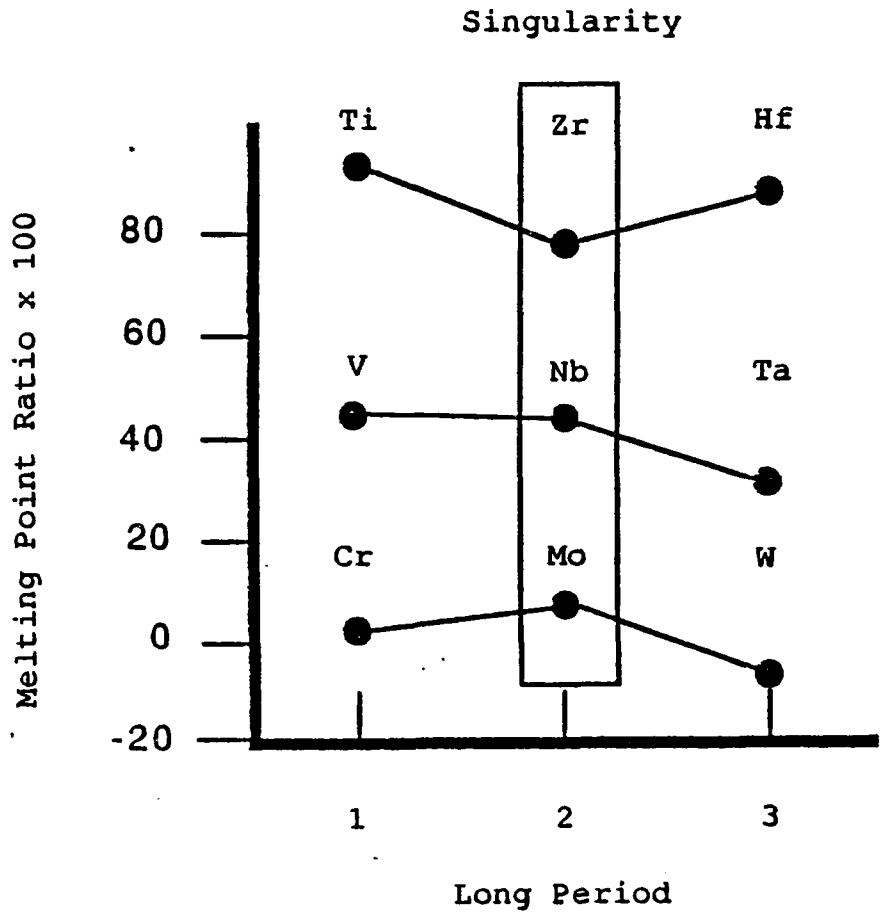

Figure 6. Melting point ratio (carbide - element)/(Element) x 100 in relation to placement in period. (After Goldschmidt)

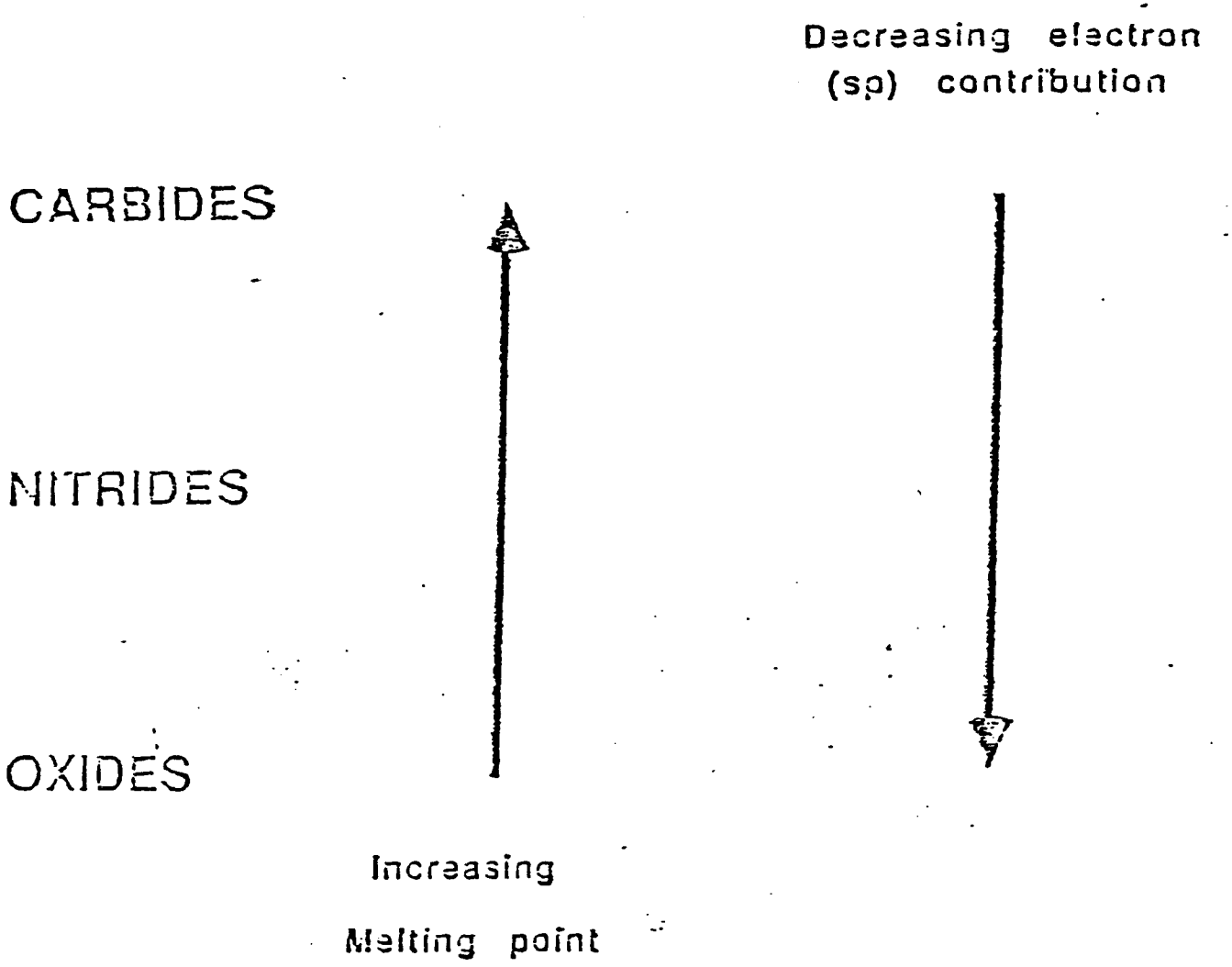

Figure 7. Ranking of electronic contribution in relation to melting point of carbides, nitrides, and oxides.

composition of the material. The detailed defect, crystal, and grain structures also control optical properties. Despite this, much work has been performed on poorly characterized or uncharacterized samples. These results are not useful to the researcher trying to make comparisons between these compounds. On the other hand, it is easy to be overly critical of such work, since characterization is difficult. Indeed, since the properties of these materials are strongly dependent on a variety of preparation and contamination conditions, and since adequate characterization techniques and standards for comparison are lacking, it is doubtful that these materials can be completely characterized (Toth, 1971). We now focus on a specific class of interstitial compounds that have the potential for application to solar energy conversion technology - the transition metal carbides and nitrides.

Solid State Chemistry Material Properties of the Transition Metal Carbides and Nitrides

The transition metal carbides and nitrides discussed here are those of the fourth and fifth group of the periodic table. Carbide and nitride formation is fairly common among the transition metals, as shown in Figure 8. As indicated earlier, of all the interstitial compounds formed between transition metals and the light elements H, B, C, N and O only the carbide and nitride compounds are the most closely related in crystal structure, phase relationships, bonding characteristics, and electrical and optical properties. This can be understood if notice is taken of the similar electronic structure, size, and electronegativity of carbon and nitrogen. These similarities do not extend to the borides, which have strong boron-boron bonds, to the oxides, which are characteristically ionic in nature, nor to the hydrides, whose properties vary widely, since hydrogen can function as either a pseudo-metal or a pseudo-metalloid. Despite the relative similarities between the

Group IV	Group V	Group VI
TiN Ti_2N	VN V_2N	CrN Cr_2N
ZrN	NbN Nb_2N Nb_2N_3 Nb_xN_{1-x}	MoN Mo_2N
HfN	TaN Ta_2N Ta_2N_2	WN W_2N

Group IV	Group V	Group VI
TiC	VC V_2C	$Cr_{23}C_6$ Cr_7C_3 Cr_3C_6
ZrC	NbC Nb_2C	Mo_2C Mo_3C_2 Mo_xC_{1-x}
HfC	TaC Ta_2C	WC W_3C_2 W_2C

Figure 8. Carbide and nitride formation in groups IV,V,VI. (After Toth)

carbides and nitrides, it is important to note that the additional electronic contribution of nitrogen does affect the electronic and optical properties of the interstitial compounds. This one electron difference causes the general properties of the fourth group nitrides to be more similar to the fifth group carbides than to the fourth group carbides. Thus, ZrN is more similar to NbC than to ZrC.

As we have mentioned, these materials share remarkably high melting points. Figure 5 compares the melting point for the elements and their carbides and nitrides. The nitrides have melting points comparable to the parent metal, while the carbides' melting points are distinctly higher. There is an interesting displacement in the maximum melting point versus group number: the elemental transition metals of Group VI have the highest melting point; the carbide and nitride maxima occur in Groups V and IV, respectively.

This stability is coupled with the ability to maintain extreme hardness at high temperatures; these compounds are among the hardest known. The binary carbides have microhardness values between 2000 and 3000 kg/mm^2 - values which place them between alumina and diamond. Typical values and other physical properties are shown in Table I. These materials also display an unusually high resistance to deformation and crack propagation. Moreover, nitride films deposited by Chemical Vapor Deposition can be produced with low compressive stress (Perry et al., 1985).

The carbides and nitrides form binary phases over a broad range of process parameters. Ideal stoichiometry is not the rule in these phases; in fact, deviations are far more common. Vacancy concentrations up to 50% can exist in some nonmetal lattices. The vacancies in TiN can occur at up to 4 atomic % stoichiometry on both the sublattices of nitrogen and titanium (Toth, 1971). The

Table 1. Survey of Selected Properties of Transition Metal Carbides and Nitrides (After Toth).

Phase	Lattice Parameter Angstroms	X-ray Density gm/cm^2	Microhardness	Coefficient of Thermal Expansion (10^{-4})
TiC	4.328	4.91	2900	7.4
$ZrC_{0.97}$	4.698	6.59	2600	6.7
$HfC_{0.88}$	4.646	12.67	2700	6.6
TiN	4.240	5.39	2000	9.35
ZrN	4.577	7.30	1500	7.24
HfN	4.526	13.8	1600	6.9

possibility of an ordered vacancy structure can be imposed on the lattice structure of the subcarbides, subnitrides and even some monocarbides. The presence of these vacancies or holes as atom equivalents, either ordered or disordered, significantly affect the properties of the compound. Different preparation techniques "lock in" different defect structures which produce diverse physical properties.

The transition metal monocarbides and mononitrides of interest nearly always assume a B1 structure; that is, a cubic close packed NaCl lattice. This simple structure forms because the radii ratio $r = r_x/r_{me}$ of these combinations has a value between 0.41 and 0.59 and these fulfill the Hägg criteria. These ratios for some transition metal compounds are presented in Table II.

If we turn to the electrical properties of these compounds, we note that the carbides and nitrides have electrical properties similar to those of the transition metal elements. These properties are presented in Table III. Here, the problem associated with imperfect characterization appears. Values for the resistivity of TiC range from 35 to 250 ohm-cm. This diversity can arise from oxygen impurities and different metalloid to metal ratios for the same nominal composition. Presumably, oxygen is ionically bound in the lattice and effectively scatters electrons, raising the resistivity. In fact, it is especially difficult to obtain Group IV nonstoichiometric carbides and nitrides free from oxygen contamination due to the tremendous chemical affinity of the group for oxygen.

Optical Properties of the Transition Metal Carbides and Nitrides

The desire to find or synthesize a material with a reflectance profile that varies as a strong function of wavelength is motivated by the desire to exploit the separation in wavelength (energy) between the incident energy spectrum of the sun

Table II. Hägg Radius Ratios for Some Transition Metal Carbides and Nitrides.

Element	Ti	Zr	Hf
Atomic Radius	1.467	1.597	1.585
Carbon/Metal Ratio	0.526	0.483	0.486
Nitrogen/Metal Ratio	0.504	0.463	0.467

Table III. Electrical Resistivities of Some Transition Metal Carbides and Nitrides (μohm-cm at room temperature).

Ti	TiC	TiN
40	52.5	25
Zr	ZrC	ZrN
42	50	7
Hf	HfC	HfN
35	45	33

and the thermal radiation spectrum of a heated collector. The wavelength separation of these two processes - capturing the sun's energy and minimizing the energy loss from the heated object - allows systems to be designed with spectral regions of complementary optical performance. Surfaces with these properties are called spectrally selective surfaces. An ideal selective surface for photothermal solar energy conversion would be similar to that presented in Figure 9. The reflectance rises from a low level at the visual wavelengths very steeply to a high and constant level in the NIR.

Seraphin and others (Roux et al., 1982; Keulsson et al., 1982) have focussed on the transition metal carbides and nitrides as potential single layer absorber materials. The interest in these materials was sparked by the reflectance data provided by Turner (Seraphin and Meinel, 1975) shown in Figure 10. Sponsored by a grant from the NSF, groups under Seraphin and Spitz collaborated by preparing an initial set of samples for ambient and high temperature optical characterization. The results are shown in Figure 11.

The materials demonstrate high temperature stability and both the carbides and nitrides exhibit a reflectance change as a function of wavelength. The reflectance of the parent metal is plotted for comparison. The gradual drop in carbide reflectance from a high value in the IR resembles that of the parent metals, while the nitrides display a rather sharp reflectance drop in the visible. This steep transition of the nitrides resembles a plasma edge characteristic of a classical free electron metal such as gold or silver. The desire to understand these optical differences motivated the extension of the initial sample set.

The work of Boehm (Boehm and Goretzki, 1972) and Knosp (Knosp and Gerold, 1969) demonstrated the possibility of changing reflectance minima and

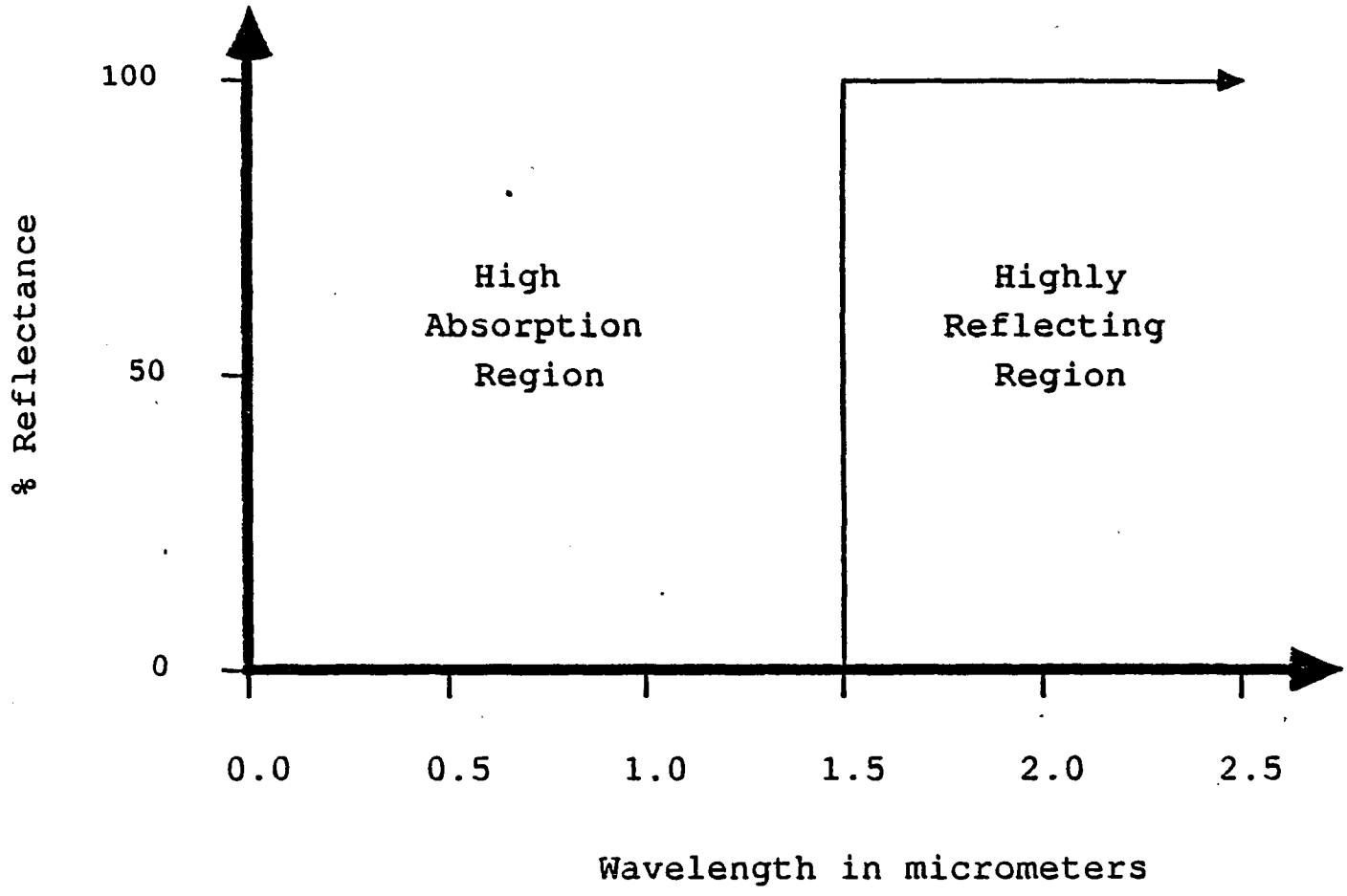

Figure 9. **Spectral profile of an idealized photothermal converter.**

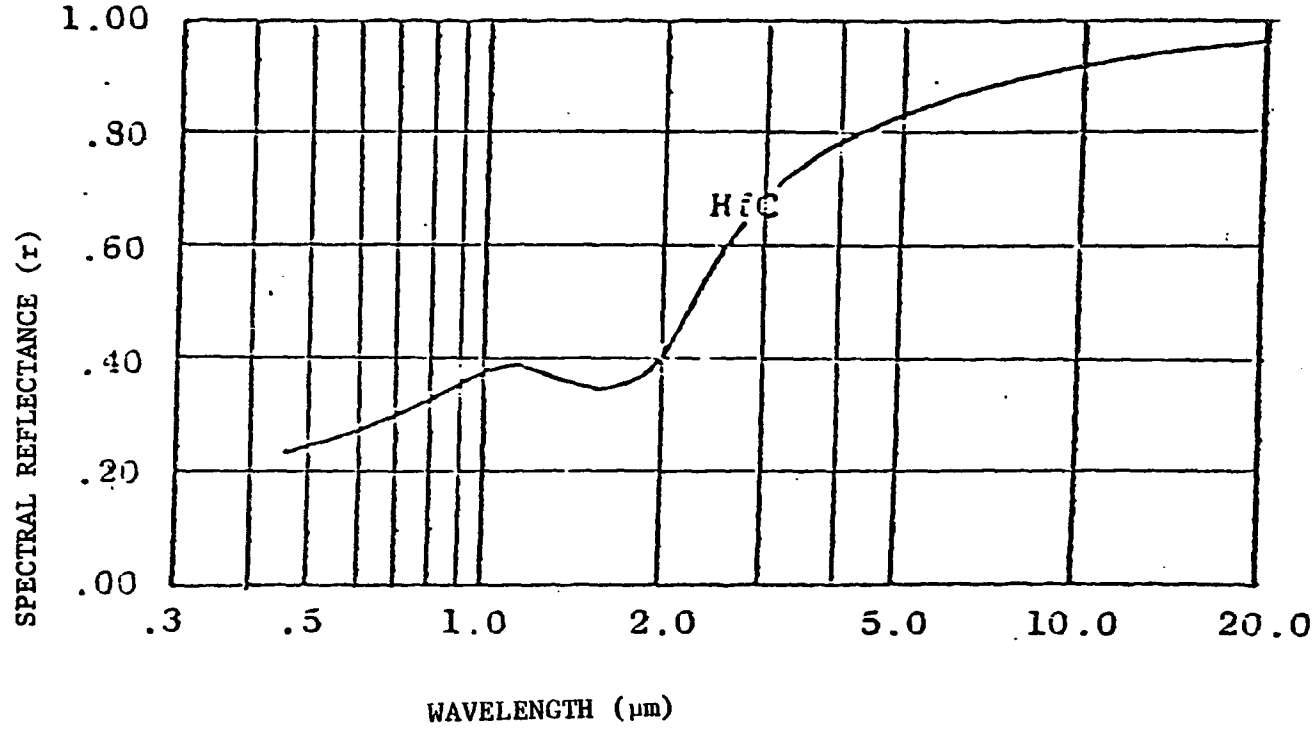

Figure 10. Specular reflectance of HfC (A. F. Turner).

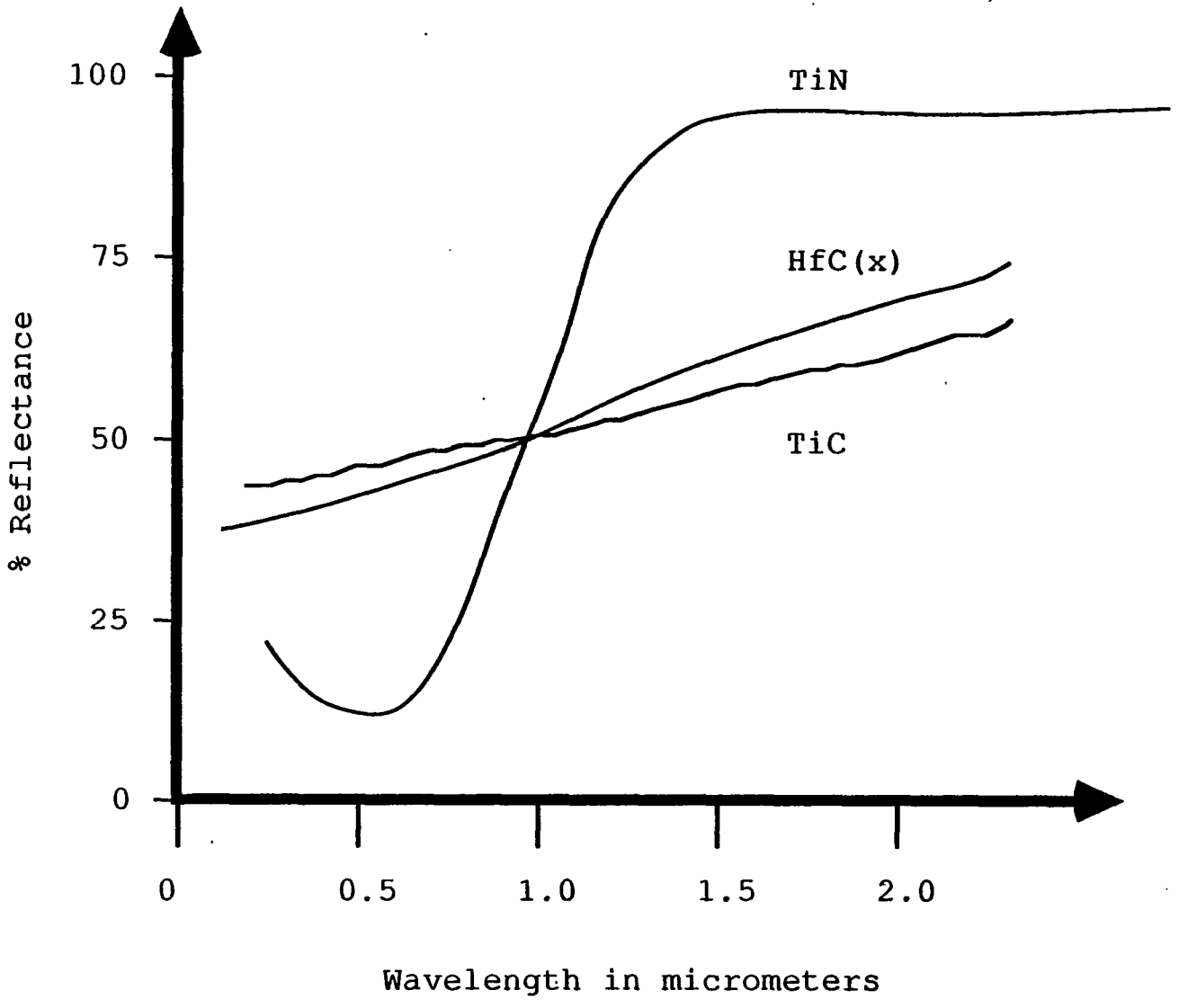

Figure 11. Hemispherical reflectance of TiN, HfC(x), and TiN.

changing the slope of the transition. These samples have a low IR reflectance (≅70-80%), indicating higher impurity concentrations, typical of powder pressed samples. This contrasts with the results obtained in this effort (see Figure 12) where the NIR reflectance of our samples is greater than 90%.

The optical properties of these materials are a direct function of the underlying electronic structure. An electronic schematic of the orbital filling of some of the free transition metals, and carbon and nitrogen is presented in Table IV. It is the interaction of the s and d orbitals of the host metal and s and p orbitals of the interstitials that form the energy bands of the compound. The interplay of these energy bands and their relation to the Fermi level are responsible for the specific material properties. In these materials, the Fermi level is situated near a minimum density of states; it is postulated that the d bands near the Fermi energy give rise to the metallic nature of these materials, while the p bands are responsible for the covalent properties (Karlsson, 1983). The exact blend and location with respect to the Fermi level of these s, p, and d bands create the differences in material properties of the carbides and nitrides. A desire to collect and characterize a wide variety of quality samples of these types led to the development of a range of optical and material characterization tools discussed in this thesis.

Summary

In summary, the transition metal compounds form a class of materials with a variety of unusual physical properties, a direct result of the outer unfilled d electron shell and the overall band structure of the material. These d electrons can neither be described by a collective electron model, as in the case of s and p type electrons, nor by the strictly localized model, as in the case of tightly bound

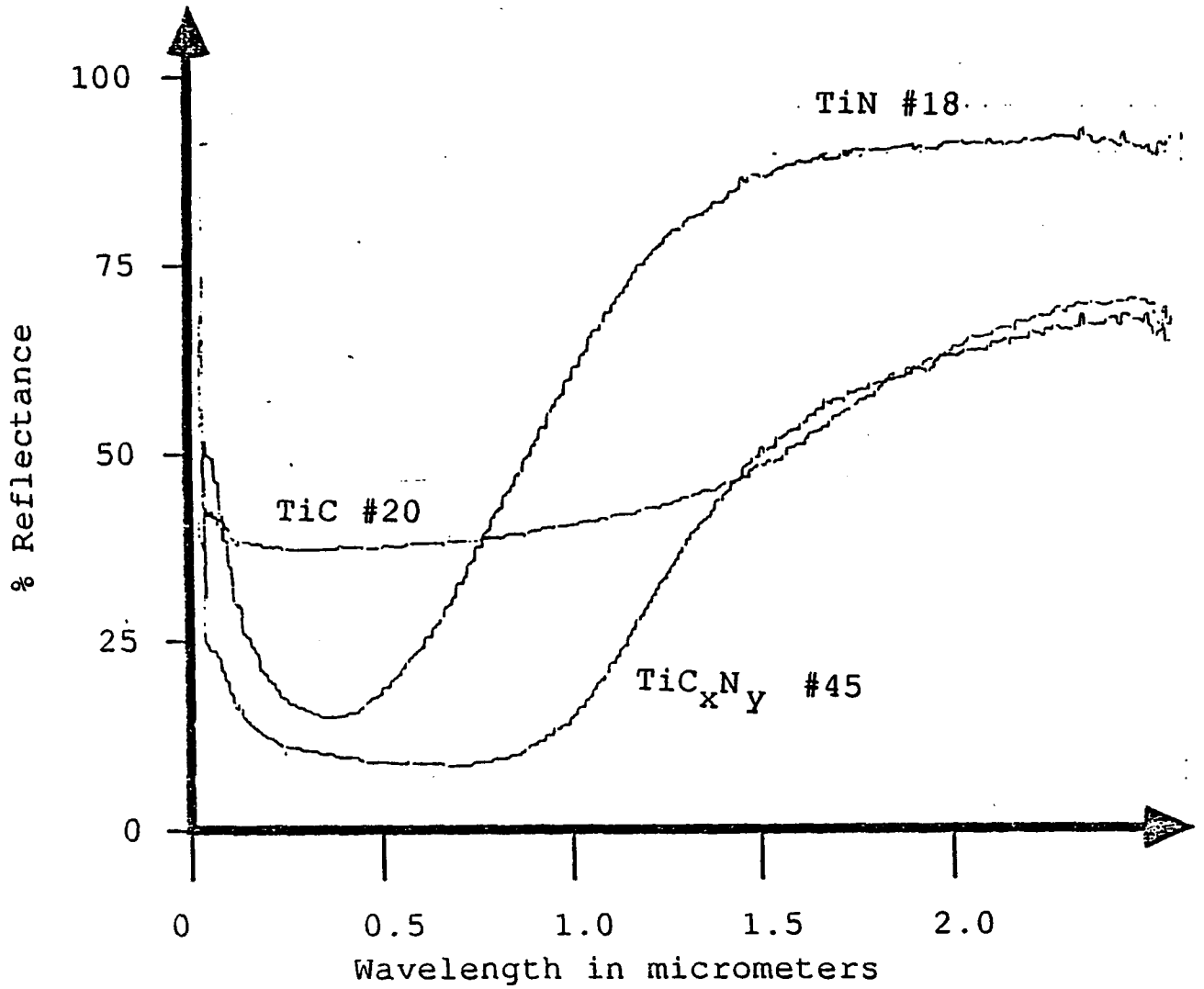

Figure 12. **Hemispherical reflectance of the OSC's titanium carbonitride series.**

Table IV. Electronic Structure of Free Atoms of Transition Metals.

Element	1s	2s	2p	3s	3p	3d	4s	4p	4d	4f	5s	5p	5d	6s
Ti	2	2	6	2	6	2	2							
Zr	2	2	6	2	6	10	2	6	2		2			
Hf	2	2	6	2	6	10	2	6	10	14	2	6	2	2
C	2	2	2											
N	2	2	3											
O	2	2	4											

f electrons. The electronic configuration of the transition metals, modified by the electron donors C and N, produce variable optical properties.

The materials are difficult to produce; rather exotic techniques must be employed to create either bulk samples or thin films of these materials. High quality samples are difficult to acquire. Typically, the laboratory with the necessary production expertise cannot characterize the samples to the level needed. With so little interest in the basic optical properties of these materials, and with adequate characterization difficult, the properties with respect to composition have been difficult to establish.

We were never able to collect a sample that matched the reflectance profile of the original HfC scan suggested by Turner. This highlighted a problem posed early on in this effort: the location of sources for these types of materials. Once we located such sources, we often necessarily accepted films made under deposition parameters of primary interest to these outside parties. We characterized these samples as fully as we could. Two groups (R. Bunshah-UCLA; J. Haygarth-Teledyne Wah Chang) were kind enough to prepare the nominal types of samples we requested. The samples produced by Dr. Haygarth at Teledyne Wah Chang were the best we received and formed the basis this work.

The variety of the samples required that we utilize a range of material characterization techniques: X-ray diffraction, nuclear techniques, scanning electron microprobe analysis and Auger analysis.

Optical characterization also demanded several approaches; measurements were made of R (front surface reflectance), R′ (back surface reflectance) where appropriate, and T (transmittance) and T_p (transmittance at 60^0) from 0.2 to 15

micrometers along with independent measurements of thickness. Measurements of both specular and diffuse reflectance were made on all samples from 0.4 to 2.4 micrometers and scatter measurements were made at 0.488 micrometers on the samples provided by Haygarth. The methods used to invert the optical measurements to basic material properties included Nestell-Christy and Kramers-Kronig analyses. The samples are of very high quality and our data compare favorably with other published work.

The overall program successfully demonstrated that it is possible to correlate these materials' optical and electronic properties and to relate these to compositional changes. Additions of carbon and nitrogen change the observed optical properties in a specific manner; the roles of these elements as electron donors and their effect on the location and population of the d electron bands with respect to the Fermi level are postulated. The reader is directed to the appendices and references for a more complete discussion of the physical models developed under this effort.

The samples were collected from many sources and there is inevitable scatter in the results. This scatter is greater than any imprecision in our measurements. Considerable efforts were made to characterize the samples as completely as possible, but it became clear during this program that further progress would require access to deposition facilities better suited for these materials. This was not possible at the OSC. Dr. Bjorn Karlsson, who was a coworker at OSC during this program, became very interested in this problem and was able to arrange a program in his own laboratory in Sweden (Karlsson and Ribbing, 1982). His group has assumed a leadership role with these materials, and has been able to elucidate the exact nature of the relationship between the

electronic structure and the optical properties of one of the most interesting sets of these compounds - the titanium carbonitrides (Karlsson et al., 1982). With access to equipment capable of depositing high quality films, he demonstrated that shifting the steep transition edge of TiN toward the IR on the order of 0.4 electron volts (.322 micrometers) with the introduction of carbon was possible without significantly changing the high IR reflectance or the steepness of that edge.

CHAPTER 2

DESCRIPTION OF THE SAMPLE SET

A complete listing of the sample set collected during the course of this investigation appears in Appendix A. The majority of these samples came from industrial laboratories with an interest in exploiting the great hardness of these materials as coatings for long wearing machining and cutting tools. While we were able to discern trends in the optical properties of a wide variety of carbides, nitrides and carbonitrides from these donated samples, they were not completely suitable for our analysis. Little chemical analysis, of sufficient accuracy for our needs, had been performed by our benefactors. Many samples were claimed to be representative of particular metal nitrides; when analyzed by Auger spectroscopy, they displayed significantly more carbon and oxygen than nitrogen. However, these samples still allowed some optical comparisons of their reflectance profiles.

All of the samples were measured in an integrating sphere reflectometer to assess their as-received (rough surface) diffuse reflectance. Many samples were deemed interesting enough to polish optically for near normal specular reflectance measurements. We then established selection criteria to choose the samples for optical constant determination. A careful review was made of the surface type, status of our chemical analysis, and the chances for a successful optical analysis; certain samples from the original sets provided by Dr. Jean Spitz and by Dr. John Haygarth were chosen for more thorough work (see Tables V and VI).

Table V. HfC_x Samples Chosen for Optical Constants Evaluation.

Sample	PCH_4(torr)	d(A)	C/Hf	Resistivity	Method
6	$8x10^{-5}$	2800	0.2	80	KK
8	$2x10^{-4}$	2500	0.5	230	KK
11	$5x10^{-4}$	2800	1.2	210	KK
13	$7x10^{-4}$	3000	1.7	250	KK
14	$1.5x10^{-3}$	3500	3.5	610	KK
1	$4.5x10^{-3}$	110	1	—	R,T,d/ln(T)
2	$4.5x10^{-3}$	230	1	240	R,T,d/ln(T)
3	$4.5x10^{-3}$	375	1	225	R,T,d/ln(T)
4	$4.5x10^{-3}$	520	1	240	R,T,d/ln(T)
5	$4.5x10^{-3}$	655	1	250	R,T,d/ln(T)

Table VI. Nitride Samples Chosen for Optical Constant Evaluation.

Sample	Type	Temperature	d(A)	N/Metal	Method
60	TiN	1000° C	8000	1	KK
61	ZrN	1170° C	8000	1	KK
62	HfN	1150° C	8000	1	KK

The Carbides - Samples From J. Spitz

The original sample set consisted of a group of hafnium carbide, titanium carbide, and titanium nitride samples (Table V) prepared and characterized for the OSC under a NSF grant by Jean Spitz's group in Grenoble. The depositions were made on visually transparent quartz, and IR transparent silicon, substrates using reactive cathodic sputtering with either a hafnium or titanium target (99.9% purity) in an argon atmosphere containing either methane or nitrogen. Determinations of film thickness, density, structure, composition and electrical resistivity were made in France. These samples were delivered to the Optical Sciences Center (OSC) for optical measurements.

At the OSC, their near normal reflectance and the stability of their reflectance profiles as a function of temperature were measured (Baraket and Seraphin, 1976). These initial high temperature measurements irreversibly changed some of the samples. For example, high temperatures caused the nonstoichiometric samples to oxidize to the point that visual interference colors from surface layers were noticeable. While these oxide layers did not present large problems when first order comparisons of the reflectance profiles were being made, our ability to make precise determinations of the optical constants was diminished. These oxidized samples represented a sizeable portion of our sample set.

The exact thickness and the exact composition of our films became issues fairly early in this program. To address these questions, independent measurements of film thickness and sample composition were undertaken at the OSC.

The Nitrides - Samples From J. Haygarth

Thin films of the nitrides of titanium, zirconium and hafnium were deposited by a CVD process on highly polished molybdenum discs. The deposition is based on the reaction of a metal chloride vapor and hydrogen and nitrogen in a vessel heated to temperatures over 1000°C:

$$MCl_4 + 2H_2 + \frac{1}{2} N_2 \xrightarrow{1000°C} MN + 4HCl$$

where M = Ti, Zr, Hf

The reaction takes place at atmospheric pressure and produces a condensed film on suitable substrates. The by-product of the reaction is HCl. The film is a dense and polycrystalline with a coarse grained columnar microstructure. The exact nature of the microstructure is a function of the deposition conditions, the coating rate, reactant gas partial pressure, and temperature.

Molybdenum discs, polished by standard metallographic techniques, served as substrates. The reaction continued until a coating of approximately 10 microns thick was achieved. The deposition conditions are shown in Table VII. Afterwards, the substrates were removed and weighed to establish film mass and thickness. Micrographs of the surface texture were then made with a scanning electron microscope. The rough surfaces of some of the samples were polished to produce a smooth, specular, though not optically flat, surface and sent to OSC for further work. The HfN and ZrN samples were received both unpolished and polished; this allowed us to investigate the effect of surface morphology on the reflectance and absorptance of the samples.

Table VII. Preparation Parameters for Nitride Depositions by CVD at Teledyne Wah Chang.

Material	P_{H_2}*	P_{N_2}*	P_{MCl_4}*	Temperature	Time
TiN	0.575	0.375	0.050	1000° C	8 hrs.
ZrN	0.339	0.642	0.019	1170° C	10 hrs.
HfN	0.386	0.610	0.004	1150° C	14 hrs.

*Total System Pressure is 0.1 MPa.

OSC Characterization

The samples provided by Drs. Spitz and Haygarth proved to be the most suitable for the optical analyses we envisioned. They were of high optical quality and relatively free from impurities. However, since we were not able to deposit these materials ourselves, it was necessary to verify their properties by extensive characterization at the OSC. The data on many vital film parameters, such as thickness, were often inconsistent or imprecise by our standards. Where analytical services were not available at the OSC or on the campus of the University of Arizona, we were able to arrange for help from other institutions to measure and understand film thickness, surface polish quality, and compositional purity.

These evaluations were necessary to complete models of the films under analysis. Such models shaped our conclusions concerning the connections between the optical properties and the chemical composition. However, some issues were left outstanding. Without access to systems capable of depositing these materials, shorter turn around time between deposition and characterization of the films, and characterization methods specifically suited to the analysis of these materials, we felt that some of these issues would never be satisfactorily resolved. Examples include the nature of a carbon phase in the carbon rich HfC sample, the types of vacancies in the lattices of all the films, and the net interstitial metalloid contribution to the lattice in the metal nitrides. The following sections describe some efforts to reduce the imprecision in our analysis.

Polishing and Material Preparation

Again, the majority of the industrial samples were fabricated to investigate the wear and hardness properties of these materials. As such, many

samples were deposited on cemented carbide tool inserts. Others were fabricated as buttons by arc melting. Both needed extensive preparation before evaluations of the optical properties could be made. We consulted with both the OSC's Optical Shop and the University's Department of Mines and Metallurgy regarding appropriate approaches for polishing and preparing these samples for optical analysis. We combined the standard metallographic specimen preparations and optical polishing methods more familiar to the optical community to generate the specularity and flatness needed for optical measurements on these very hard materials.

To prepare samples for polishing we cut the arc melted samples to expose the largest dimension of the as-received buttons. These sliced samples and some of the other samples were then mounted by embedding them in two inch diameter cells of a commercially available thermosetting epoxy with a diamond saw in the OSC's modulation spectroscopy's preparation lab. Once set up, these cells allowed for easy sample handling and for polishing the rough surfaces of the crystal face left by the slicing operation.

The polishing followed the guidelines set forth in the paper by R. E. Parks et al. (1977). The samples from Sandvik, Batelle, Kennametal, Adamas Carbide, Ti Coating, Materials Technology, LASL, and some of those provided by Haygarth were all polished at the OSC, allowing us to correlate both specular and hemispherical reflectance properties. Polishing proceeded under continuously finer grit diamond pastes. Starting with 6 micron diamond grit, we progressed to a 0.25 micron final polish. We gratefully employed a suggestion provided by Mr. R. Sumner, head of the OSC's Model Shop, and added glycerine to the slurry to

reduce the onset of undesirable polishing artifacts when working with the harder samples.

In general, the results of polishing were quite satisfactory. Although this operation was tedious because of the extreme hardness of these materials, the ability to make specular measurements on this larger sample set proved to be worth the effort. By quickly making our measurements after our polishing sequences we hoped for a measurement surface free from handling contamination and presumably free from bothersome oxides. The only potential defects assumed to exist in these samples might be the mechanical work damage done to the surface by our polishing techniques. We assumed that hardness and good polishing practice would minimize these surface defects; this was established by the low scatter measured from the polished surfaces. Comparisons were also made between specular and hemispherical reflectance at wavelengths below 0.45 micrometers, these comparisons indicated low scatter surfaces.

Spectral Measurements

The samples were measured by several spectrophotometric instruments in the OSC's Measurement Laboratory. Specular measurements of reflectance and transmittance in the range 0.2 to 2.7 micrometers were made on a Perkin Elmer Model 450 dual beam spectrophotometer. The instrument has a tungsten light source and dual quartz prisms. Photomultipliers cover the visible to 0.75 micrometers; a lead sulfide detector covers the near IR out to 2.7 micrometers. All measurements were made in the double beam mode. Transmittance was measured relative to air and reflectance was measured relative to a freshly evaporated aluminum sample at near normal (10^0) incidence.

The specular measurements from 2.5 to 15 micrometers were performed on a Perkin Elmer Model 137 spectrophotometer. This instrument employs NaCl prisms for dispersion and a thermopile for detection. Since these films are highly absorbing in the IR, transmittance measurements were impossible at these wavelengths. All reflectances were determined at near normal incidence (10^0) relative to a freshly evaporated aluminum sample.

Measurements of the hemispherical reflectance of non specular samples were made in a double beam integrating sphere reflectometer developed at the OSC (Jacobson et al., 1979). The instrument is based on a modified Perkin Elmer 21 Spectrophotometer. It contains a tungsten source, a quartz prism, and a solid state two color silicon/lead sulfide detector with a range of 0.4 to 2.5 micrometers. This instrument primarily measured the as-received reflectance profile. Only the specular measurements of the high quality samples were used for analysis.

The aluminum samples serving as spectrophotometric references were very important since our analysis required absolute values of reflectance; our measurements were all made with respect to aluminum samples. The aluminum reference samples were deposited in the OSC's Thin Film Lab. They were flash evaporated at 10^{-5} Torr in a diffusion pumped coating chamber. We found that the rate of evaporation had a profound influence on the UV performance of the reference film. This is precisely the region where our analysis becomes the most sensitive to errors in our data, and where the number of our data points was limited. A careful culling process was undertaken to insure that only high quality mirrors, deposited by rigorous techniques, became references. The reflectances of the aluminum references were assumed to be similar to those of Bennett et al. (1962) deposited under similar conditions. These values were combined with those

of Hass and Hadley (1963) by reducing the latter by 1% to match those of Bennett's high vacuum aluminum values at 0.4 micrometers (see Figure 13). The trend of Bennett's values was extrapolated down to 0.2 micrometers and formed the basis for converting our relative measurements to absolute values.

Scatter

The intensity of the light scattered out of the specularly reflected beam conveys information about the surface texture of materials. Measurements of the angular distribution of this scattered energy have been used by a variety of researchers to characterize surface roughness (Bennett and Burge, 1980; Bennett, 1985; Shack, 1974; Rodgers, 1976; Eastman and Baumeister, 1974). Studies of the practical limitations of radiant energy collection imposed by scattering from surfaces of high performance optical instruments, and interest in the theoretical aspects of the coupling of electromagnetic energy to rough material surfaces, are areas of active research. Because of ongoing activity in scattering studies, we were able to make use of existing instrumentation at the OSC. In particular, Dr. Seppo Sari had established instrumentation to investigate the effect of surface roughness on surface plasmons in silver films. Use of this facility was kindly extended to us to characterize our films.

An argon laser operating at 0.488 micrometers was directed through a polarizer to illuminate the sample. An analyzer and detector on a movable arm were swung through a range of angles and measurements of the distribution of energy intensity were recorded. The samples were all good metallic conductors; thus, all scattering was attributed to surface roughness as opposed to any bulk scattering contribution.

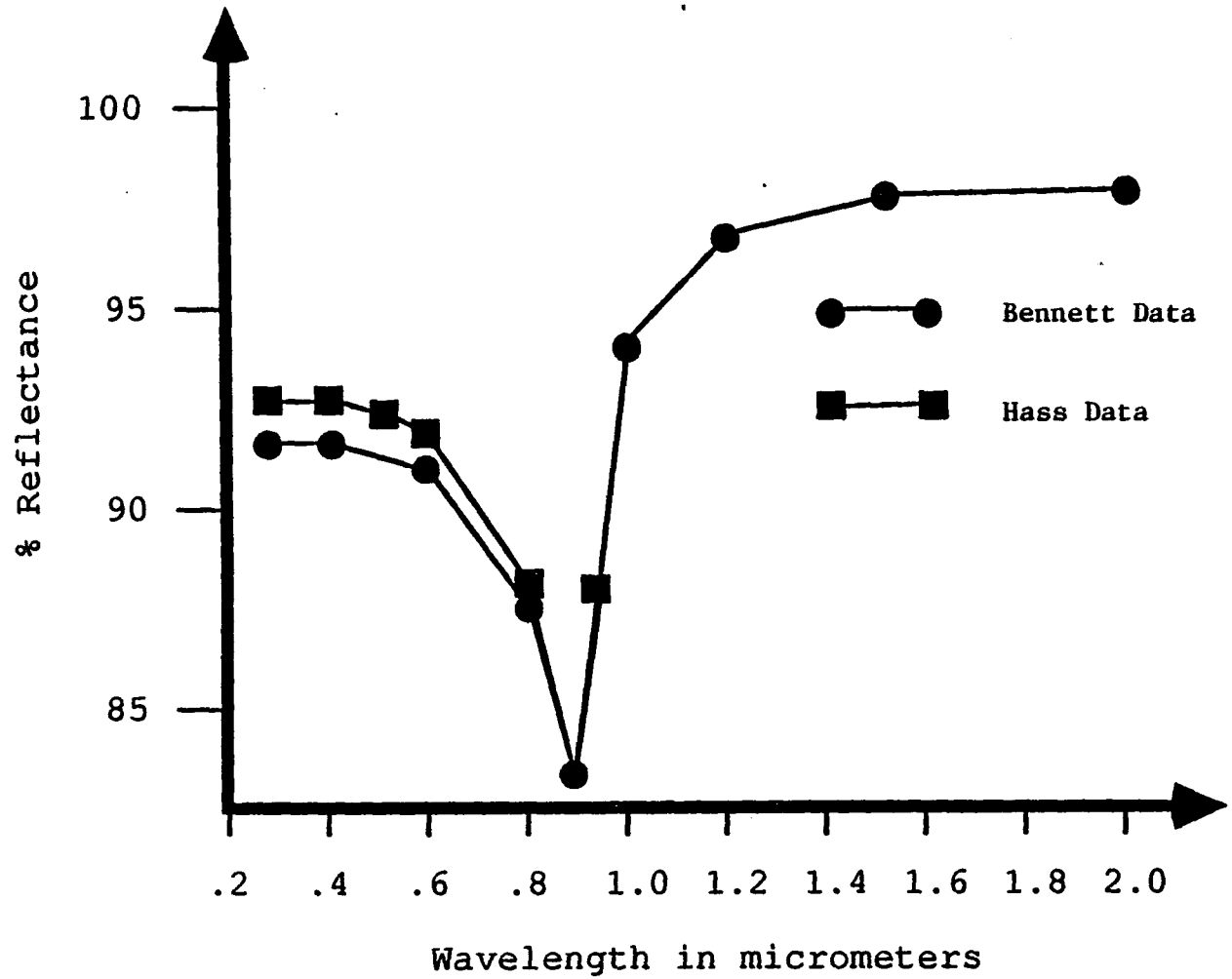

Figure 13. Absolute reflectance of aluminum thin films.

Generally speaking, a figure of merit for establishing whether a surface is of high optical quality is that the rms surface roughness divided by the wavelength should be less than 1/40. This figure of merit corresponds to optically smooth surfaces that scatter less than 10% of the incident energy. Comparisons below 0.45 micrometers between measurements of specular reflectance from the Perkin Elmer 450 and the hemispherical reflectance measured in the integrating sphere verified that our samples scattered less than the 2% combined measurement error of the instruments. At a typical visible wavelength, 0.5 micrometers, this figure of merit would demand that the rms roughness of an optical quality surface be less than 125 A. This order of roughness is seen as the upper limit for our samples and the surface quality observed for the metal nitrides was probably much better. It was important to establish that the polished nitride samples had fine optical surfaces to insure that consistent measurements were made of the reflectance values in the UV (0.2 micrometers). Typical results of these measurements for the specular nitride samples and some of the rough as received samples (ZrN, HfN) from Haygarth are presented in Figures 14 and 15. In addition, a scanning electron micrograph of the surface condition of the as received ZrN sample is presented in Figure 16.

Auger Analysis

To establish a working composition model of the samples supplied by Dr. Spitz, and to address some of the inconsistencies in previous characterizations of these samples, we sent a corner section of each coated substrate to Dr. Wehner's laboratory at the University of Minnesota for analysis by Auger spectroscopy. Dr. Tilak Raj kindly analyzed the full set (all 19) of our carbide and nitride samples.

He also analyzed the four hafnium samples sent to us by Prof R. F. Bunshah's Material Science Group at UCLA.

This technique allows one to identify elements in films by analysis of the energy of the Auger electrons emitted as a result of radiationless Auger transitions. This emission is a three electron process; since emitted electrons at such energies cannot travel far, it is essentially a surface phenomenon. To investigate material composition as a function of thickness, this surface analysis is usually coupled with an apparatus that sputters away film material. "Snapshots" of the material composition are typically made after periodic material removal. The signal generated by Auger electrons is quite small, so the first derivative of the number of Auger electrons with respect to the electron energy is measured. This method quantitatively identifies elemental distribution in the sample.

Identification of chemical bonds are not easily made, since a knowledge of the density of states of the electronic levels is needed to determine chemical shifts. Quantitative analysis is difficult since these relative measurements are converted to absolute concentrations with respect to calibrated standards of like materials, which were not available for our set of materials.

Typical output for the metal carbides (sample HfC No. 11) is shown in Figure 17. A sputtering removal rate of 140 A per minute (relative to a Ta_2O_5 standard) was assumed throughout the analysis to provide composition as a function of thickness. The carbide results contrast with those obtained from the nitrides (see Figures 18 and 19). The titanium peak at 380 eV and the nitrogen peak at 387 eV overlap and preclude attempts at quantitative analysis. Even the use of the higher spectroscopic resolution shown in Figure 19 does not adequately resolve the peaks. This electronic spectroscopy reveals another difference between

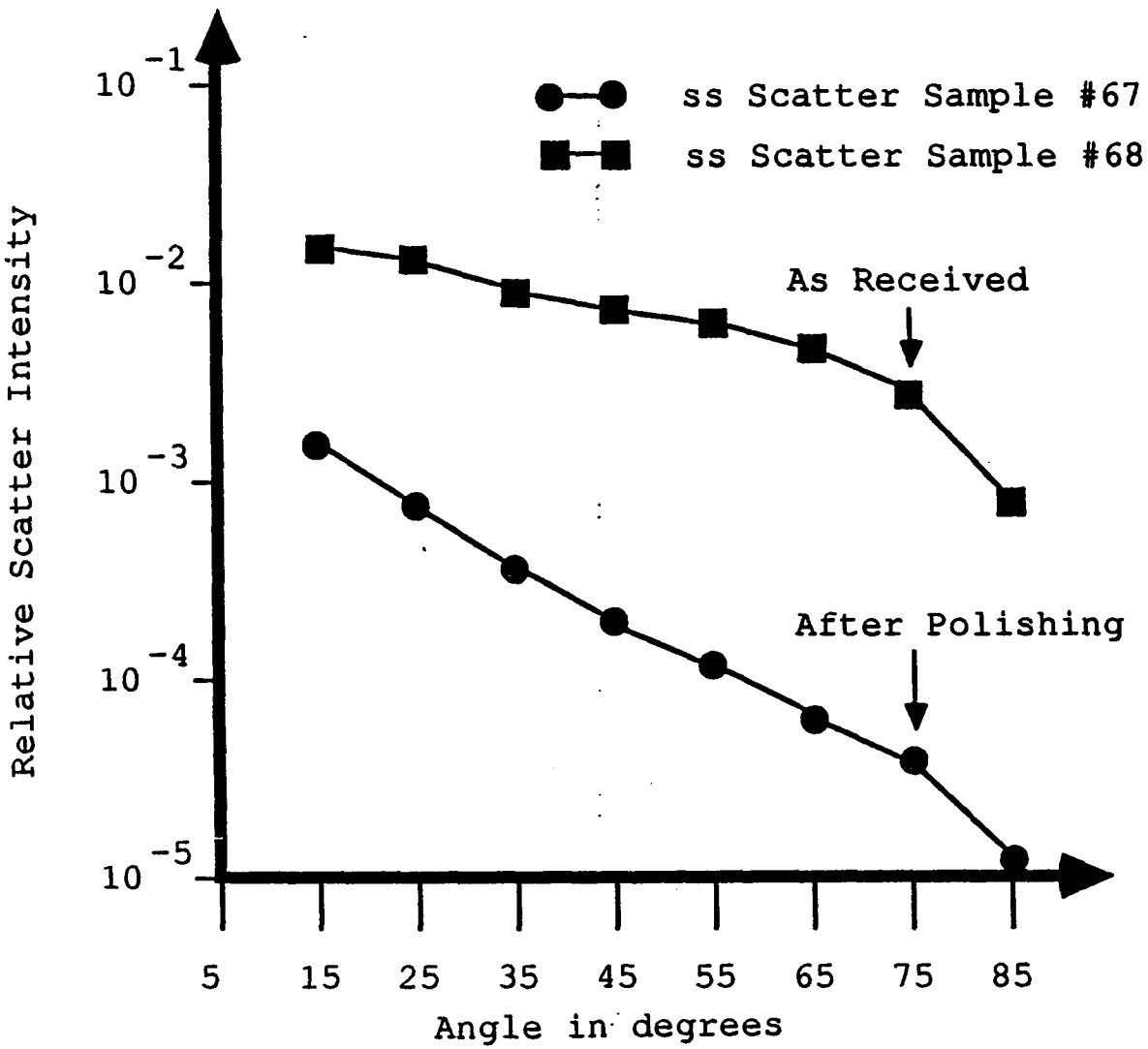

Figure 14. Relative scatter profile (ss) of samples No. 67 and No. 68 of CVD ZrN

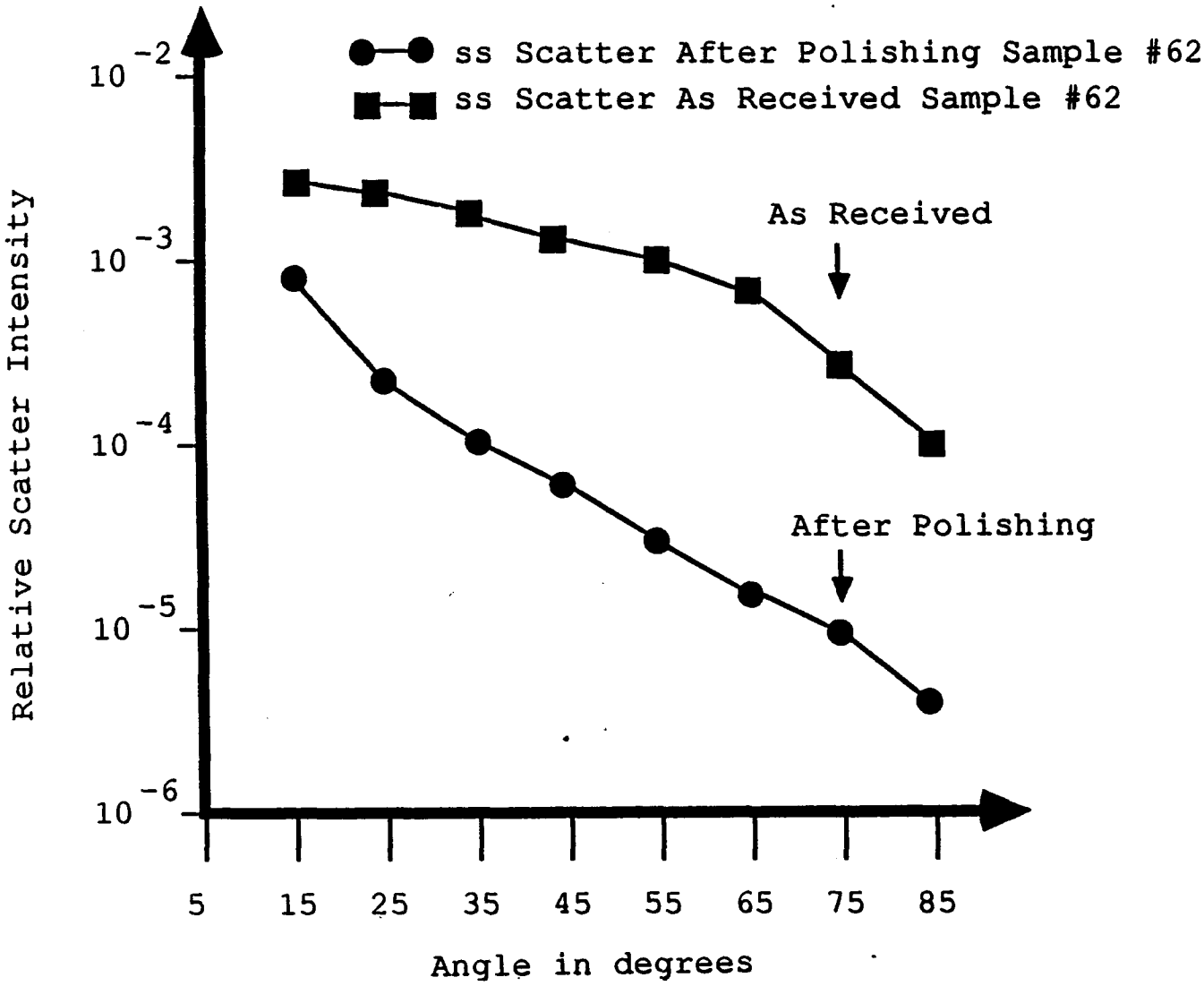

Figure 15. Relative scatter profile (ss) of sample No. 62 of CVD HfN.

Figure 16. Scanning electron micrograph of the surface profile of CVD ZrN (Sample No. 67 at 10,000 X).

the titanium carbides and nitrides. The core electrons of nitrogen reside at the same energy level as those of titanium while carbon electrons are bound at a much lower level (269 eV).

In general, the hafnium carbide samples were covered by a surface oxide layer on the order of 100 A thick (see Figure 20). The oxygen content fell off rapidly below this surface oxide layer to a background level of about 8 atomic %. The presence of this oxide layer was evident on all of the samples in the Spitz set.

A small argon signal was detected in some of the samples. The argon signal was just above the detection limit, but was present throughout the film. The samples which were exposed to a high temperature (500^{0}C) also revealed high levels of oxygen throughout (see Figure 21); the oxygen appeared to have diffused throughout the entire film.

The analysis of the titanium carbide sample (No. 20) provided by our French collaborators also indicated a significant amount of nitrogen. The overlap of the titanium and nitrogen peaks makes quantitative analysis difficult, but it appeared that the nitrogen content was below 15 atomic %. The titanium nitride samples also had surface oxide layers and low levels of oxygen and argon in the films.

Measurement of the Hf:C ratio of the hafnium carbide samples, also prepared by the French group, was based on a plot (see Figure 22) of the composition determined by nuclear techniques versus the partial pressure of methane. This analysis technique was good to within 5%. The compositions of the samples we received were never directly measured, but interpreted from

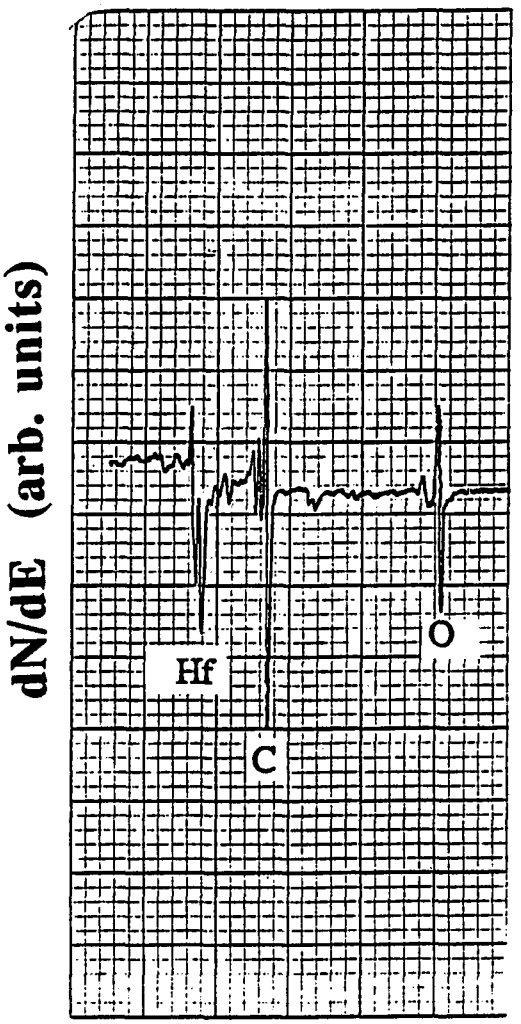

Figure 17. Auger spectrum of HfC(x).

The Auger lines identified are:

Hf	=	172 and 185 eV
C	=	270 eV
O	=	511 EV

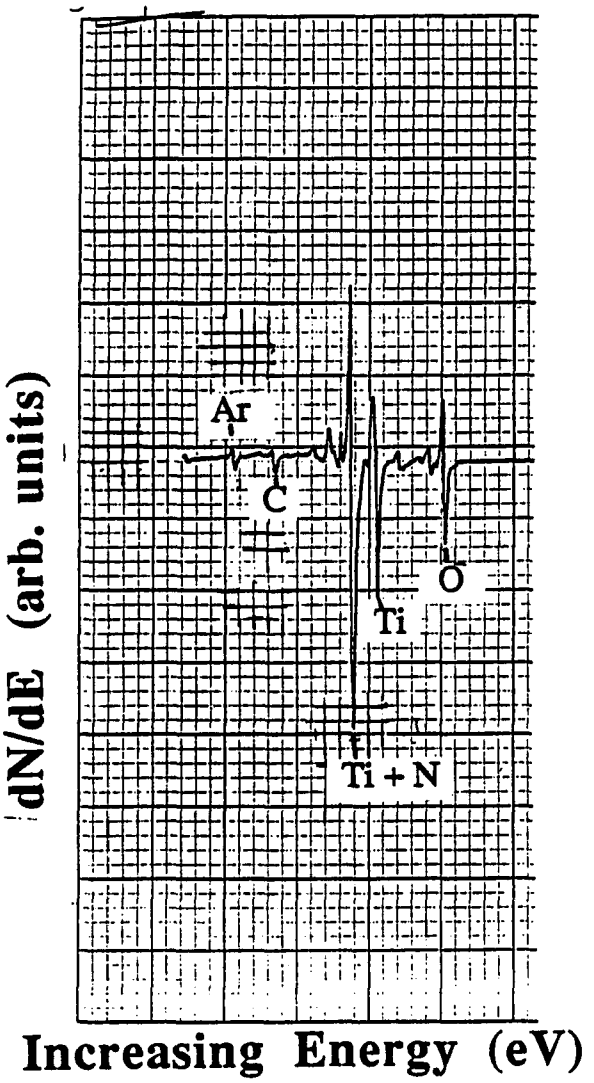

Figure 18. Auger spectrum of TiN at nominal resolution.

The Auger lines identified are:

Ar	=	208 eV
C	=	270 eV
Ti+N	=	381 eV
Ti	=	418 eV
O	=	511 eV

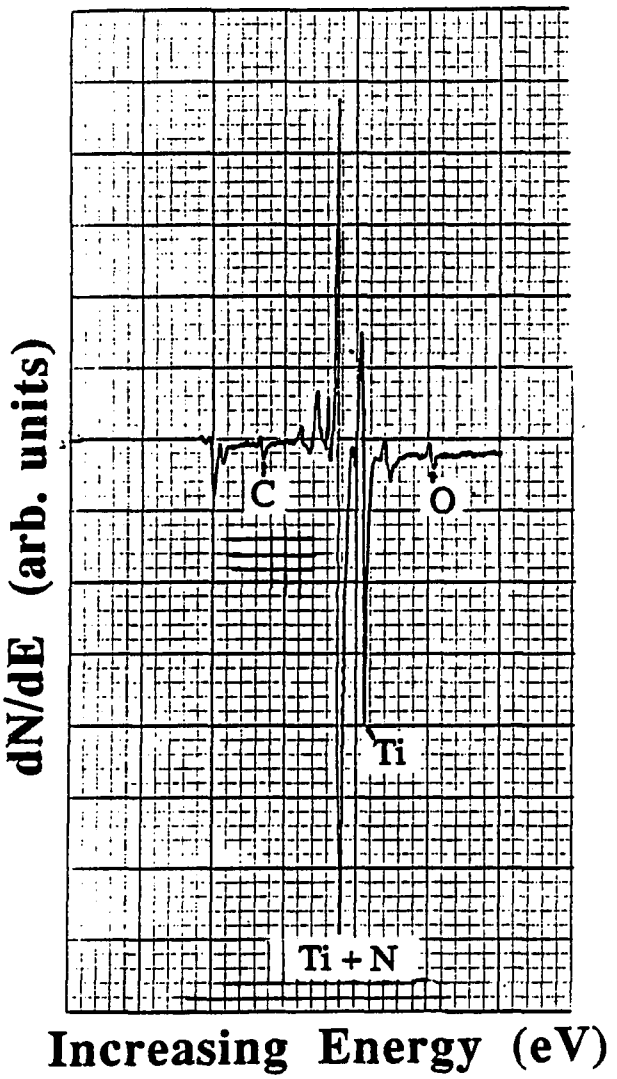

Figure 19. Auger spectrum of TiN at increased resolution. The Auger lines identified are:

C	=	270 eV
Ti+N	=	381 eV
Ti	=	418 eV
O	=	511 eV

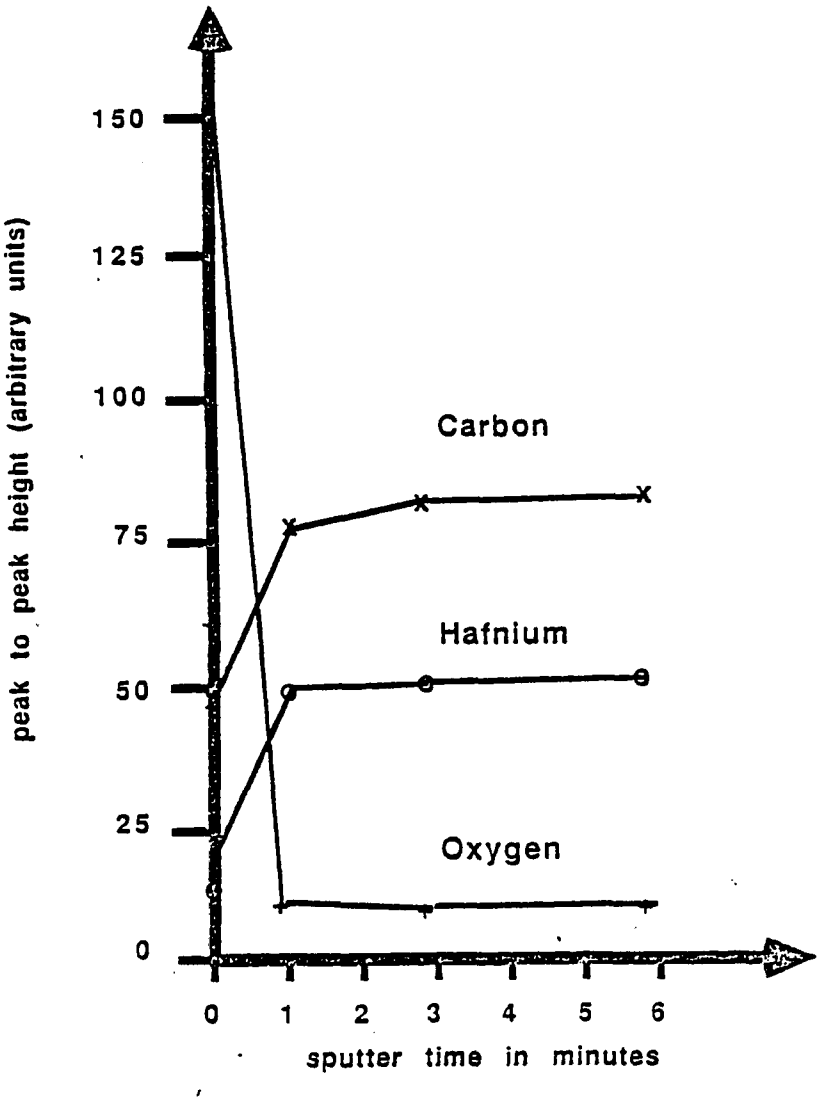

Figure 20. Auger analysis results of sample 26AG (HfC) before measurement in the high temperature reflectometer.

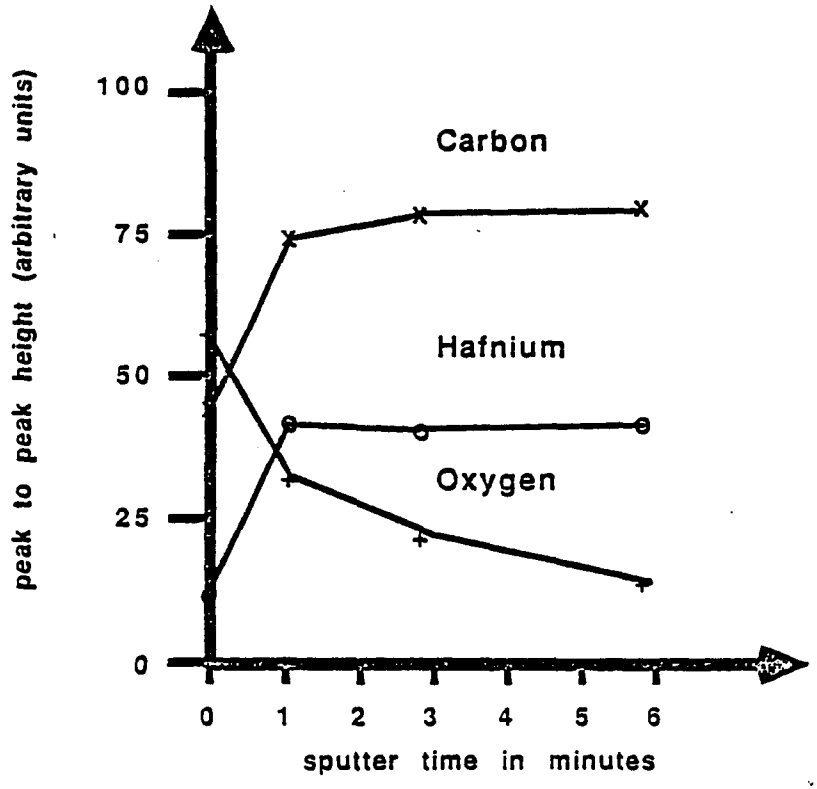

Figure 21. Auger analysis of sample 26AD (HfC) after measurement at 500°C in the high temperature reflectometer (HTR).

values obtained from this plot. We hoped that Auger analysis would confirm these values. Instead, due to the lack of reference standards for these films, this analysis could only reliably provide data on the impurity content of the films.

Nonetheless, the depth profiling of these films helped to establish the thickness of the surface oxide and to estimate the impurity level of the films. The low indicated level of impurities (O and C) analysis demonstrated the relatively high quality of these films compared to others in our sample set.

X-Ray Diffraction Analysis

X-ray diffraction analysis using Copper Kα radiation (1.542 A) was undertaken to identify the carbon phase in the carbon rich hafnium carbide samples provided by Spitz. We also established the presence of the oxide layer by this method. With access to the X-ray diffractometer system at the University's Department of Mines and Metallurgy, we could make these measurements conveniently.

By using X-rays of known wavelength and measuring the diffraction angle, we determined the spacing of the various crystal planes. This spacing is unique to the various periodic atomic structures that many materials and compounds form. This structural analysis can identify materials and is often used to distinguish the phases of unknown mixtures. Ideally, we would have preferred thicker films (on the order of 5000 A) but since transition metals have fairly large X-ray mass absorption coefficients, we were able to analyze these relatively thin films.

These measurements indicated improvement in the analytical precision was in order. A plot made of the nominal film thickness versus the intensity of the diffracted X-rays indicated deviations from a smooth absorption curve (see Figure 23); a plot of the given film thickness versus intensity of the primary

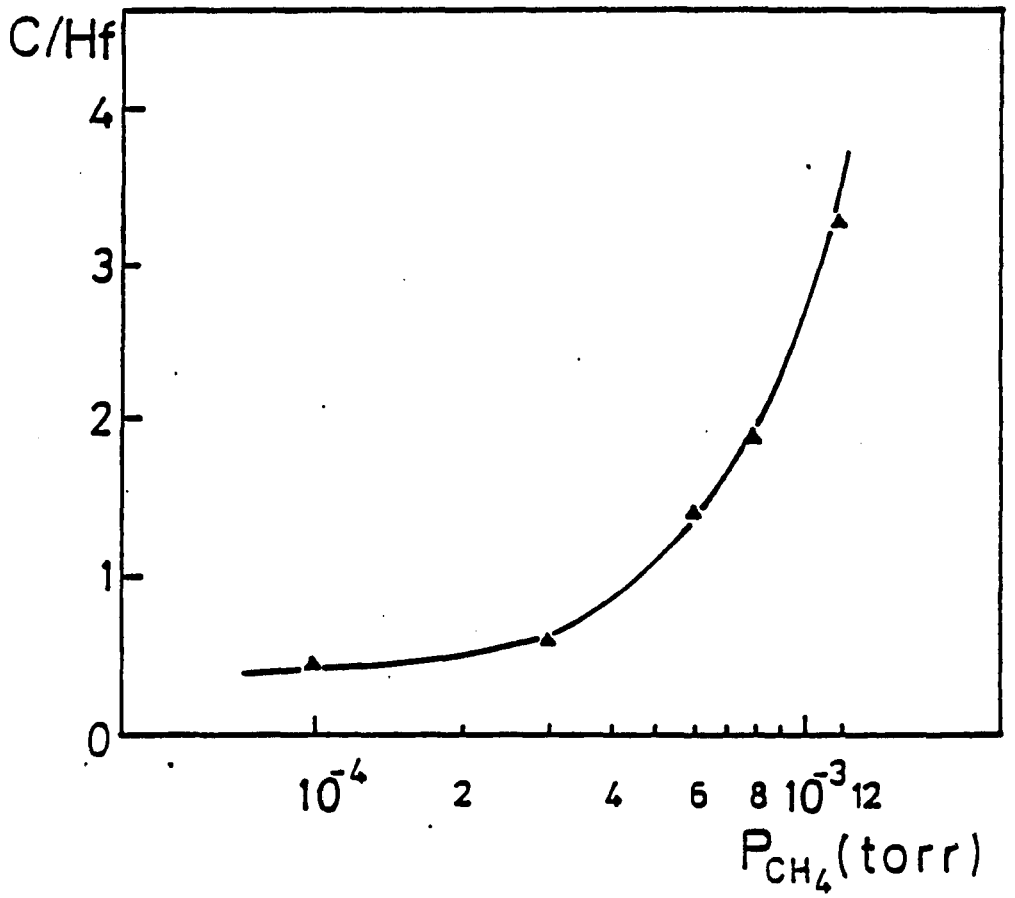

Figure 22. Composition of HfC as function of methane partial pressure.

diffraction plane should produce a smooth curve with no discontinuities. Moreover, the characterization of the visually discernible oxide layers proved to be difficult due to their thinness, but they pointed to a porous oxide layer, HfO_x on the order of 100 A thick. We were unable to find any indication of a second phase of carbon in the carbon rich hafnium carbide samples using this technique.

X-ray analysis of the TiN sample produced by CVD showed a matrix structure with a lattice parameter a = 4.24 A. This value was very nearly that attributed to the stoichiometric compound (Toth, 1971). This was the only X-ray measurement performed on the Haygarth samples.

Electron Microprobe Analysis

The electron microprobe in the Lunar and Planetary Laboratory at the University of Arizona heavily contributed to our film analysis. The technique is nondestructive and provides moderate accuracy with efficiency. The accelerated electron cascade excites a pear shaped volume in the sample, from which X-rays emerge. Thus, the detected signals provide an average volume analysis over depths of up to several micrometers. If the excitation depth exceeds the film layer thickness, the substrate will influence the results.

An electron beam accelerated to 6 KeV is directed at the sample and a crystal (Si:Li) detector attached to a multichannel analyzer records the energy spectrum of X-rays emitted by the sample. This energy dispersive mode allows for the simultaneous analysis of multiple elements. Its main drawback is the limited elemental detection range. Typically, elements with mass numbers less than 11 (Na) are difficult to detect. By working with lower acceleration potentials (6KeV instead of the usual 10-25 KeV, good reference standards, and a PET crystal, we made excellent measurements on the elemental metal composition (better

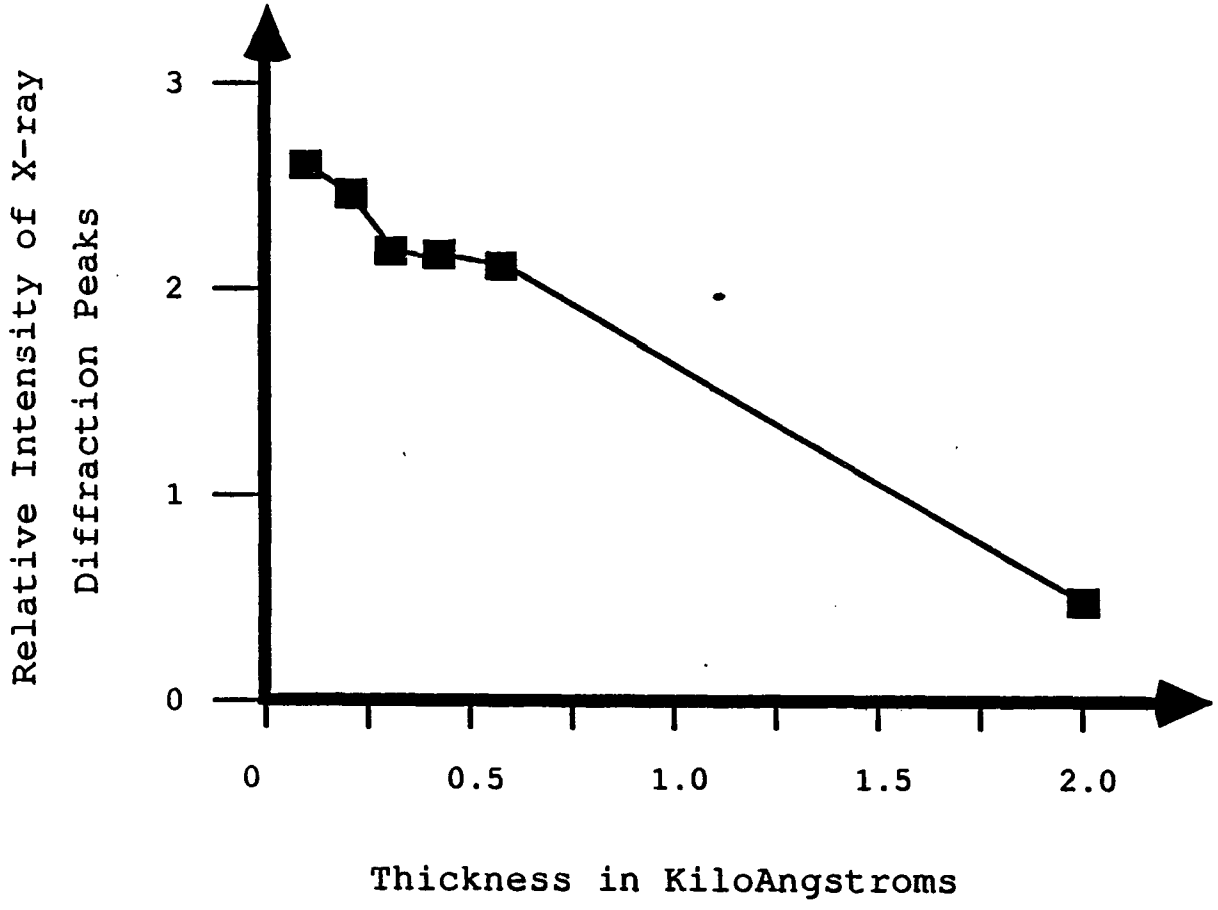

Figure 23. Relative intensity of X-ray diffraction peaks of the HfC films.

than 0.1 %), good measurements of the carbon content (± 0.2%), and fair measurements of the oxygen content (± 1%). We had difficulty with the nitrogen determination for two reasons; the lack of a good reference standard and the low spectroscopic resolution (on the order of 120 eV). This limited our ability to resolve the overlapping titanium and the nitrogen peaks of the titanium nitride sample.

The samples from Spitz proved to be too thin (3000 A maximum) for this technique. With a penetration depth of approximately 1 micrometer and a pear shaped excitation volume of around 1 cubic micrometer below the film surface, the signals from the excited Si and 0 in the quartz substrates dominated at even the lower acceleration voltages.

The results obtained from the analysis of the Haygarth samples are displayed in Table VIII. The values for the metals appear to be very reasonable and correspond to those obtained at the laboratories at Teledyne. For the titanium values we turned to the L X-ray emission peaks rather than the normally analyzed K emissions. The presence of zirconium in the HfN sample (see Table VIII) was verified by Haygarth (1979). Since $ZrCl_4$ contaminates the $HfCl_4$ reactant gas (Haygarth, private communication) and ZrN deposits preferentially during the course of the film growth, the 7 atomic % ZrN we found in our HfN analysis is reasonable.

The values obtained for the oxygen and the carbon impurities are also reasonable for these samples. The values for nitrogen are questionable since we were never able to obtain a suitable standard. The nitrogen peak was completely obscured by the titanium emission; we were unable to distinguish the peaks even using their L emission lines (see Figure 24).

Table VIII. Compositional Analysis of the CVD Nitrides by Energy Dispersive Analysis.

Sample	Type	% Metal	% Carbon	% Oxygen	% Nitrogen
60	TiN	93 wt.%* Ti	<0.2 wt.%	No trace	Undetermined**
67	ZrN	96 wt.% Zr	<0.2 wt.%	<1 wt.%	.12±.06 wt.%**
61	HfN	93 wt.% Hf 4 wt.% Zr	<0.2 wt.%	No trace	.09±.06 wt.%**

*Based on Ti L emission spectra. All others based on Ti K Emissions.

**These data added for reference only. Emission peak overlaps were so large that accurate evaluations could not be made.

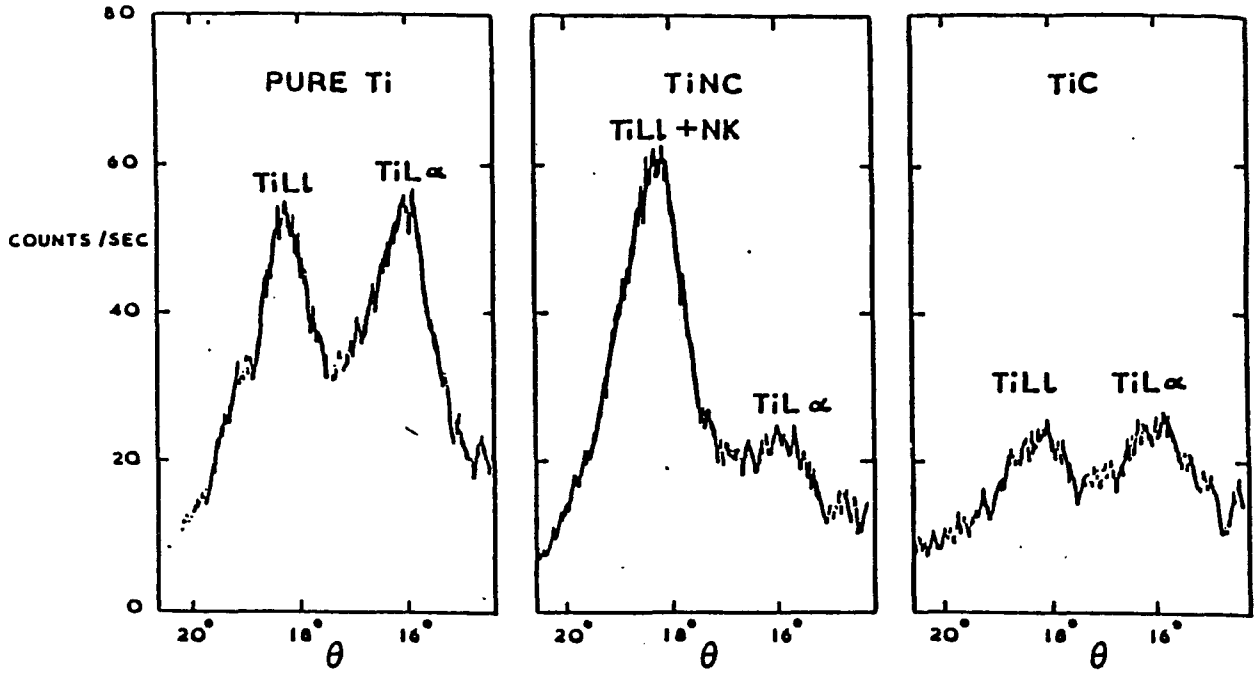

Figure 24. Obscuration of Ti(L) and N(K) peaks due to overlap in spectrometer.

Aging Effects

A concern arose early in the program over the nature of the oxide film on these samples. The duration of this program - the samples from Dr. Spitz were presumably made prior to 1976 while the analysis was undertaken in the period from 1977 to 1979 - and indications that the room temperature UV spectral reflectance had changed were worrisome. This change was noticed even on samples that had not been exposed to the high thermal loads found in the High Temperature Reflectometer. Our assumption was that these changes were due to surface oxide growth. This oxide was assumed to form at a logarithmic rate (Beensch-Marchwinka and Berlicki, 1979); usually, after a thin surface layer oxidizes, the reaction self quenches due to the protective nature of this outer oxide layer, unless cracks or other defects occur. However, some indications suggested that the thinnest films continued to oxidize; comparisons of measurements made over a period of two years showed a reduction on the order of 1% in the UV. Alternative explanations for this reaction might be measurement errors or changes in the performance of our aluminum reference sample.

The oxides of these materials tend to have large band gaps and consequently little or no absorption. In fact, oxides of these materials routinely appear in laser and UV coatings because of their low UV/visual absorption and hardness. A plot of the theoretical reflectance of HfC calculated using the constants derived from this work with and without a 100 A oxide layer are presented in Figure 25. These values compare favorably with our experimental results.

This apparent aging effect triggered our efforts to characterize samples at the OSC. Once the question of sample composition was raised, we felt that these initially unplanned characterizations would be essential.

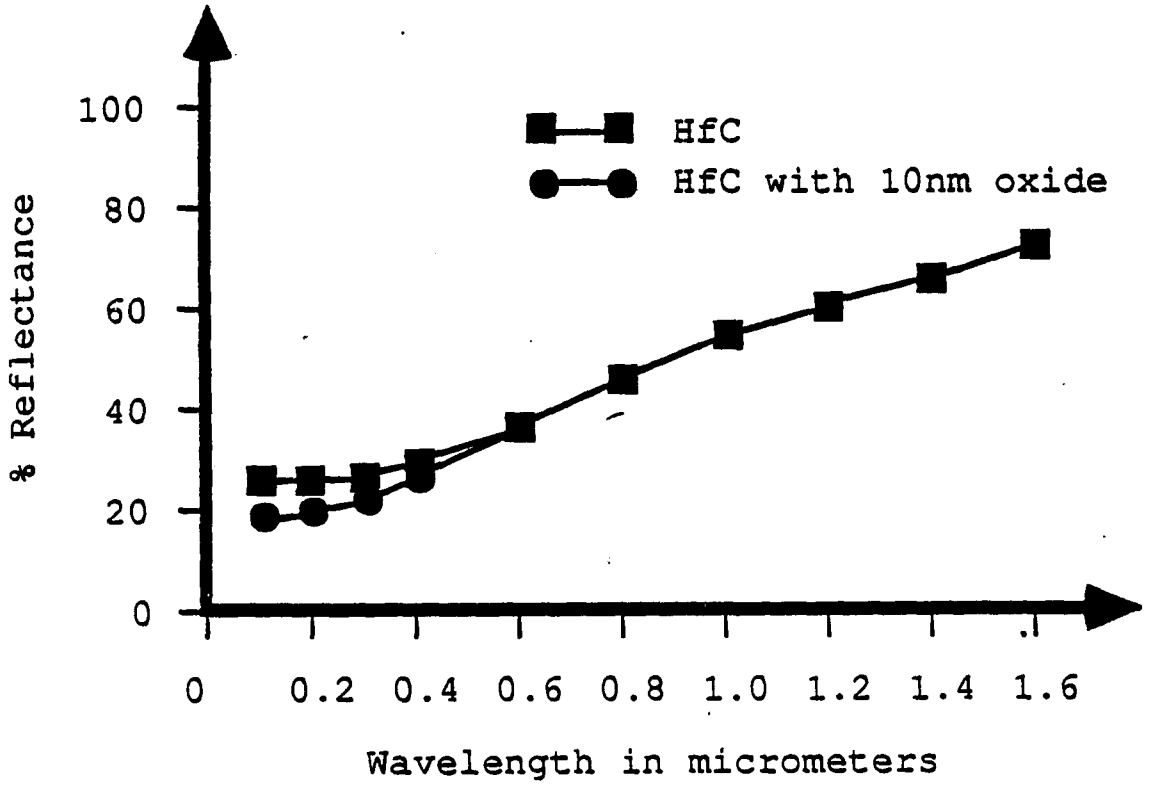

Figure 25. Theoretical effect of oxide growth on the reflectance of an HfC thin film.

Thickness

Our need for a greater degree of precision in thickness measurement than the nominal values provided with the semitransparent film samples led us to consider the problem in more detail. During the deposition, thickness monitoring was based on elapsed time. After deposition, thicknesses were measured with a stylus instrument with an accuracy of ± 100 A. This posed a problem, since some films were only about 100 A thick. Plots of the French measurements of resistivity versus thickness produced discontinuous results similar to the plot of the X-ray mass absorption versus thickness (Figure 23).

We adjusted the thicknesses of the samples to fit a smooth curve of resistivity versus thickness. Thickness determinations provided by an interference technique using fringes of equal chromatic order (FECO) of the coating sample edges were also made. While the precision of the latter method is excellent, the samples had not been prepared so as to facilitate this measurement. Ideally, sharp edges produced by physical masking generate the sharply defined fringes needed for accurate FECO analysis. Problems due to nonuniform thickness or edge roll off in our samples could not be discounted.

This problem was finally eliminated with measurements of the optical thickness determined by near normal reflection and transmission, and the transmission of p polarized light at 60^0 incidence angle. These measurements suitably overdetermined a thickness solution for the film and these values and those obtained from FECO were averaged to obtain those used in our analysis. The decision to employ optically derived thicknesses was justified on the basis that our analytical goals were ultimately related to optical properties.

Optical Microscopy

All of the samples were monitored during the polishing cycle by the Leitz microscope equipped with standard objectives and an interference (Mirau) attachment for determining sample height variations. These observations kept track of the surface quality and topography. A photographic record of the complete sample set was made at the conclusion of the polishing cycle.

Physical Models of the Films

The model derived for the semitransparent samples appears in Figure 26. The oxide layer was present in all cases on the films from Spitz and tended to diffuse into the hafnium carbide matrix at high temperatures. Three of the semitransparent samples were exposed to temperatures greater than 500°C. The titanium nitrides and carbides were also covered by this surface oxide. However, due to our inability to measure the actual thickness of this layer and since it affected our optical measurements on the order of 1% (which is about the best accuracy we could claim for the Perkin Elmer instruments), we decided to neglect this oxide contribution and accept an uncertainty of 2% in our optical data.

The optical measurements of the samples provided by Haygarth were probably more accurate than 2%. Since we were able to polish and measure them immediately, this presumably removed any oxides. They were also measured within the month of deposition and had not been exposed to any high temperature environments prior to our measurements. There was little hesitancy in using simple models with these films.

The physical models of the films on which this analysis is based are presented in Figures 26 and 27. We assumed that the films were homogeneous

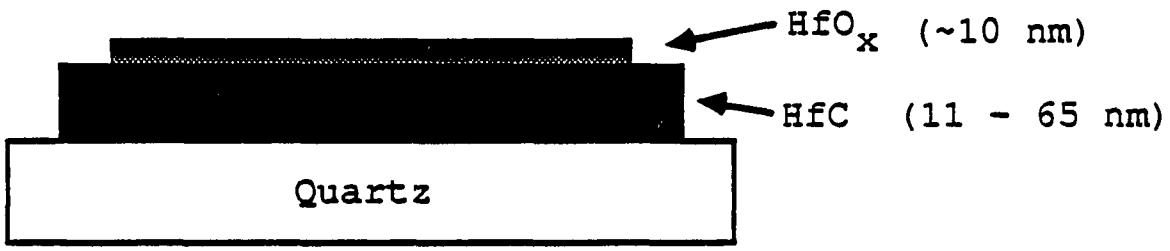

Figure 26. Physical model of the hafnium carbide films after OSC characterization.

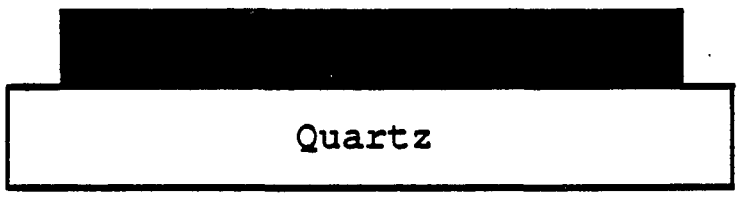

Figure 27. Physical model of HfC films used in our analysis.

and uniformly thick. We also assumed that the quartz substrates did not produce measurable bulk scattering. All interfaces were assumed to be abrupt and plane parallel.

These simple models were also predicated on the fact that we already had enough variables to satisfy even the most fanatical statistician with a yen for fitting data. Moreoever, we could not assure ourselves that more complex models would be accurate; they would require knowledge of uncertain quantities, such as refractive index and density of the oxide layers, that we did not determine.

CHAPTER 3

INVERSION OF SPECTRAL MEASUREMENTS TO OPTICAL CONSTANTS

The interaction between an external electromagnetic field and the atoms of a homogeneous material can be completely characterized by two frequency dependent numbers - the so called optical constants. Despite the efforts of numerous individuals, there is no direct method for obtaining these optical constants. A variety of methods coupling measurement sequences and inversion techniques exist, but no experiment has been devised which will yield the values of n and k outright. All of the methods which match experimental data with the underlying optical constants are model dependent, and typically involve the over-determination of enough optical parameters to reduce the inherent ambiguities of an inversion scheme. Hundreds of scientific papers have been written and complete careers have been made by experimentalists working on this problem. No one method is clearly superior for all cases; the limitations of each become readily apparent shortly after the choice is made, and long before any valid results emerge.

We have chosen two well-established methods. The first is based on work by Nilsson (1968) and Nestell and Christy (1965). This approach was first implemented at the OSC by Hahn (1976); it is based on using values of R and T obtained from spectrophotometric measurements. This data is then manipulated in

an iterative search process to develop solutions of n and k that will minimize the differences between the measured reflectances and theoretical reflectance values calculated from these n and k values.

The second method is based on the dispersion relations developed by R. Kronig (1926) and H. Kramers (1927). These dispersion relations were first applied to the analysis of reflection spectroscopy by T. Robinson (1952). The Kramers-Kronig dispersion relations express an exact relationship between the real and imaginary parts of the optical constants. These relationships allow measurements of the single surface reflectance to be converted to both the real and imaginary optical constants of the material.

The program to measure optical constants began with semitransparent film samples from Spitz. Because of unsatisfactory results additional samples were collected and better analysis methods developed. The following sections detail the evolution of our capabilities.

Reflection, Transmission and Thickness (R, T, d) Method

A subset of the hafnium carbide samples provided by Spitz were deposited with the same nominal stoichiometry, but with differing thicknesses. It was hoped that these thickness variations would ease the analysis needed to determine the optical constants and that the code developed by Hahn would succeed. Neither of these aspirations were realized.

Our work built on that of Hahn and extended his three modes of analysis to include three additional measurement and analysis modes. These were developed as a direct result of the measurement sequence possible with the Spitz samples. Substantial new code was generated and loaded into the OSC's in-house Eclipse computer. It allows the iterative search for optical constants using up to

5 spectral measurement combinations. For a time, this code was one of the only available tools for rigorously calculating the theoretical performance of absorbing films on absorbing substrates.

This first method was based on making measurements of near normal reflectance (R) and normal transmittance (T) as shown in Figure 28. These measurements coupled with film thicknesses are input using Mode 2.0 of the computer code listed in Appendix B; then, solutions for n and k are sought. Great pains were taken to assure ourselves that the spectral measurements were the best possible evaluations that our samples and instrumentation would allow.

Unfortunately, the weak spectral variation of both n and k, the similar numerical values of n and k, and difficulties in determining the film thickness limited the program's ability to determine n and k for these films. This problem becomes evident in the plots of constant reflectance and transmittance in the n and k plane as shown for two thin film thicknesses in Figures 29 and 30. These values for R and T cross at broad, nearly tangential intersections, which make precise determinations of n and k impossible. In some cases, no overlap occurs. After measurements and remeasurements of R, T, and d produced no better convergence, this analysis method was changed to include a new approach.

Following the method of Nestell and Christy, measurements of the transmission of p-polarized light at 60^0 incidence angle were made; the sequence is depicted in Figure 31. These measurements are sufficiently independent that, in principle, a film thickness can be established. With this optically determined thickness as an input into our code, we hoped that we could get convergent optical constants for these films. The basis for this hope is evident, if a comparison is made between the contours of constant R and T in n-k plane for T

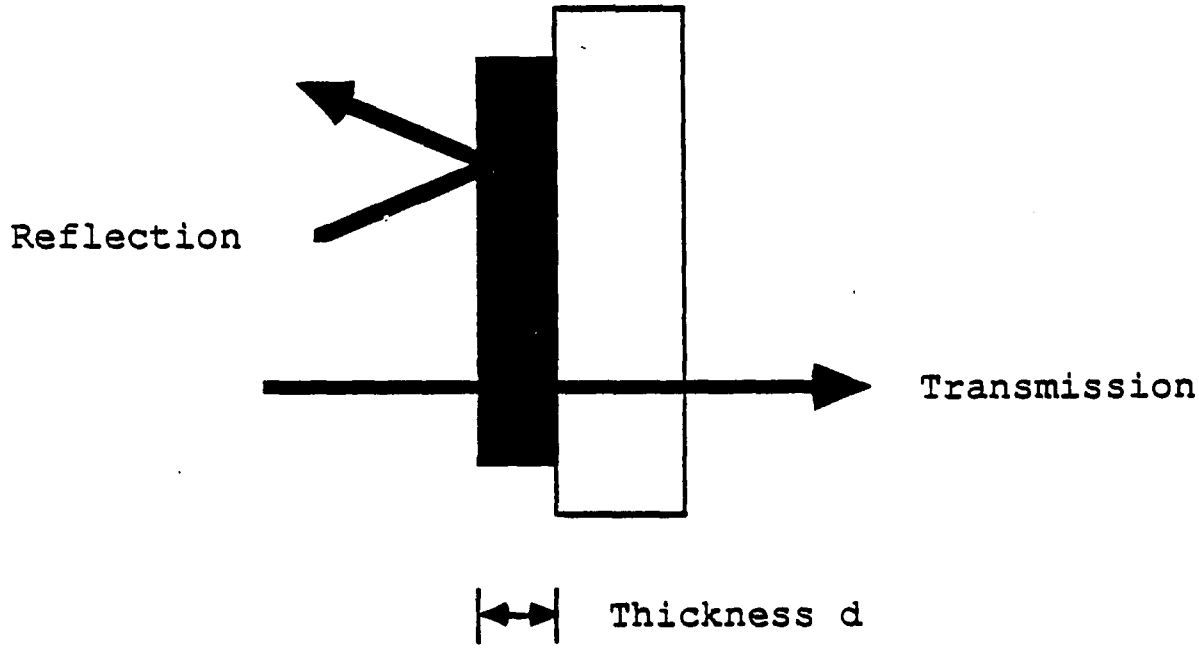

Figure 28. Schematic representation of our reflection and transmission (R,T) measurements.

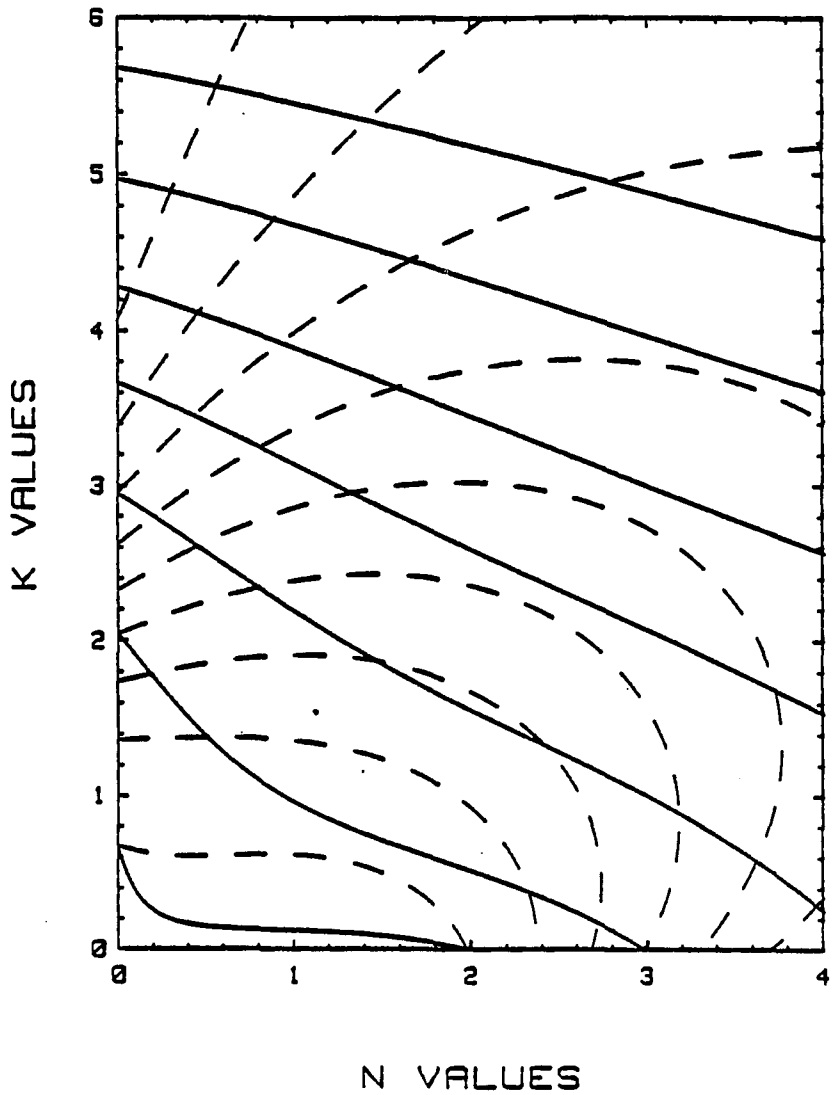

Figure 29. Contours of constant reflectance and transmittance in the n and k plane for a film thickness to wavelength ratio of 0.5. (Reflection = -; Transmission = —).

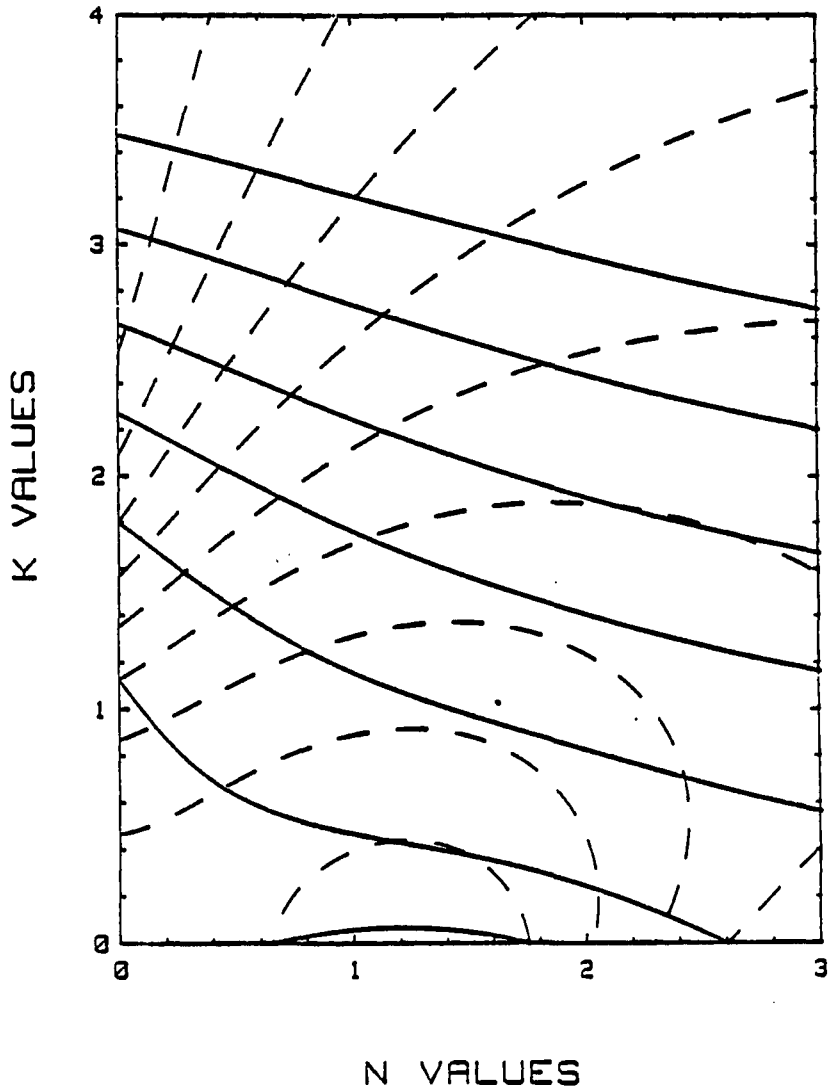

Figure 30. Contours of constant reflectance and transmittance in the n and k plane for a film thickness to wavelength ratio of 0.1. (Reflection = -; Transmission = —).

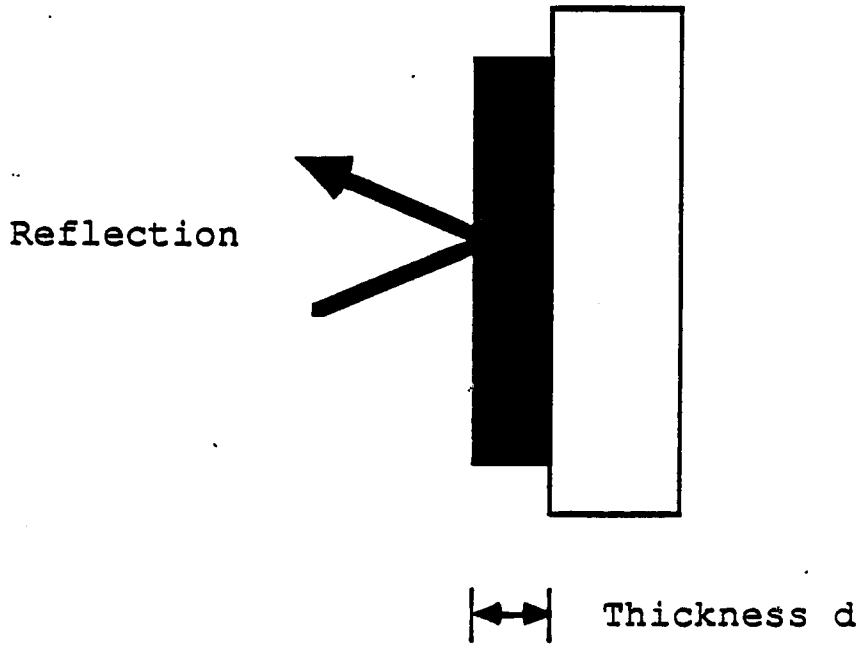

Figure 31. Schematic representation of the measurement of near normal reflectance used in our Kramers-Kronig (K-K) analysis.

(normal) (Figure 30) and T_p (60^0) (Figure 32) (polarized at 60^0 incidence). Much steeper intersection points appear in Figure 32 and allow the program to "find" clear cut solutions.

The code was modified again for this purpose. One of the calculation routines, Mode 0.0, was converted to incorporate measurements of $T'_p(60^0)$. A thickness solution was the first output of this analysis, which was then input back into the code along with the measurements of normal R and T that originally determined this film thickness, and searches for n and k solutions were initiated again. This approach again proved unsatisfactory. A check of the quality of our analysis was made by taking the logarithm of the transmission [log(T)] of samples with differing film thicknesses. This method should produce consistent values for the absorption factor k of our films. The values of the log(T) for films of differing thicknesses did not correlate with the optical constants obtained from the iterative search. Thus, the only results from this entire effort which we trusted were the film thicknesses. The most consistent results of n and k values for our sample set were derived using the data from the logarithm of the transmittance only. Using this analysis approach and assuming that the oxide was similar on all these films of differing thicknesses, the problem of surface oxide contamination should factor out (Hunter, 1985).

The difficulties encountered in determining the film thickness values to an accuracy better than 10 A, the errors in measurements of the spectral properties, numerically similar values of n and k, and the questions arising from surface contamination were all too great for the R, T and d method to overcome. We felt we had invested considerable effort in analyzing these films and could not develop

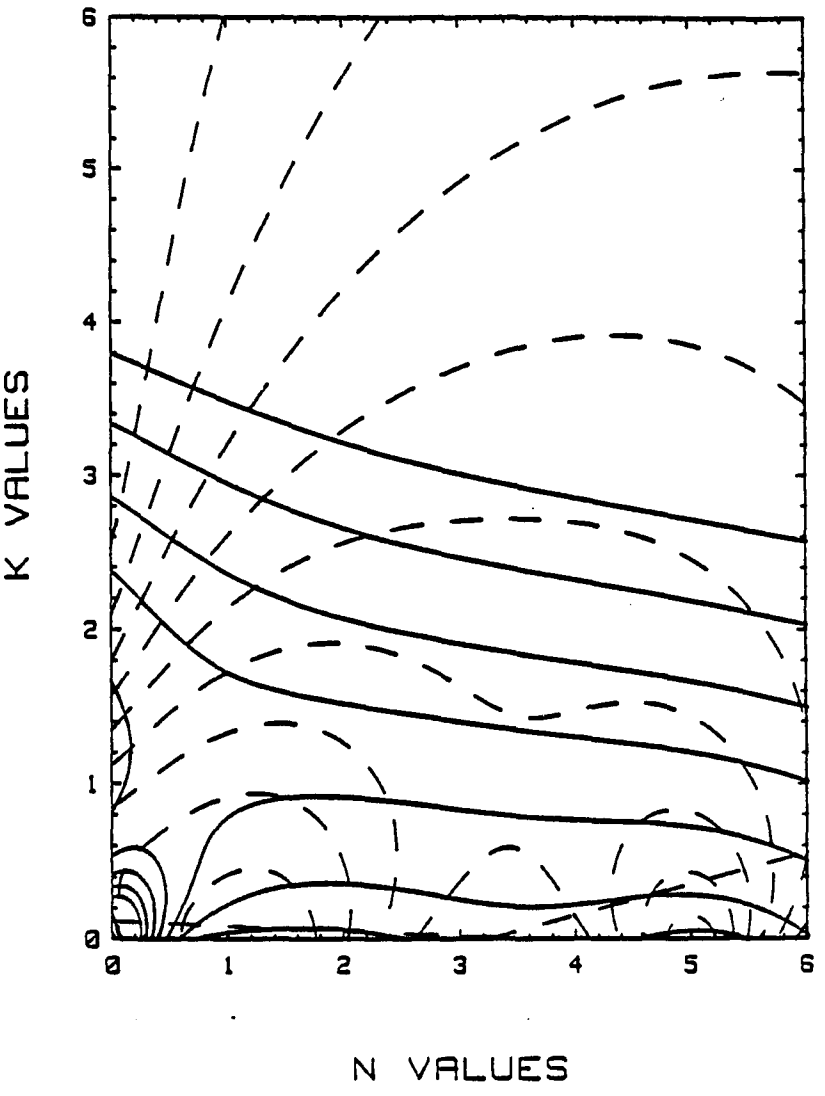

Figure 32. Contours of constant reflectance and transmittance for T(p) at 60 degrees. The thickness/wavelength ratio in this example is 0.1.

consistent results; perhaps more progress could be made on the program by changing our sample set and by using a different analysis approach.

Kramers-Kronig (KK) Analysis

Since the majority of the samples we obtained were opaque, we needed a technique that could be used to determine the optical constants from reflectance measurements only. The Kramers-Kronig (KK) method was chosen to address these needs.

We measured the near normal reflectance of the opaque samples as shown in Figure 33. Invoking such principles as causality and realizing that optical constants are analytically continuous functions with real and complex components, we can express the optical constants n and k as:

$$n = \frac{1-r^2}{1+r^2-2r\cos\theta} \text{ and } k = \frac{-2r\sin\theta}{1+r^2-2r\cos\theta} \tag{1}$$

Here we follow the treatment of Rossler (1965) and Mitra (1985) and use the normal conventions for our expression. The experimentally determined reflectance R is equal to r^2 in our expression. The phase difference theta (θ) between the incident and reflected wave can be written:

$$\theta_c = \frac{1}{\pi}\int_0^\infty \frac{d\ell n(r)}{d\omega}\,\ell n\,\frac{\omega+\omega_c}{\omega-\omega_c}\,d\omega$$

$$= 2\,\frac{\omega_c}{\pi}\int_0^\infty \frac{\ell n(r)(\omega)-\ell nr(\omega_c)}{\omega^2-\omega_c{}^2}\,d\omega \tag{2}$$

The evaluation of the phase at a particular frequency (ω_c) is related to reflection spectrum $R(\omega)$ by means of this integral transform. It is not an independent quantity. This integral is solved numerically using the computer code

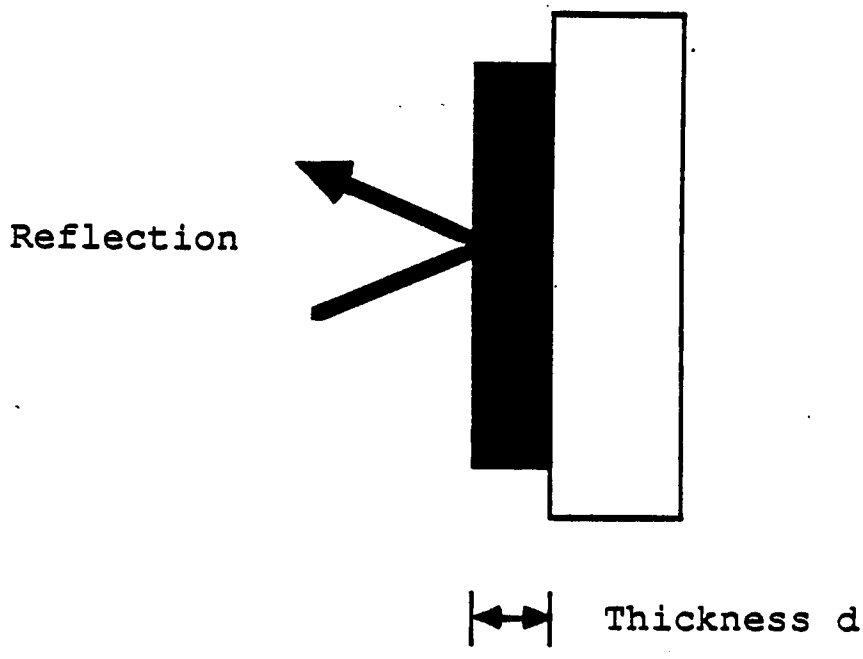

Figure 33. Schematic representation of the measurement of near normal reflectance used in our Kramers-Kronig (K-K) analysis.

listed in Appendix C. These rather formidable limits of integration for the frequency ω (0 to ∞) reduce to two extrema where the reflection hopefully approaches constant values. This points out the basic problem associated with this type of analysis: it is difficult to get R values from zero to infinite frequency. Actual data below 0.2 micrometers (above 6 eV) is difficult to acquire without a synchrotron and must be extrapolated. Errors at any wavelength may influence the results of the analysis.

The extrapolations used for the nitrides were based on the following arguments. The low energy reflectance data $R(\omega)$ are extrapolated using the relationship

$$R(\omega) = 1 - \left[\frac{\omega}{s}\right]^2$$

where the adjustment parameter s was chosen to provide long wavelength continuity.

Since these materials display a distinctly metallic behavior in the infrared, it was felt that this extrapolation, based on a Hagen-Rubens relationship, would be justified. This follows well accepted practice (Stern, 1963; Hauser et al., 1978). Literature results (Schlegel et al., 1977) on the reflectance of these materials (TiN, ZrN, HfN) were employed in the energy range 6.2 to 12 eV. The ZrN and HfN extrapolations were treated similarly since at the time this work was done no data existed for HfN. The close similarity between the HfN and ZrN reflectance profiles was also used in making this decision. A multiplication factor had to be applied to the more extensive TiN data in the literature to match our results. We needed to shift the shape of the reflectance curves in the literature to higher values. We believed that we needed this multiplicative factor as a result of our

access to higher quality (higher reflecting) samples. Our samples closely resembles the data from TiN single crystals. This is not true for the reflectance levels of the other TiN values. Beyond 12 eV, the reflectance was extrapolated in the conventional manner (R proportional to $1/(\omega)^2$ for energies between 12 and 36 eV and R proportional to $1/(\omega)^4$ for energies beyond 36 eV). Since the spectral variations occurred primarily within our measurement region, we felt confident of our results. Our work compares favorably with recent analysis of the nitrides (Roux et al., 1982; Martin, 1982; Valkonen et al., 1983, 1986; Pfluge, 1984, 1985).

CHAPTER 4

RESULTS

Analysis techniques established for this effort provided the tools needed to develop an understanding of the underlying physical processes of these materials. The physical models of the electronic processes were developed primarily by my colleagues, B. Karlsson and B.O. Seraphin. However, a brief overview of the results and the models will be given here.

We made measurements on some samples to understand their composition. Deviations from nominal stoichiometry, the presence of impurities and oxide overlayers, and other aspects which would affect our film model were noted where possible. This was an important step and a major undertaking for some of our samples. After we reached a point where we had difficulty making further progress characterizing the samples at our facility, we proceeded to make our spectral characterization. Measurements of transmission and reflection of our semitransparent films are presented in Figures 34 and 35.

The spectral data combined with determinations of film thickness were inverted and used to search the n and k plane for solutions which would match our spectral data. It was difficult to develop consistent results for our semitransparent sample set. A somewhat arbitrary average of all the semitransparent results was developed. This was supported by similar conclusions from Kramers-Kronig results of the opaque samples. These results were within 10% of each other. The results of our analysis for the semitransparent samples

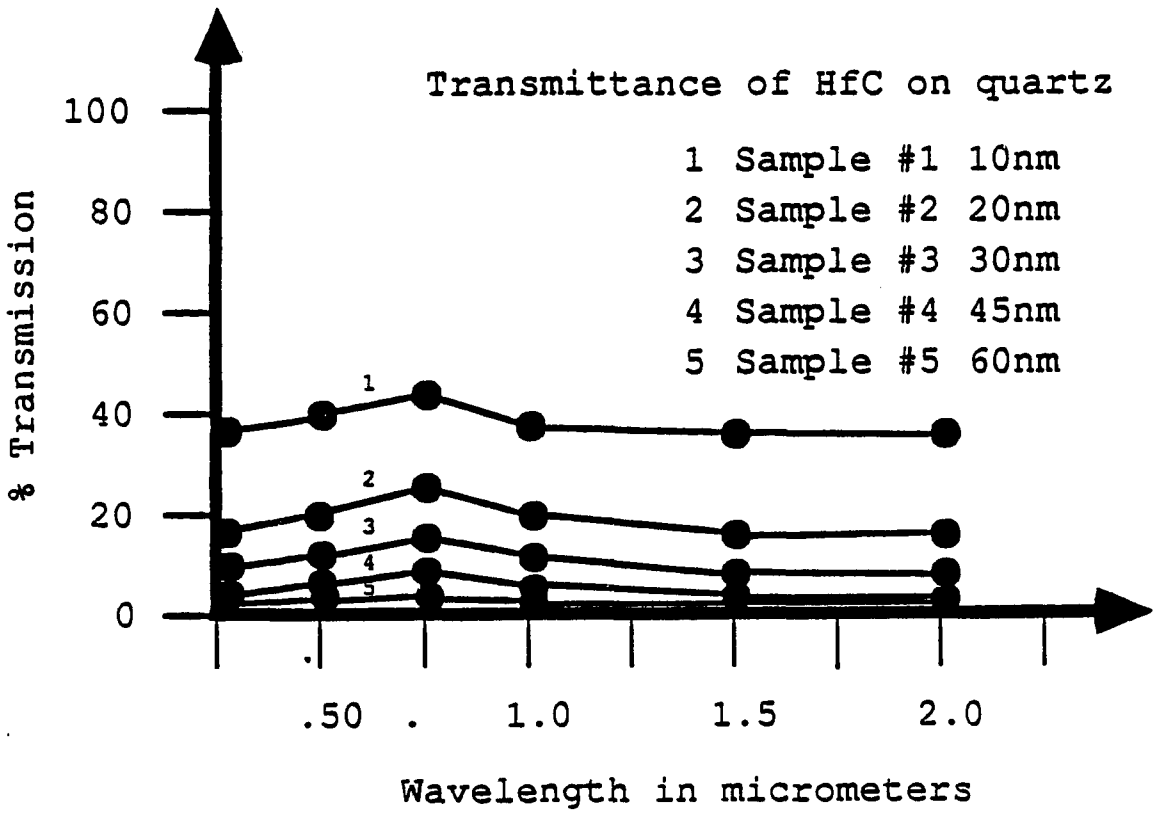

Figure 34. Transmittance of HfC films of various thickness on quartz.

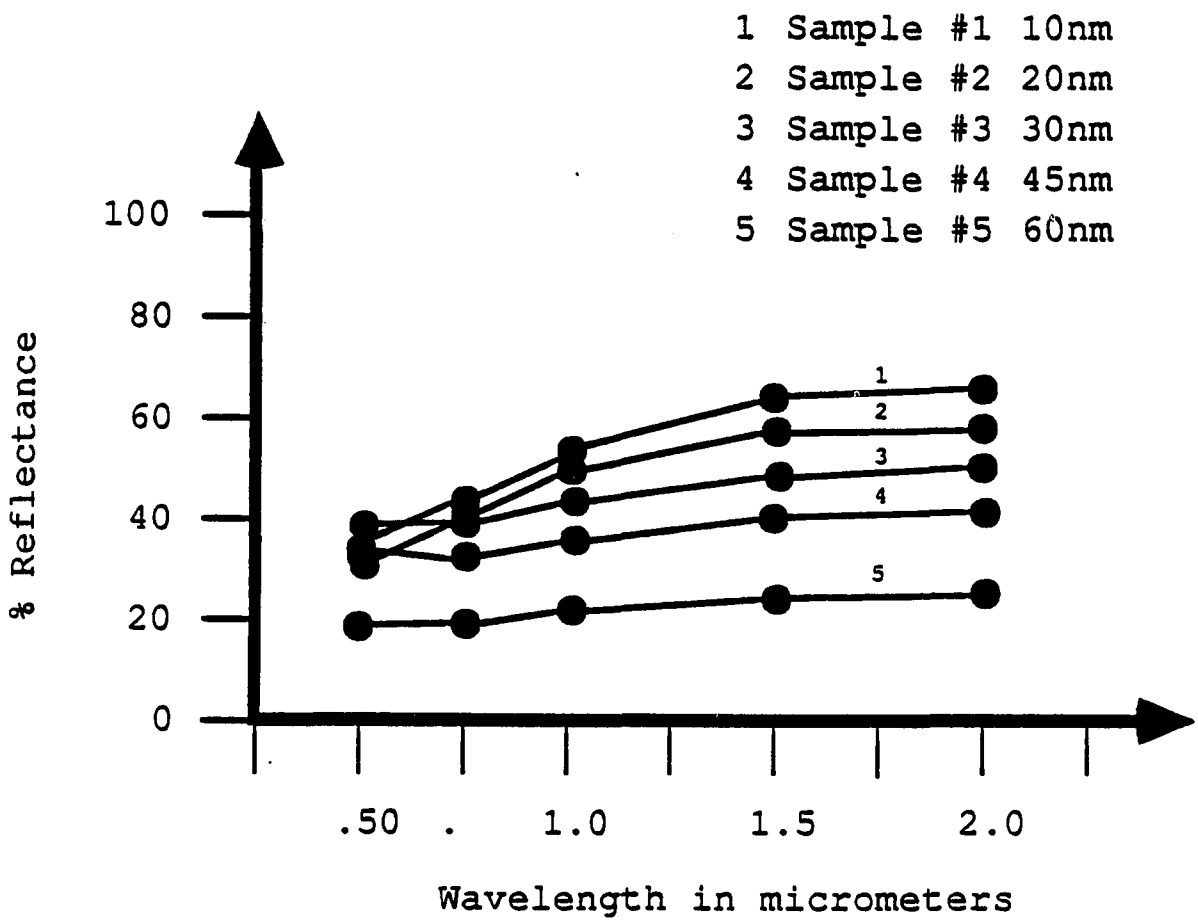

Figure 35. Reflectance of HfC films of various thickness on quartz.

are shown in Figure 36. Note the weak spectral variation on n and k. This is typical of most transition metals and transition metal compounds.

The Kramers-Kronig analysis of the nitrides proved to be more rewarding. Measurements of the spectral reflectance of our samples is presented in Figure 37.

As noted earlier we used well accepted extrapolations for our measurement data and developed data for n and k which is presented in Figure 38. The TiN data compares favorably with more recent work (Valkonen et al., 1986) and we expect our data for the other materials to stand up as well. We attribute this to the consistent CVD process of Haygarth which proceeds under near equilibrium conditions. They condense at high temperatures (approximately 1000^0 C) and at a slow rate (about 0.015 μm/min). These films were slowly cooled to preserve equilibrium in the lattice.

The nitrides display a highly metallic optical response similar to the noble metals, in distinct contrast to the carbides. It is possible to model these nitrides with a simple Drude approach.

This Drude behavior is unexpected for these materials, but can be explained by looking at a schematic representation of the density of states distribution as shown in Figure 39. Our model proposes that this difference from other transition metal compounds is explained by the lack of hybridization of the d-bands around the Fermi level E_f. Dipole selection rules will not allow d to d transitions. These pure d bands localized around E_f produce the Drude like behavior. The effective mass and the relaxation times of the d electrons thus dominate the optical properties. This is in direct contrast to the hybridized sp bands encountered in the carbides. In those cases the compounds tend to mimic the optical response of the elementary transition metal. Our colleague, Karlsson,

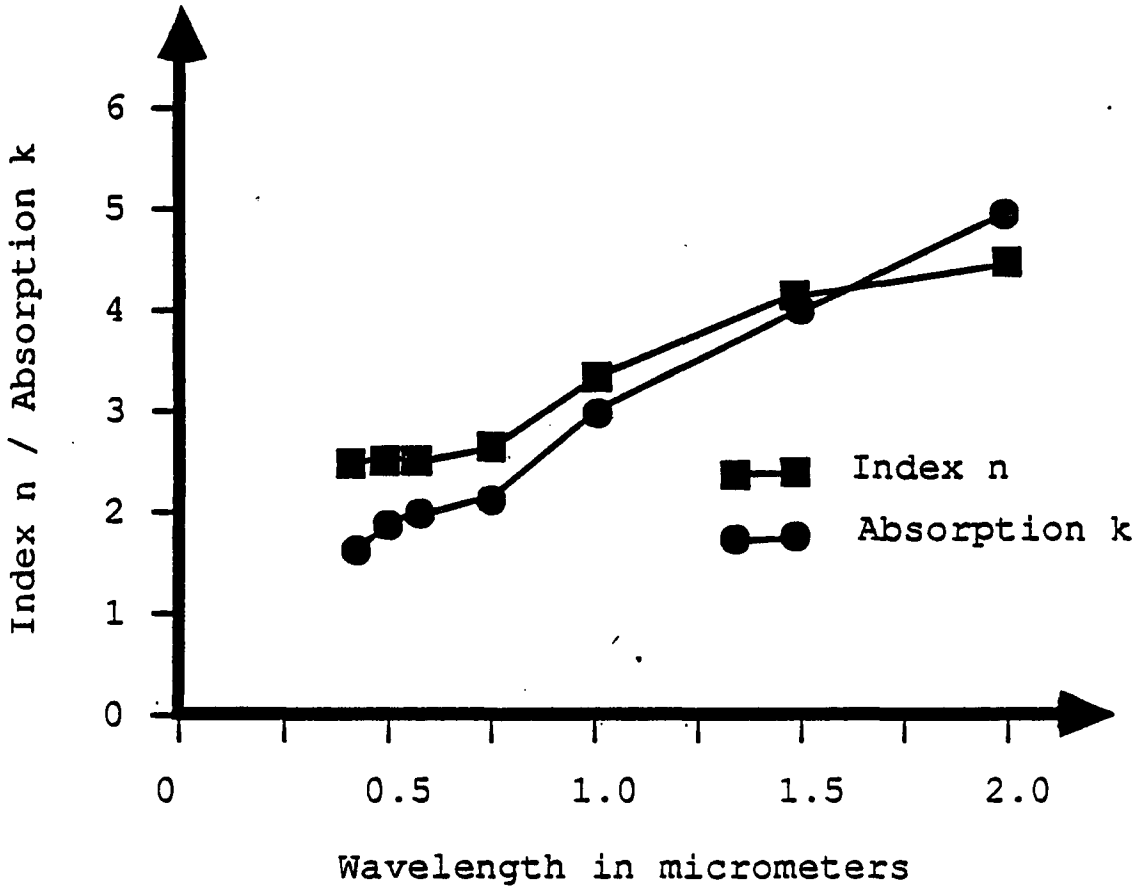

Figure 36. Optical constants for HfC for all samples calculated from R and T measurements.

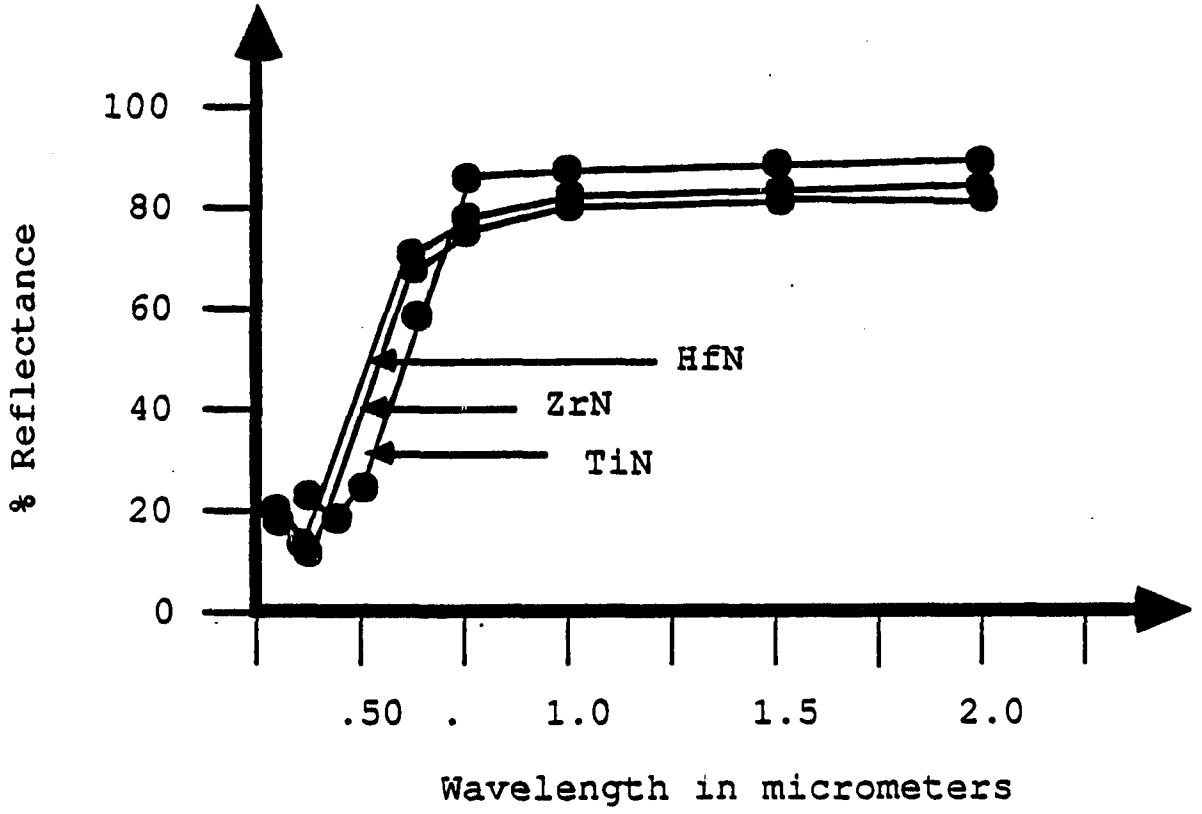

Figure 37. Total hemispherical reflectance of TiN, ZrN, and HfN samples deposited by CVD.

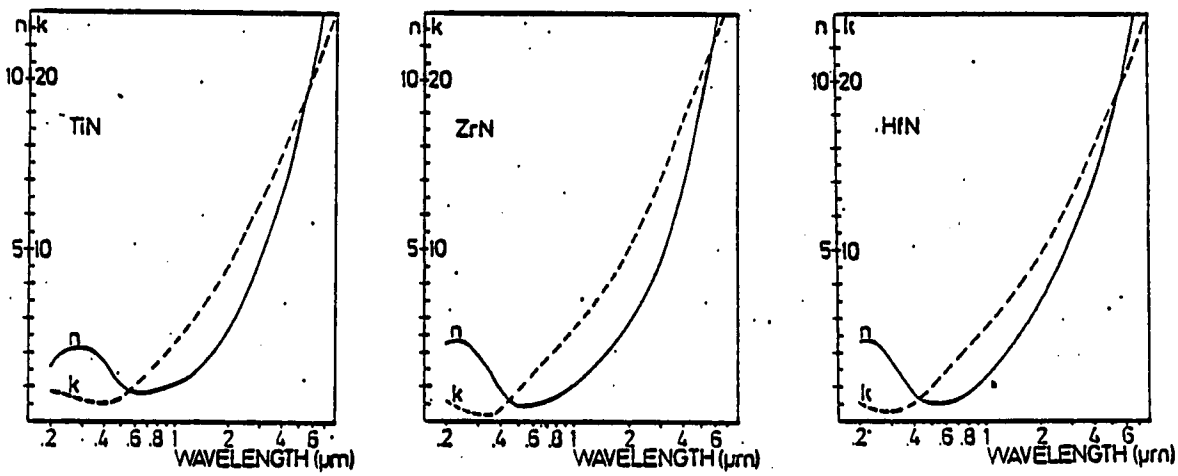

Figure 38. Optical constants of TiN, ZrN and HfN deposited by CVD.

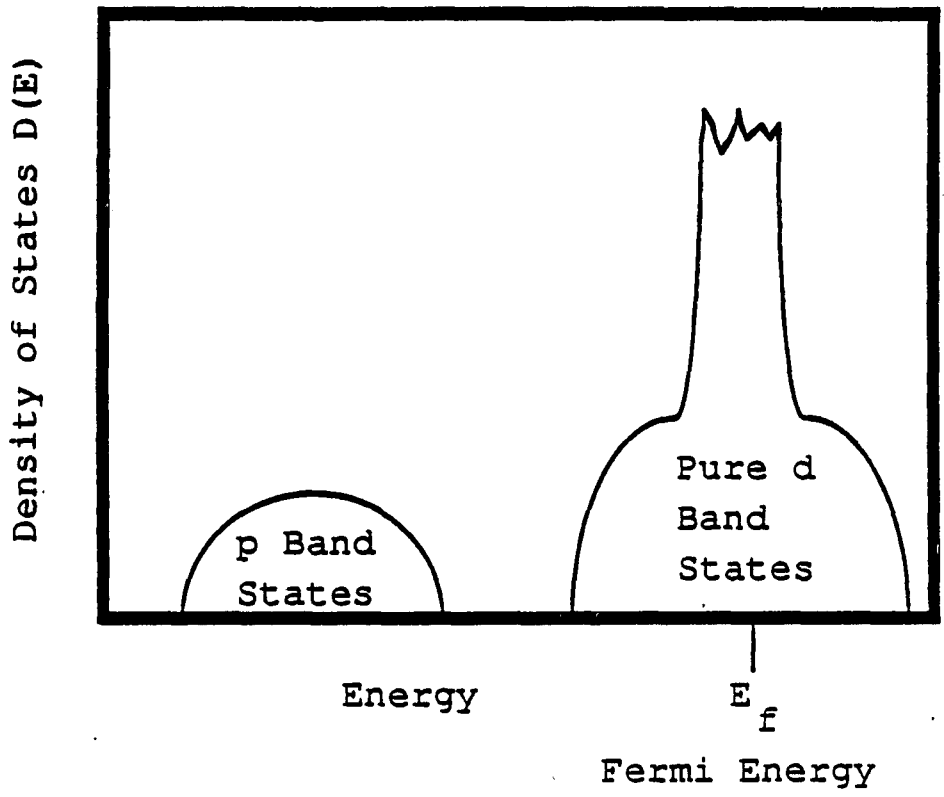

Figure 39. Schematic picture of the density of states distribution for the transition metal nitrides.

has extended this model to describe a variety of wavelength selective materials (T. Karlsson and B. Karlsson, 1984).

Recent work by Perry et al. (1986) extends and compares the contribution of composition to the location and slope of the TiN reflectance curves with the effect of expansions of the crystal lattice. With the wide range of composition available in TiN_x and the small lattice volume changes available, it had been expected that composition effects would dominate these shifts in the reflectance profile. This is consistent with our results. Perry has shown that it is possible to achieve comparable shifts in the visual reflectance profile (i.e. color) of his plasma enhanced films. Our samples were used as the basis for his comparison as shown in Figure 40.

CHAPTER 5

SUMMARY

The optical properties of a group of high-temperature materials have been investigated as potential candidates for single-layer absorber coatings. Ideally, these selective absorber coatings would be applied as thin films for use in high-temperature photothermal conversion systems. While these materials can be produced in thin-film form and are capable of withstanding high temperatures without degradation of their optical and mechanical properties, they do not possess the required spectral selectivity. This has been verified by independent efforts (B. Karlsson, 1982; Roux, 1982).

A model of the mechanisms underlying the spectral profile of these materials is postulated; it explains spectral differences of the metal carbides and nitrides. This model implies some ability to modify the spectral properties of these materials; however, it appears that the materials investigated are not capable of achieving the required spectral profile as single layers. The moderate spectral selectivity these materials possess will not justify the cost of applying these materials to photothermal solar energy conversion systems.

However, many applications do require the combination of properties that these materials demonstrate. Further work on understanding the many different material combinations and their resulting optical and material properties is justified.

Toward this end, an extensive set of samples of Group IV interstitial transition metal carbides and nitrides have been assembled. The samples were prepared by sputtering, CVD, arc melting, and both reactive sputtering and reactive evaporation. The samples were catalogued and suitably prepared for optical measurements. A database of spectral data for these samples has been established and extensive material characterization has been performed on some of the most interesting samples. Well established optical analysis methods were implemented to determine their fundamental optical properties. Some of the pitfalls of implementing both the methods of material and optical characterization have been discussed. We recommend that further work be done wholly in one institution or with the close cooperation of a facility capable of producing these films on short notice and according to the program management schematic shown in Figure 41.

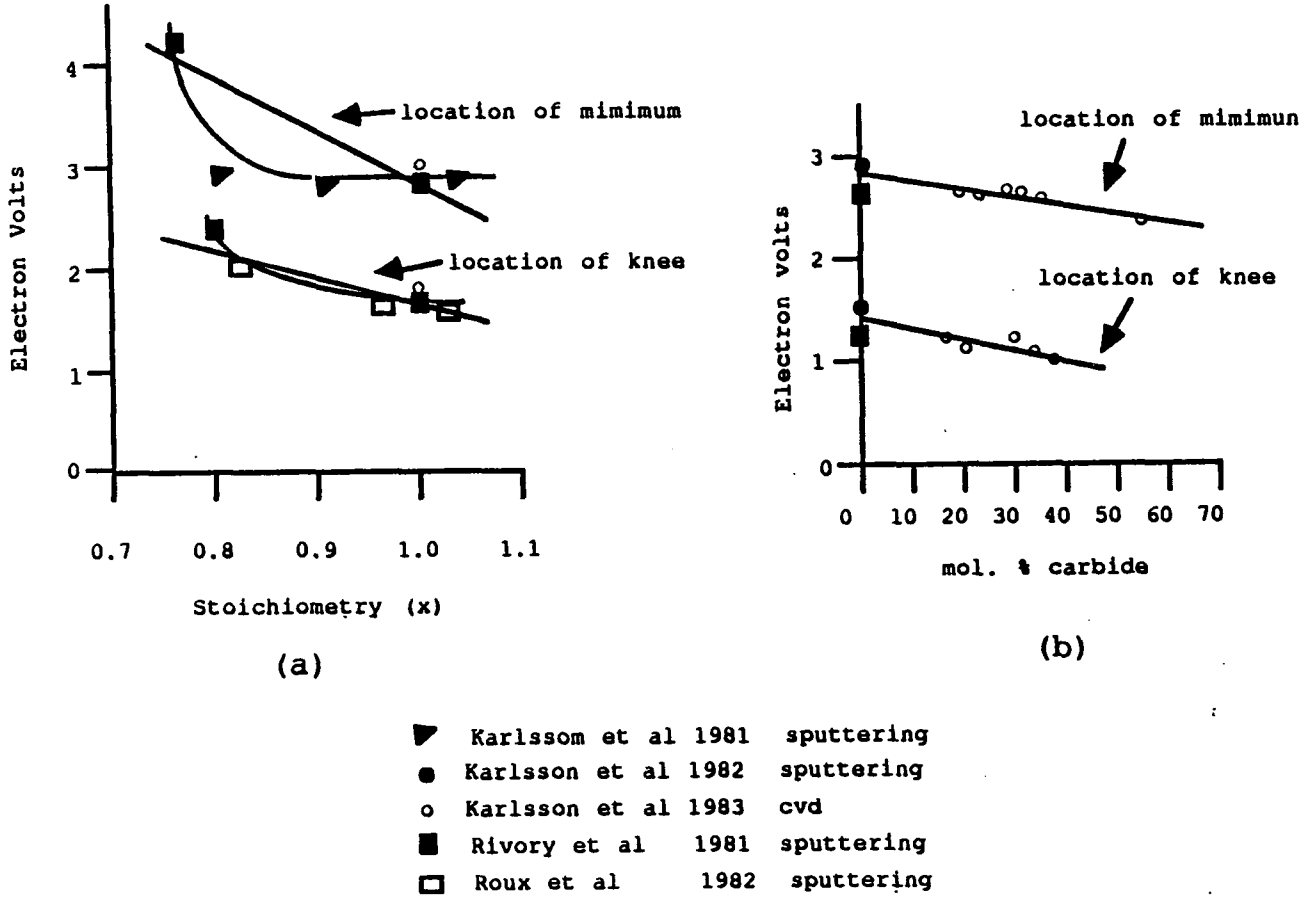

Figure 40. Comparison of reflectance change for stoichiometry (a) and lattice expansion (b) for TiN. (After Perry, 1986).

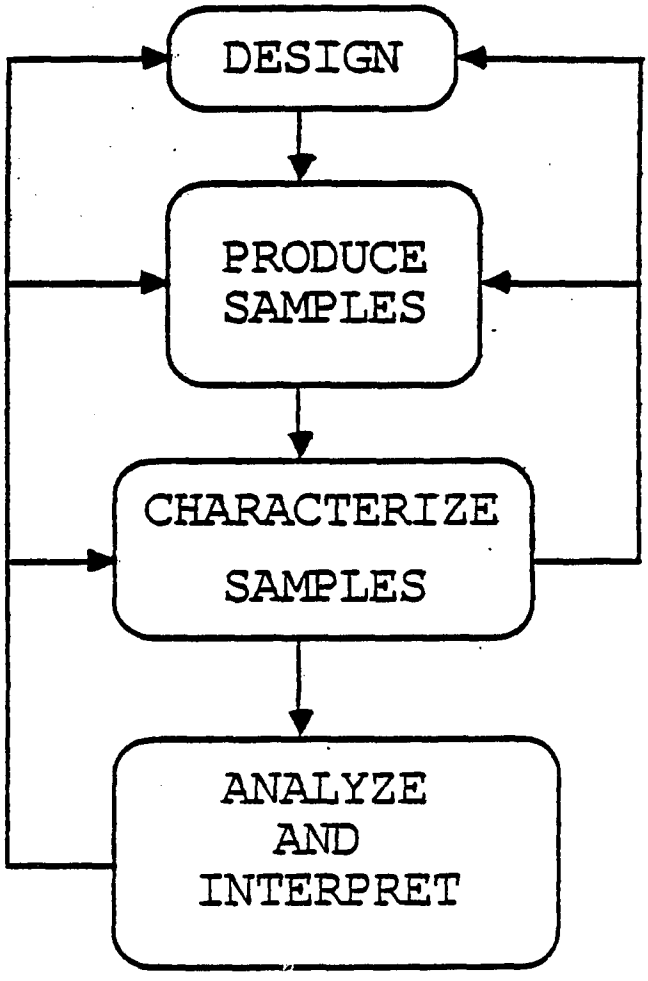

Figure 41. Proposed optimal workflow.

APPENDIXES

APPENDIX A

COMPLETE SAMPLE LISTING OF INTERSTITIAL TRANSITION METAL COMPOUNDS

The table included in this Appendix is the master list of all samples collected by the OSC's Solar Energy Group from 1975 to 1979. It lists the sample number, the type of material and nominal composition as stated by the group donating the sample, the method of deposition, the substrate used in the deposition, and the as-received surface condition (i.e., specular or rough).

Complete Listing of Interstitial Transition Metal Compounds.

#	TYPE	SOURCE	COATING-METHOD	SUBSTRATE	SURFACE
1	HfC 31A	Spitz-Grenoble	Reactive Sputtering	Quartz Si	Specular
2	HfC 31B	" "	" "	" "	"
3	HfC 31C	" "	" "	" "	"
4	HfC 32A	" "	" "	" "	"
5	HfC 32B	" "	" "	" "	"
6	HfC 27AG	" "	" "	Quartz	"
7	HfC 27AD	Missing "	" "	"	"
8	HfC 28AG	" "	" "	"	"
9	HfC 28AD	" "	" "	"	"
10	HfC 26AG	" "	" "	"	"
11	HfC 26AD	" "	" "		
12	HfC 29C	" "	" "	"	
13	HfC 29D	" "	" "	"	
14	HfC 27C-G	" "	" "	"	"
15	HfC 27C-D	" "	" "	"	"
16	HfC 27B	" "	" "	Si	"
17	HfC 26B	" "	" "	"	
18	TiN 22A	" "	" "	Quartz	"
19	TiN 22B	" "	" "	"	"
20	TiN 21A	" "	" "	"	"
21	TiN ?	" "	?	"	"
22	HfC 32C ? TiN 20B, TiI 22C, TiC 23A, TiC 24B sent back	" "	Sputtered from HfC target	"	
23	TiN 8301-25	Sandvik	CVD	Carbon Insert	Rough
24	TiN 80	"	"	" "	"
25	TiC	"	"	" "	"
26	HfC 6LS1	"	"	" "	"
27	HfN 7810	"	"	" "	"
28	TiC	Batalle	Arc Melting	--	"
29	ZrC	"	" "	--	"
30	HfC	"	" "	--	"
31	NbC	"	" "	--	"
32	TiNC, 6	Kennametal	CVD	Carbon Insert	"
33	samples of	"	"	" "	"
34	different	"	"	" "	"
35	shades	"	"	" "	"
36		"	"	" "	"
37		"	"	" "	"
38	TiC, 6	"	"	" "	"
39	samples of	"	"	" "	"
40	different	"	"	" "	"
41	shades	"	"	" "	"
42		"	"	" "	"
43		"	"	" "	"
44	TiC	Adams Carbide	"	Cemented WC	"
45	TiCN	Materials Tech.	"	Ti6Al4V	
46	TiN	" "	"	WC	"
47	Al2O3 + Ti2O3	" "	"	"	"
48	TiC	" "	"	"	"

Complete Listing of Interstitial Transition Metal Compounds (continued).

#	TYPE	SOURCE	COATING METHOD	SUBSTRATE	SURFACE
49	TiC 4.4,	Ti-coating	CVD	Cemented	Rough
50	4.8,5.3	"	"	Carbide bars	"
51	um,3samples	"	"	"	"
52	TiN 15um	"	"	"	"
53	Al2O3	"	"	"	"
54	TiC Ti-H-274	Bunshah	Reactive Evap.	Steel	"
55	TiC-N Ti-Ni-C-17	"	" "	"	"
56	TiN Ti-F-20	"	" "	"	"
57	TiN Ti-F-33	"	" "	"	"
58	V,TiC V-Ti-A-5	"	" "	"	"
59	TiC Ti-H-17	"	" "		"
60	TiN 7/10-78	Teledyne	CVD	Mo	Specular
61	HfN-1 6/26-78	"	"	"	"
62	HfN-2 6/26-78	"	"	"	Rough
63	HfN-3	"	"	"	Sp/Rgh
64	HfN-4	"	"	"	"
65	AMRC-488	Blickensderfer	Sputtering	Glass	Specular
66	AMRC-489	"	"	"	"
67	ZrN-1	Teledyne	CVD	Mo	"
68	ZrN-2	"	"	"	Rough
69	TiC(0.8)	Storms(LASL)	Arc melting	--	"
70	TiC(1.2)(TiC+C)	"	" "	--	"
71	ZrC(0.69)	"	" "	--	"
72	NbC(0.79)	"	" "	--	"
73	NbC(0.92)	"	" "	--	Specular
74	NbC+C	"	" "	--	Rough
75	NbN(1.04)	"	" "	--	Sp/Rgh
76	VC(0.85)	"	" "	--	"
77	MoC(0.66)	"	" "	--	Specular
78	LaB6+LaB9	"	" "	--	Sp/Rgh
79	V-TiC-A-2	Bunshah	Reactive Evap.	Steel	Rough
80	V-TiC-A-4	"	" "	"	"
81	V-TiC-A-6	"	" "	"	"

APPENDIX B

COMPUTER CODE (OPKON) FOR INVERSION OF R, T, d into n,k AND ϵ_1,ϵ_2

A general description and listing of a program (OPKON) to invert the measurements of reflectance, transmittance and thickness of a film into the dielectric (ϵ_1,ϵ_2) and optical constants (n,k) is presented. The basis for this program was established by the work of Nestell and Christy (1965), Nilsson (1968), and Bennett and Booty (1966). Hahn (1976) implemented this approach in work done for his dissertation. His early program was called OPTPROP. The FORTRAN program originally ran on the University's CDC 6400 computer system. We transferred the code to the OSC's in-house Data General Eclipse computer. During the transfer process substantial new code was added to address the type of measurements appropriate for our samples and the sequence originally proposed for this effort.

The program takes initial values (good guesses) of n and k for the film/substrate system under consideration, and then calculates values of the theoretical film reflectance and transmittance which are compared to the measured values. A series of three nonlinear equations with three unknowns is set up and successive comparison iterations are made using a Newton-Raphson technique. Under the best circumstances, this method will converge to optical constants that match the measured values throughout the measurement spectrum. After a set

number of iterations, a best fit output of n,k and ϵ_1,ϵ_2 for the given measurements is produced.

In some instances no convergence occurs. This can be a result of inaccurate measurements or an underlying problem. In some cases, especially for absorbing materials (with n approximately equal to k), the curves of R and T do not intersect at steep angles. Instead, the intersections may be tangential or not occur; the broad intersections restrict the code's ability to locate correct points of convergence. These are not the only reasons why numerous measurement combinations are required for various modes of the program. Any inversion method takes measurements of a film/substrate system and attempts to fit them to a model. Any deviation from this assumed model due to film inhomogeneities, surface or interface roughness, or film surface layers may prevent convergence.

The OPKON program has five modes of data analysis. We have added two additional modes to Hahn's code that aided this effort. The OPKON program modes are as follows:

MODE 0.0 Reflectance and transmittance of films on a nonabsorbing substrate and reflectance of films on an absorbing substrate determine the optical constants.

MODE 1.0 Reflectance of a film on an absorbing substrate and transmittance of the film on a nonabsorbing substrate plus an independent thickness measurement determine the optical constants.

MODE 2.0 Reflectance and transmittance of film on a nonabsorbing substrate plus an independent evaluation of film thickness determine the optical constants. (This was the primary mode used for our work.)

MODE 3.0 Reflectance and thickness of film sample one on a nonabsorbing substrate and reflectance and thickness of film sample two on a nonabsorbing substrate determine the optical constants.

MODE 4.0 Transmission and thickness of film sample one on a nonabsorbing substrate and transmission and thickness of film sample two on a nonabsorbing substrate determine the optical constants.

Auspicious choices of the modes of analysis are helpful and numerous cross checks of any results are prudent.

```
C  ************************************************************************
C
C PROG TO CALC THE OPT KONSTANTS AN THICKNESS OF A SINGLE FILM GIVEN   **
C THE MEASURED REFLECTANCE AND THE TRANSMITTANCE USING NEWTON RAPHSON   **
C
C PROG CAN BE USED IN THREE MODES
C
C MODE 0.0---CALCULATES N,K,D GIVEN RG,TG,RM
C MODE 1.0---CALCULATES N,K GIVEN TG,RM,D
C MODE 2.0---CALCULATES N,K GIVEN RG,TG,D
C MODE 3.0--- CALCULATES N,K GIVEN R1"RG",R2"RM",D1,D2
C MODE 4.0--- CALCULATES N,K GIVEN T1"TG",T2"TM",D1,D2
C
C ************************************************************************
C
C
C OP SWITCH PROVIDES FOR A PRINT OUT OF N,K AFTER EACH ITERATION
C OP=1 PRINTS OUT LAST ITERATION ONLY
C OP=-1 PRINTS OUT ALL ITERATIONS
C
C """""""""""""""
C
C
      DIMENSION A(4),B(4),C(4),D(2),E(2),F(2)
      COMPLEX NSH,NF,DNF,CNS,DNFN,DNFK,FCSNF,DELTANF
      COMPLEX NFO
      REAL IDNO,N,K,RBULK
      REAL NO,LAMBDA,NS,NFK,NFN,DELTAK,DELTAN,DELTADF,MODE
C """""""""""""""
C IDENTIFICATION NUMBER (IDNO) MUST BE GREATER THAN ONE  """
C """""""""""""""
      INPUT=9
      OUTPUT=12
   95 MODE=0.0
      READ FREE (INPUT) IDNO,NFO,DFO,D2,MODE,OP
      NF=NFO
      DF=DFO
C """""""""""""""
C TEST FOR END OF DATA
C """""""""""""""
      IF (IDNO.GE.1) GO TO 105
      GO TO 210
C """""""""""""""
C PRINT OUT INITIAL VALUES
C """""""""""""""
  105 WRITE (OUTPUT,130) IDNO,NF,DFO,D2,MODE
  130 FORMAT(1H1,//,11X,23HIDENTIFICATION NUMBER= ,I5,//11X,26HINITIAL FILM
     1 INDEX     N= ,F10.6,  5X,3HK= ,F10.6  /11X,27HINITIAL FILM THICKNESS
     2 (UM),2X,"D1=",F8.6,3X,"D2=",F8.6,/
     3 11X,"MODE=",2X,I1,//)
C """""""""""""""
C CHANGE INDEX TO N-IK
C """""""""""""""
      NF=CONJG(NF)
C """""""""""""""
C ENTER LAMBDA,INDEX AND MEASURED REFLECTANCE AND TRANSMITTANCE VALUES
C """""""""""""""
```

```
  110 READ FREE (INPUT) LAMBDA,NS,NSM,RG,TG,RM,TM
      IF (NS.LE.0.001) GO TO 95
      WRITE(OUTPUT,140) NS,NSM,RG,TG,RM,TM
  140 FORMAT(" ",10X,18HSUBSTRATE INDICES , 5X,12HGLASS   N= ,F10.5/
     1 34X,12HMETAL    N= ,F10.5,5X,3HK= ,F10.5///
     2 11X,"R1GLASS= ",F8.6,2X,"T1GLASS= ",F8.6,2X,//
     3 11X,"R2METAL= ",F8.6,2X,"T2METAL= ",F8.6,//
     4 " ***************************************************************"
     5 "******************"/)
C ****************
C [illegible]
C ****************
      NSM=CONJG(NSM)
      NF=CONJG(NFC)
      DF=DFO
      NO=1.0
      CNS=CMPLX(NS,0.0)
C ****************
C CALC INIT R AND T VALUES BASED ON THE INIT PNT
C ****************
      CALL RATCALC(LAMBDA,NO,NF,DF,CNS,RGCALC,TGCALC)
      CALL RATCALC(LAMBDA,NO,NF,D2,NSM,RMCALC,TMCALC)
C ****************
C PRINT OUT HEADER FOR ITERATIVE LOOP
C ****************
      IF (LP.EQ.1) GO TO 151
      WRITE(OUTPUT,145)
  145 FORMAT(" LAMBDA [illegible] K [illegible]
     1 2")
  150 DO 200 I=1,42
C ****************
C DEFINE THE THREE EQAUTIONS TO BE SOLVED
C ****************
      FONE=RGCALC-RG
      FTWO=TGCALC-TG
      FTHREE=RMCALC-RM
      FFOUR=TMCALC-TM
C ****************
C WE WILL USE THREE TOTAL DERIVATIVES,SET THEM EQUAL TO THE CURRENT
C VALUES OF THE FUNCTIONS AND SOLVE FOR THE INCREMENTS OF N,K AND DF
C CALCULATE THE PARTIALS W.R.T. RE(NF) AND PUT IN  EQ A
C ****************
      DN=0.0001
      DNFN=NF+DN
      CALL RATCALC(LAMBDA,NO,DNFN,DF,CNS,RGDIFF,TGDIFF)
      CALL RATCALC(LAMBDA,NO,DNFN,D2,NSM,RMDIFF,TMDIFF)
      A(1)=(RGDIFF-RGCALC)/DN
      A(2)=(TGDIFF-TGCALC)/DN
      A(3)=(RMDIFF-RMCALC)/DN
      A(4)=(TMDIFF-TMCALC)/DN
C ****************
C CALC PARTIALS W.R.T.IM(NF) AND PUT IN B
C ****************
      NFN=REAL(NF)
      NFK=AIMAG(NF)
      DK=-0.001
      NFK=NFK+DK
      DNFK=CMPLX(NFN,NFK)
```

```
      CALL RATCALC (LAMBDA,NO,DNFK,DF,CNS,RGDIFF,TGDIFF)
      CALL RATCALC (LAMBDA,NO,DNFK,D2,NSM,RMDIFF,TMDIFF)
      B(1)=(RGDIFF-RGCALC)/DK
      B(2)=(TGDIFF-TGCALC)/DK
      B(3)=(RMDIFF-RMCALC)/DK
      B(4)=(TMDIFF-TMCALC)/DK
C ****************
C
C TEST TO SEE IF THE THICKNESS IS TO REMAIN CONSTANT
C ****************
      IF (MODE-3.5) 151,151,300
C ****************
C CALC PARTIALS W.R.T. DF AND PUT IN C
  151 DI=0.0001
      DD=DF+DI
      CALL RATCALC(LAMBDA,NO,NF,DD,CNS,RGDIFF,TGDIFF)
      CALL RATCALC(LAMBDA,NO,NF,DD,NSM,RMDIFF,TMDIFF)
      C(1)=(RGDIFF-RGCALC)/DI
      C(2)=(TGDIFF-TGCALC)/DI
      C(3)=(RMDIFF-RMCALC)/DI
C ****************
C WANT SUM OF DIFF AND FUNC TO GO TO ZERO
C SOLVE THREE EQUATIONS FOR DELTAN,DELTAK--ELIMINATE N,
C THEN N AND GET SOLN FOR CHANGES IN THE VARIABLES
C DEFINE SOME OF THE RESULTING COEFFS
C ****************
      D(1)=A(1)*FTWO-A(2)*FONE
      E(1)=A(1)*B(2)-A(2)*B(1)
      F(1)=A(1)*C(2)-A(2)*C(1)
      D(2)=A(1)*FTHREE-A(3)*FONE
      E(2)=A(1)*B(3)-A(3)*B(1)
      F(2)=A(1)*C(3)-A(3)*C(1)
      G=E(1)*D(2)-E(2)*D(1)
      H=E(1)*F(2)-E(2)*F(1)
C ****************
C CALC THE INCREMENTS
C ****************
      DELTADF=-G/H
      DELTAK=(-D(1)-F(1)*DELTADF)/E(1)

      DELTAN=(-FONE-B(1)*DELTAK-C(1)*DELTADF)/A(1)
C ****************
      D2=DF
C CHECK TO SEE THAT THE INCREMENTS ARE NOT TOO LARGE
C ****************
  161 IF(ABS(DELTAN).LT.0.3) GO TO 164
      IF (DELTAN)      162,162,163
  162 DELTAN=-0.3
      GO TO 164
  163 DELTAN=0.3
  164 IF (ABS(DELTAK).LT.0.3)   GO TO 167
      IF (DELTAK)     165,165,167
  165 DELTAK =-0.3
      GO TO 167
  166 DELTAK=0.3
  167 IF (ABS(DELTADF).LT.0.0030) GO TO 170
      IF (DELTADF) 168,168,169
  168 DELTADF=-0.0030
      GO TO 170
```

```
  169 DELTADF=0.0030
C ***************
C CHECK THAT K LT 0 AND NGT 0.0001
C ***************
  170 IF ((AIMAG(NF)+DELTAK).GT.0.0)   DELTAK=-AIMAG(NF)
      IF((REAL(NF)+DELTAN).LT.0.0001)  DELTAN=-(REAL(NF)-0.0001)
C ***************
C CALC NEW FILM PARAMETERS
C ***************
      DELTANF=CMPLX(DELTAN,DELTAK)
      NF=NF+DELTANF
      DF=DF+DELTADF
C ***************
C CALC NEW VALUES FOR RGCALC,TGCALC,RMCALC
C ***************
      CALL RATCALC(LAMBDA,NO,NF,DF,CNS,RGCALC,TGCALC)
      CALL RATCALC(LAMBDA,NO,NF,D2,NSM,RMCALC,TMCALC)
      POSNF=CONJG(NF)
      IF (CP.EQ.1) GO TO 193
      WRITE (OUTPUT,191) LAMBDA,POSNF,RGCALC,TGCALC,RMCALC,TMCALC,I
  191 FORMAT(" "7(F7.5,2X),I4/)
C ***************
C TEST FOR CONVERGENCE OF N,K,DF
C ***************
  193 IF(ABS(DELTADF).LT.0.0002$1 .AND.ABS(DELTAK).LT.0.0002$1.AND.
     1 ABS(DELTAN).LT.0.0002$1) GO TO 22$
  200 CONTINUE
  220 IF(I.EQ.43) GO TO 179
      NFO=POSNF
  179 WRITE(OUTPUT,180)I
  180 FORMAT(" ",//," NUMBER OF ITERATIONS= ",I3//)
      WRITE (OUTPUT,181)
  181 FORMAT(" ***********************************************************"
     1 "******************",//
     2 " R1GLASS   CALC    T1GLASS    CALC    R2GLASS   CALC
     3  T2GLASS     CALC"/)
  182 WRITE(OUTPUT,184)RG,RGCALC,TG,TGCALC,RM,RMCALC,TM,TMCALC
  184 FORMAT(" ",8(F7.5,2X)/)
  186 WRITE (OUTPUT,188)
  188 FORMAT("  LAMBDA      D1        D2        N         K         E1
     1         E2     RBULK"/)
      N=REAL(POSNF)
      K=AIMAG(POSNF)
      E1=N*N-K*K
      E2=2*N*K
      RBULK=((N-1)*(N-1)+K*K)/((N+1)*(N+1)+K*K)
C ***************************************************************************
C WE HAVE JUST CALCULATED RBULK, E1 AND E2 FROM N AND K
C
C***************************************************************************
  192 WRITE (OUTPUT,194) LAMBDA,DF,D2,POSNF,E1,E2,RBULK
  194 FORMAT(" ",8(F7.4,2X),I4////)
C ***************
C READ MORE DATA
C ***************
      GO TO 110
  300 CONTINUE
      IF (MODE-1.5) 305,305,400
```

```
      SUBROUTINE RATCALC (LAMBDA,NO,NF,DF,NS,R,T)
C SUB TO CALC R AND T FOR A SINGLE FILM ON AN ABSORBING OR NONABSORBING
C SUBSTRATE GIVEN NO, NS,DF,NF
C PROG BASED ON EQS GIVEN BY BERNING IN PHYSICS OF THIN FILMS ..
      REAL NUM,DENOM,NO,LAMBDA
      COMPLEX PHIF,A,B,C,EO,HO,NS,NF
      PI=3.141592654
C CALC THE COMPLX PHASE THICKNESS OF THE FILM
      PHIF=(2*PI*NF*DF)/LAMBDA
C CALC THE MATRIX COEFF FOR THE FILM
      A=CCOS(PHIF)
      B=CMPLX(0.0,1.0)
      B=B*NF*SIN(PHIF)
      C=NF**2*B
C CALC THE E AND H FIELDS AT THE SURFACE
      EO=A+NS*B
      HO=C+NS*A
C CALC R AND T
      NUM=CABS(EO-(HO/NO))
      DENOM=CABS(EO+(HO/NO))
      R=(NUM*NUM)/(DENOM*DENOM)
      T=(4.0*REAL(NS))/(NO*DENOM*DENOM)
C     CALC THE BACKSIDE R
      R2=(NS-1)/(NS+1)
      R2=R2*R2
      T2=1-R2
      T1=T
      R1=R
      R=(R1-R1*R1*R2+T1*T1*R2)/(1-R1*R2)
      T=(T1*T2)/(1-R1*R2)
      RETURN
      END
```

APPENDIX C

COMPUTER CODE (KK) FOR KRAMERS-KRONIG ANALYSIS OF REFLECTANCE

This brief description and source listing of a FORTRAN program "KK" presents a technique useful for inverting the reflectance spectra of a sample into the dielectric (ϵ_1,ϵ_2) and optical (n,k) constants of a sample. The code originated in the Solid State Physics Group at the University of Uppsala in Sweden. The code was transferred and loaded into the OSC's in-house Data General Eclipse. This method contributed extensively to this effort; many of our samples lent themselves to this type of evaluation only.

In general, measurements of near normal reflectance are made on a sample in some restricted wavelength range; our range was .2 to 15 micrometers (6.2 to .083eV). The quality of the measurements and the extrapolations of the data are important. Rigorous implementation of the Kramers-Kronig dispersion relations can only be based on reflectances from a very broad energy range. The inability to collect extensive R data forces one to extrapolate the measured data at both ends of the data interval. The high energy extrapolation must contain at least one adjustable parameter; typically a power law. The low energy data is extrapolated for metals with a Hagen-Rubens relation and for semiconductors and insulators with a constant reflectance.

Despite the drawbacks, there is a vast body of data describing dielectric and optical properties of materials derived from this analysis approach. Again, it is important when correlating optical properties with composition by using the Kramers-Kronig analysis to have as complete a physical model as possible for the sample. This emphasizes accurate nonoptical characterization of the film properties. For example, the nature of surface roughness and oxide layers inherent in all real samples must be known.

```
:UDD:USSOLAR:DSK12 MEASURE:KK.FR                    19-JUN-79  16:36:11  PAGE 1

C KRAMERS KRONIG ANALYZIS OF REFLECTANCE DATA
C
C ********************************************
      DIMENSION W(400),R(400),WS(8),RS(8),TH(400)
      DIMENSION NQ(400),TQ(400),RQ(400),NQ1(400),T10(400),T20(400),T30(400)
      INPUT=9
      OUTPUT=12
C*************************************************
CREAD THE DATA
C*************************************************
  100 PI=3.141593
      N=0
C*************************************************
      WRITE(OUTPUT,101)
  101 FORMAT(" ",///,"KRAMERS KRONIG ANALYSIS OF REFLECTANCE")
      READ FREE(INPUT)NKORT,P
  107 WRITE(OUTPUT,108)NKORT
  108 FORMAT(" ",///,"NUMBER OF CARDS=",I3)
      DO 111 I=1,NKORT
      READ FREE(INPUT)W(I),R(I)
  102 FORMAT(F8.1,F7.4)
      IF(P.EQ.1)GO TO 117
      W(I)=1.23978/W(I)
  117 CONTINUE
  111 CONTINUE
      N=NKORT
      NS=0
C
C CALCULATION OF N AND K
C
      NS=N-1
      DO 700 I=2,NS
      WI=W(I)
C
      D=(ALOG(R(2)/R(I))-ALOG(R(1)/R(I)))/(W(2)-W(1))
      E=((ALOG(R(3)/R(I))-ALOG(R(2)/R(I)))/(W(3)-W(2))-D)/(W(3)-W(1))
      A=ALOG(R(1)/R(I))-D*W(I)-E*W(I)*W(2)
      B=D-E*(W(I)+W(2))
      C=E
C
      T=-1/(2*PI)*((A+C*WI**2)*ALOG(ABS((W(2)+W(3)-2*WI)*(W(I)+WI)/
     1  (W(2)+W(3)+2*WI)/(W(1)-WI)))+B*WI*ALOG(ABS(((W(2)+W(3))**2-
     2  4*WI**2)/(4*(W(1)**2-WI**2))))+C*WI*(W(3)+W(2)-2*W(1)))
      T10(I)=T
      NSS=NS-1
      DO 400 J=3,NSS
      D=(ALOG(R(J)/R(I))-ALOG(R(J-1)/R(I)))/(W(J)-W(J-1))
      E=((ALOG(R(J+1)/R(I))-ALOG(R(J)/R(I)))/(W(J+1)-W(J))-D)/
     1(W(J+1)-W(J-1))
      A=ALOG(R(J-1)/R(I))-D*W(J-1)+W(J-1)*W(J)*E
      B=D-E*(W(J-1)+W(J))
      C=E
C
      T=T-1/(2*PI)*((A+C*WI**2)*ALOG(ABS((W(J)+W(J+1)-2*WI)*(W(J-1)+
     1  W(J)+2*WI)/(W(J)+W(J+1)+2*WI)/(W(J-1)+W(J)-2*WI)))+
     2  B*WI*ALOG(ABS(((W(J)+W(J+1))**2-4*WI**2)/((W(J-1)+W(J))**2-
     3  4*WI**2)))+C*WI*(W(J+1)-W(J-1)))
C
```

```
      T20(I)=T-T10(I)
  400 CONTINUE
C
      D=(ALOG(R(N-1)/R(I))-ALOG(R(N-2)/R(I)))/(W(N-1)-W(N-2))
      E=((ALOG(R(N)/R(I))-ALOG(R(N-1)/R(I)))/(W(N)-W(N-1))-D)/
     1(W(N)-W(N-2))
      A=ALOG(R(N-2)/R(I))-D*W(N-2)+E*W(N-2)*W(N-1)
      B=D-(W(N-2)+W(N-1))*E
      C=E
C
      T=T-1/(2*PI)*((A+C*WI**2)*ALOG(ABS((W(N)-WI)*(W(N-2)+W(N-1)+
     1  2*WI)/(W(N)+WI)/(W(N-2)+W(N-1)-2*WI)))+
     2  B*WI*ALOG(ABS(4*(W(N)**2-WI**2)/((W(N-2)+W(N-1))**2-
     3  4*WI**2)))+C*WI*(2*W(N)-W(N-1)-W(N-2)))
C
      T=T-1/(2*PI)*ALOG(R(N)/R(I))*ALOG(ABS((W(N)+WI)/(W(N)-WI)))
C
      TH(I)=T
      T30(I)=TH(I)-T20(I)-T10(I)
  700 CONTINUE
  701 READ FREE(INPUT)TH1,W1,TH2,W2
      I=0
    2 I=I+1
      IF(W(I).LT.W1)GO TO2
      DTH1=TH1-TH(I)
      IF(W2.LT.0.0001)GO TO4
    3 I=I+1
      IF(W(I).LT.W2)GO TO3
      DTH2=TH2-TH(I)
      B2=PI/(W2*W2-W1*W1)*(-DTH1/W1+DTH2/W2)
      B0=(DTH1*PI/W1)-(W1*W1*B2)
      GO TO 5
    4 B0=PI/W1*DTH1
      B2=0.0
    5 CONTINUE
      WRITE(OUTPUT,80)
   80 FORMAT(" WI       TH1       W2       TH2")
      WRITE(OUTPUT,90) W1,TH1,W2,TH2
   90 FORMAT (" "4(E7.3))
      WRITE(OUTPUT,6) B0,B2
    6 FORMAT(" B0=",E10.7," B2=",E10.7)
C
CWRITE OUT THE TABLE HEADING
C
      WRITE(OUTPUT,205)
  205 FORMAT(" OMEGA     E       R       N.      K       EPS1    EPS2    THTOT
     I   THEXP")
C WRITE THE TABLE OUT
      WRITE(OUTPUT,206) W(I),R(1)
  206 FORMAT(" ",F5.1,F8.4)
C
      DO 503 I=2,NS
      WI=W(I)
      T=TH(I)+WI/PI*(B0+WI*WI*B2)
      R1=SQRT(R(I))
      R2=1+R(I)-2*R1*COS(T)
      RN=(1-R(I))/R2
      RR=2*R1*SIN(T)/R2
```

```
:UDD:USSCLAR DSK12 "F"SUPE:KK.FR                    19-JUN-79  16:36:11  PAGE 3

      EPS1=RN**2-RK**2
      EPS2=2*RN*RK
      E=W(I)
      THETA=P
      RTM1=EPS2/(EPS1**2+EPS2**2)
      RTM2=EPS2/((EPS1+1)**2+EPS2**2)
      EPS1C=1-EPS1
      EPS1D=EPS1C*W(I)**2
      EPS1W=EPS1*W(I)
      EPS2W=EPS2*W(I)
      IF(P.EQ.1)GO TO 550
      W(I)=1.23979/W(I)
  550 CONTINUE
C
      WRITE(OUTPUT,600)W(I),E,P(I),RN,RK,EPS1,EPS2,THETA,TH(I)
  600 FORMAT(" ",F6.3,F6.3,F8.4,F7.2,F7.2,F8.2,F9.4,F8.3,F9.3)
C
  700 CONTINUE
      END
```

APPENDIX D

PRESENTATION OF A MODEL CORRELATING THE DRUDE PROPERTIES OF TiN, ZrN, and HfN WITH THE BAND STRUCTURE OF THE MATERIAL

Solar Energy Materials 7 (1983) 401–411
North-Holland Publishing Company

OPTICAL PROPERTIES OF CVD-COATED TiN, ZrN AND HfN

B. KARLSSON†, R. P. SHIMSHOCK, B. O. SERAPHIN*
Optical Sciences Center, University of Arizona, Tucson, AZ 85721, USA

and J. C. HAYGARTH
Teledyne Wah Chang Albany, P.O. Box 460, Albany, OR 97321, USA

Received 3 May 1982

The reflectivities of TiN, ZrN and HfN have been measured in the spectral energy range 0.1 to 6.2 eV. The optical constants have been determined by means of a Kramers–Kronig analysis. A separation into interband transitions and free electron behaviour was carried out. The extended free electron region is explained and the interband transitions are compared with allowed transitions in the density of states distribution. The possibility of improving the optical selectivity by shifting E_F is discussed.

1. Introduction

The carbides and nitrides of the fourth and fifth column of the periodic table exhibit interesting optical properties. Related compounds, like TaC compared to $TaC_{0.8}$ or TiC compared to TiN, show remarkedly different optical properties. TaC and TiN are golden while $TaC_{0.8}$ and TiC are metallic grey [1]. Therefore optical spectroscopy is supposed to be an important probe for investigating their electronic structure. The possible use of them as a high-temperature stable selectively absorbing layer on a solar absorber has also increased the interest in their optical properties. Hafnium-carbid has been a early example as one of few bulk materials which exhibits a reflectance profile resembling that of an ideal selective surface.

The reflectance and optical constants of HfC_x at room temperature and at elevated temperatures were recently reported [2] and we now turn to CVD-coated TiN, ZrN and HfN. There exists a number of earlier investigations of the optical properties of TiN prepared in different ways, but very few reports on the optical properties of ZrN and HfN. It is also of a special interest to investigate the optical quality of CVD-coated films since this technique is already developed for industrial production, although not much tested for optical applications [3].

*Visiting scientist at the International Centre for Theoretical Physics, P.O. Box 586 – Miramare, I-34100 Trieste, Italy.

†Present address: Institute of Technology, University of Uppsala, S-75121 Uppsala, Sweden.

0165-1633/83/0000–0000/$03.00

2. Sample preparation and characterization

Interstitial transition-metal compounds, of which TiN, ZrN and HfN are examples, have long been prepared by CVD [4]. A practical preparation for these compounds is by reaction of the metal chloride vapor with hydrogen and nitrogen near 1000°C [5] and at atmospheric pressure:

$$MCl_4 + 2H_2 + \tfrac{1}{2}N_2 \rightarrow MN + 4HCl.$$

Under these conditions the nitride forms exclusively as a dense, polycrystalline layer on suitable substrates. For this work molybdenum was chosen, since it is otherwise inert to reactants and products, its thermal expansion adequately matches that of the nitrides and it is rigid and capable of taking a high polish.

Discs, diameter 32.6 mm, thickness 6.5 mm were cut from commercial molybdenum sheet-stock and polished on one side by techniques used normally in preparation for metallographic examination to yield a specular, though not optically flat, surface. Nitride coatings approximately 10 μm thick were then applied using the above reaction by placing the discs in a stream of the reactant gas mixture in a suitable apparatus. Compositions of the reactant gas mixture and other conditions are given in table 1. After coating, the discs were repolished, resulting in removal of 1–2 μm of the nitride layer to give a specular surface.

The composition of the films was studied by electron micro-probe analysis. The TiN and HfN showed less than 0.2 wt% C and no traces of O, but the HfN contained possibly up to 4 wt% Zr. The metals Hf and Zr are chemically similar, and therefore hard to separate. The ZrN-sample contained less than 1 wt% O and less than 0.2 wt% C. The lattice parameter was determined for TiN only by X-ray diffraction and gave $a = 4.24$ Å, close to the stoichiometric value [1].

Table 1
Conditions for nitride deposition

	$p^*_{H_2}$	$p^*_{N_2}$	$p^*_{MCl_4}$	T (°C)	Time (h)
TiN	0.575	0.375	0.050	1000	8
ZrN	0.339	0.642	0.019	1170	10
HfN	0.386	0.610	0.004	1150	14

*Total system pressure ≈0.1 MPa.

3. Reflectivity measurements

The room temperature, specular reflectance of the samples was measured over a wavelength range extending from 0.20 to 2.7 μm with a Perkin–Elmer model 450 spectrophotometer, and from 2.5 to 15 μm with a Perkin–Elmer model 137 spectrophotometer. The reflectance was measured relative to a freshly evaporated Al-mirror. The Al-mirror was flash-evaporated at 10^{-5} Torr in a diffusion-pumped

vacuum system. The reflectance values of the Al-films are assumed to agree with those of Bennet prepared under similar conditions [6, 7]. Bennet's data were then extended from 0.4 μm out to 2 μm with reflectance values reported by Hass [8]. Hass' values were reduced by 1% in order to coincide with Bennet's at 0.4 μm. In order to increase the relative accuracy within the set of samples all three were measured simultaneously versus the same reference. The reflectance was reproducible to an accuracy of 2% unit. The spectrals reflectances for TiN, ZrN and HfN are shown in figs. 1, 2 and 3, respectively.

To be able to examine the optical quality of these CVD-coated films, the typical data of our films are compared with those of others for the same materials in table 2. The overall impression is that these CVD-films exhibit a high optical quality, i.e. a

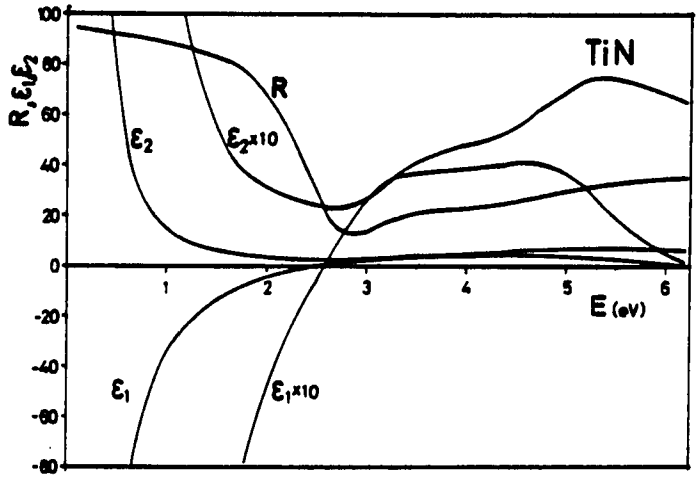

Fig. 1. Spectral reflectance, real and imaginary parts of the dielectric constants for TiN.

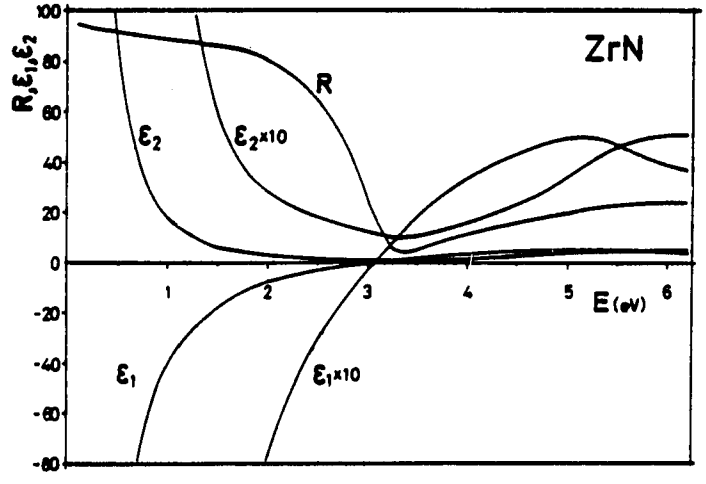

Fig. 2. Spectral reflectance, real and imaginary parts of the dielectric constants for ZrN.

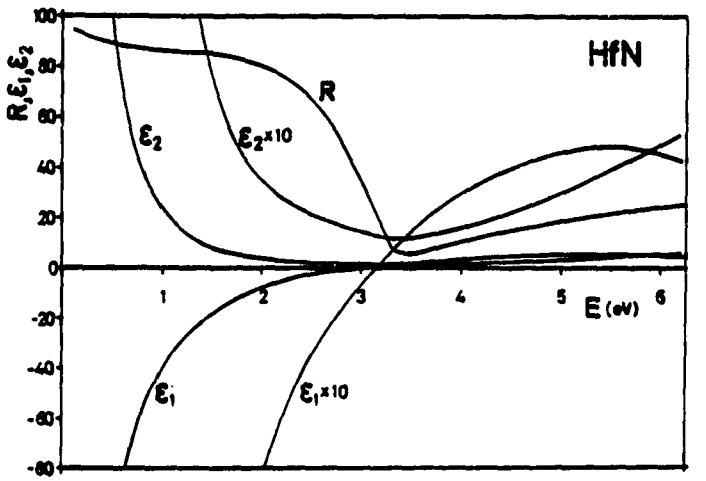

Fig. 3. Spectral reflectance, real and imaginary parts of the dielectric constants for HfN.

Table 2

Compound	Refl. (1 eV)	Refl. (at min.)	Pos. of min. (eV)	$\hbar\omega_p$ (eV)	$\hbar/\tau$ (eV)
TiN CVD-film [present data]	0.88	0.12	2.88	6.69 (6.63)	0.30
TiN solid solution [9]	0.75	0.21	3.65	8.9	1.22
TiN single cryst. [10]	0.81	0.18	3.4	6.9	0.6–0.8
TiN single cryst. [11]	0.95	0.13	2.8		
TiN ion plating [12]		0.12	2.88		
TiN react. sputt. [13]	0.77	0.15	2.9		
TiN react. sputt. [14]	0.75	0.17	2.8	8.7	1.3
ZrN CVD-film [present data]	0.88	0.04	3.38	7.17 (7.12)	0.35
ZrN solid solution [15]	0.90	0.02	3.55	6.77	0.24
ZrN single cryst. [10]	0.86	0.14	3.6	7.3–7.8	0.53–0.62
HfN CVD-film [present data]	0.86	0.05	3.48	7.32 (7.15)	0.45
HfN single cryst. [16]	0.70	0.12	3.75	8.63	1.40

high IR-reflectance and a deep reflectance minimum in the visible. The locations of the minima seem to agree with the results of most others.

4. Analysis

The reflectance spectra of TiN, ZrN and HfN in figs. 1, 2 and 3 have been analysed by means of the Kramers–Kronig relation. The reflectance below 0.1 eV was extra-

polated with

$$R(\omega) = 1 - (\omega/s)^{1/2},$$

in accordance with Hagen–Rubens relation [17] and s chosen to adjust the extrapolation to the low energy part of measured spectra.

The reflectance between 6.2 and 12 eV for TiN and ZrN have been extrapolated with Schlegel's [10] experimental results, the only modification being that the TiN-data had to be multiplied with a factor 1.16 to match our reflectance at the high energy side of the measured spectrum. Above 12 eV the reflectance has been extrapolated in a conventional way with $R \sim 1/\omega^2$ between 12 and 36 eV and with $R \sim 1/\omega^4$ above 36 eV for all three compounds. This extrapolation is in accordance with Schlegel's [10] procedure. Identical extrapolations have been applied for both HfN and ZrN since their reflectances agree at 6.2 eV and no literature values are available for HfN. This somewhat arbitrary method of extrapolation is supposed to give reasonable result since the most prominent structure of the spectral reflectance is situated within the measured wavelength region. The level of the IR-reflectance, the steepness of the reflectance-knee and the absolute value of the reflectance minima are to a large extent determining the behaviour of the optical constants within the measured wavelength interval. In order to test the reliability of this extrapolation it was applied to reflectance data with corresponding known optical constants of TiN from Chassaing [13] and of ZrN from Knosp [18]. This test showed good agreement between expected and calculated optical constants and partly justified the chosen extrapolations.

The derived optical constants of the nitrides are shown in figs. 1, 2 and 3. For low energies the reflectances and the optical constants seem to be characterized by intraband transitions of quasifree conduction electrons according to the Drude model. Strong deviations from that model are indicated by the increasing reflectance above

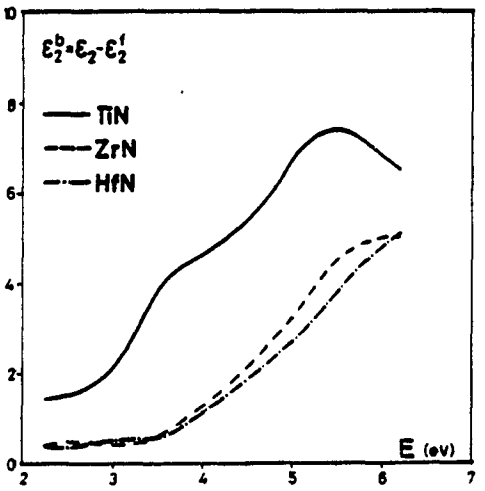

Fig. 4. Contribution to ε_2 from bound electron ε_2^b for TiN, ZrN and HfN.

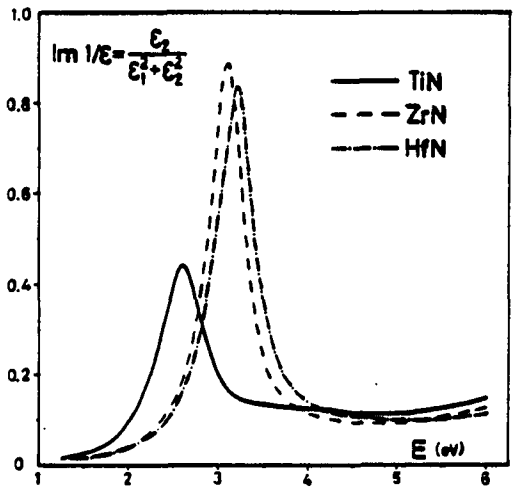

Fig. 5. Spectral dependence of the loss function $\varepsilon_2/(\varepsilon_1^2+\varepsilon_2^2)$ for TiN, ZrN and HfN.

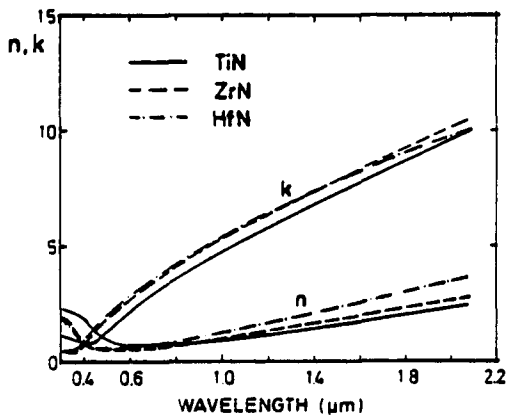

Fig. 6. Real and imaginary part of the refractive index, n and k.

the minima at around 3 eV. In order to separate the contributions to the optical constants from intraband- and interband-transitions, conventional Drude-plots were prepared [19]. From these plots the free-electron collision time τ and the plasma frequency ω_p were deduced. The values of $\hbar/\tau$ are 0.3, 0.35 and 0.45 for TiN, ZrN and HfN, respectively. This procedure gives ω_p-values of 6.69 eV for TiN, 7.17 eV for ZrN and 7.32 eV for HfN. From these parameters the contribution from intraband transitions to the optical constants was calculated over the full experimental region and the total dielectric constant was separated into contributions from free and bound electrons as shown in fig. 4. Fig. 5 shows peaks in the energy loss function $-\operatorname{Im}\varepsilon^{-1}(\omega)=\varepsilon_2/(\varepsilon_1^2+\varepsilon_2^2)$ at the energies where ε_1 vanishes, thus indicating that the conditions for plasma resonance are satisfied. Finally fig. 6 present the spectral dependence of the real and imaginary part of the refractive index, n and k.

5. Discussion

5.1. Optical model

A brief look at the optical data indicates that they for low energies are free-electron like according to the Drude picture with a high and constant reflectance. The dispersion of the spectral reflectance indicates a plasma resonance at around 7 eV. But positive contribution to ε_1 from bound electrons shifts to lower energy the point at which $\varepsilon_1(\omega)=0$. At this energy the loss function shows a maximum, a screened plasma resonance is obtained and the reflectance is sharply decreasing. This behaviour is surprisingly similar to that for the noble-metals, particularly Ag, for which interband transitions cause $\varepsilon_1(\omega)$ to change sign at 3.9 eV instead of at 9.2 eV as expected from the Drude-value of $\hbar\omega_p$ [20]. The similarity between these nitrides and the noble-metals are further underlined by the low values of the real part of the refractive index as shown in fig. 6. No one of the common transition metal have n-values below 1.0 like these nitrides and naturally the noble metals [21]. The main difference between these nitrides and the noble metals is the significantly shorter relaxation time and the weaker plasma resonance.

5.2. Conduction electron properties

As can be seen in table 2 there are large discrepancies in the reported properties of the conduction electrons, i.e. ω_p and τ. These discrepancies can partly be explained by difficulties in performing the Drude-fits because of the short relaxation-interval. It can also be explained by the different methods used in finding ω_p and τ. But mainly the differences are due to varying properties of the investigated samples. This is clearly pointed out in table 2 which shows the connection between a low IR-reflectance and a short τ which indicates the importance of scattering of conduction electrons versus impurities. In order to check the values obtained from the classical Drude-fits, ω_p was also calculated by integrating the optical absorption $\omega\varepsilon_2(\omega)$ up to the onset of interband transitions [22]. Fig. 7 shows the partial sum rule on ε_2

$$\int_0^{\omega_c} \omega\varepsilon_2(\omega)\,\mathrm{d}\omega = \tfrac{1}{2}\pi\left[\frac{N_A e^2}{\varepsilon_0 m}\right] n_{\mathrm{eff}}(\omega),$$

where N_A is the density of atoms and n_{eff} is defined as the effective number of electrons per atom, contributing to the optical absorption over a finite frequency range. The integration up to the onset of interband transitions at 2.6 eV for TiN and 3.5 eV for ZrN and HfN resulted in electron densities corresponding to plasma energies of 6.64, 7.12 and 7.15 eV for TiN, ZrN and HfN, respectively. These values which are in good agreement with the values from the Drude-plots are given in parentheses in table 2.

To estimate the effective optical mass m^* of the conduction electrons of TiN it is assumed that only the electrons above the minimum in the density of states contribute to ω_p. The number of electrons between the minima and E_F is estimated from fig. 8 to be 0.9 per formula-unit TiN. That number would imply a plasma energy $\hbar\omega_p$ of 8.04 eV, which means that the effective mass of the d-electrons contributing to the

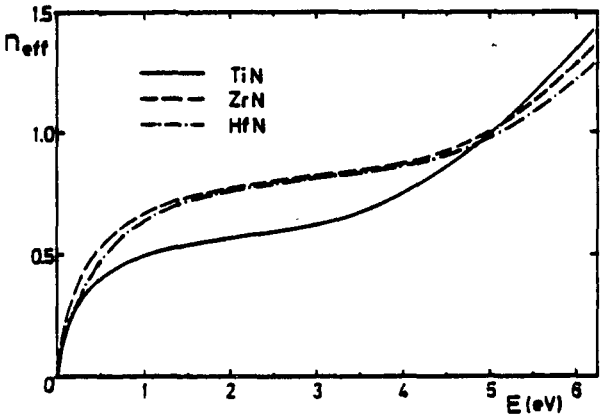

Fig. 7. The effective number of electrons per molecule-unit determined from the partial sum rule.

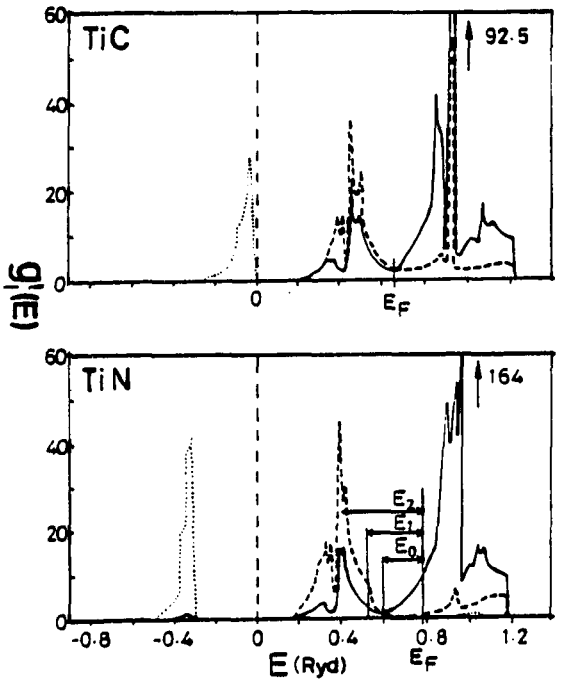

Fig. 8. LCAO partial density of states $g_l^i(E)$ (states of both spin per Ryd and unit cell) for TiC and TiN. Dotted curves: $g_s^X(E)$; broken curves: $g_p^X(E)$ (with X = C or N); full curves: $g_p^{Ti}(E)$. From Neckel [28].

conduction electron properties $m^* = 1.44$. Since the density of electrons does not vanish completely at the minimum of the density of states the energy bands interacting with the light at low energies and characterizing the plasma-frequency contain more electrons that are given from our assumption. This means that the procedure gives a lower limit to the effective mass.

5.3. Bandstructure interpretation

The Drude-like behaviour of the optical constants up to an energy of 2.6 eV for TiN and 3.5 eV for ZrN and HfN, where we have an onset of interband transitions, is unexpected for materials with partly filled d-bands [23]. The difference in optical properties between these nitrides and all other transition metals and transition metal compounds including metallic Ti, Zr and Hf [24] and the nearly related TiC [25], HfC [2] and ZrC [26] is striking. In Ti and other transition metals the Fermi level intersects the s-, p- and d-bands. Interband transitions set in at very low energies and cause the reflectance to drop almost immediately from the high values when ω increases from zero. TiN, ZrN and HfN are to our knowledge the only transition metal compounds which exhibit a wide Drude region with a high and constant reflectance. The importance of this has not been pointed out before.

An attempt to explain this property will be done using fig. 8 where the electronic density of states of TiN and TiC, as calculated by Neckel [27] from APW-bands, is given. The total density of states is decomposed into partial LCAO densities. The Fermi-energy of TiN is situated above the minimum of the density of states where the metal d LCAO partial density of states dominates. The contribution of the metalloid p LCAO partial density of states is very small. This means that interband-transitions of low energies must be weak since selection rules prevent transitions between d-bands. The low energy interval, where the optical properties of TiN are characterized by intraband transitions, is interrupted by an onset of interband-transitions at 2.5 eV. They can be identified as transitions between the increasing number of p-states 2.5 eV below E_F and d-states at E_F. These transitions are denoted as E_0 in fig. 8. The situation for TiC is different. Here the Fermi-energy E_F intersects the density of states curve where the contributions from metallic d-orbitals and metalloid p-orbitals are comparable and the interband transitions may occur at low energies. This is clearly exhibited in the reflectance curve which shows no Drude-like behaviour at low energies [25].

We have not been able to carry out the same discussion for ZrN and HfN since no bandstructure and density of states distribution are available. The optical data show the onset of interband transition at 3.5 eV, i.e. a shift of around 1 eV compared to TiN, and also indicate a corresponding shift of the distance between the p-like band and the Fermi-energy. The greater plasma energy for ZrN and HfN corresponds in our model to an increased number of d-electrons between E_F and the minimum in the density of states distribution.

5.4. Previous measurements

The overall agreement between the optical constants of our CVD TiN and the reactively sputtered reported by Chassaing [13] and Rivory [14] is good. The two peaks in ε_2 at 3.7 eV and 5.3 eV can be understood as transitions from p-states below E_F and d-states just above E_F. These peaks denoted in fig. 8 as E_1 and E_2, respectively, are also identified in the spectra of Chassaing [13] and Rivory [14]. Schlegel's [10] data are different since his reflectance minimum is shifted towards higher energies.

The powder-pressed TiN investigated by Böhm [9] exhibits a very low NIR-reflectance, a weak minimum at high energy, which is also reflected in the values of the optical constants. The reported data of ZrN by Knosp [15] and Schlegel [10] are in good agreement with ours apart from a small shift of the reflectance minima. The only known reported data on HfN are from Flück's [16] measurements performed on a powder-pressed sample. It showed a low NIR-reflectance and a relatively weak minima displaced 0.3 eV to higher energy compared to our sample.

5.5. Optical selectivity

To increase the solar-optical selectivity, the reflectance-knee of TiN (which is the nitride with the reflectance step at the lowest energy to begin with) should be displaced towards lower energies. This can, within the framework of our interpretation, be attained by lowering the Fermi energy. That should decrease the number of conduction electrons and thus the plasma-energy, it should also give the onset of transitions of p-electrons to the Fermi-level at a lower energy. Both these effects would cause ε_1 to change sign at a lower energy and simultaneously move the reflectance-knee to a lower energy. But a non-desirable effect would be that the density of states at E_F would be decreased as well as the long wavelength reflectance. One way to downshift the Fermi-energy is to replace some N-atoms with C-atoms [28], which have one p-electron less in the atomic state. The effect of introducing vacancies on some N-sites should also be evaluated. The presence of charge transfer will complicate the effect of that change. Therefore it is not obvious in which direction a lowered N/metal-ratio will move the Fermi-energy. Introduction of scattering-centers will certainly have the undesirable effect to decrease the IR-reflectance and smear out the plasma-edge.

Acknowledgements

One of us, B. K., wants to thank the Solid State Optics Group for its support and help during the time of tenure at the Optical Sciences Center. His stay there was made possible by a grant from the Swedish Council for Building Research. We would like to thank Prof. A. R. Mackintosh, Univ. of Copenhagen, for pointing out the importance of the partial densities of states. The authors are grateful to Dr. C. G. Ribbing, Univ. of Uppsala, for important suggestions and comments. We thank B. F. Kieffer and M. Östermann of Teledyne Wah Chang Huntsville, Huntsville, Alabama, for providing the molybdenum discs.

References

[1] L. E. Toth, Transition Metal Carbides and Nitrides, Refractory Materials, vol. 7 (1971).
[2] B. Karlsson, N. Baraket, R. P. Shimshock, B. O. Seraphin, A. Aubert, M. Borel and J. Spits, Solar Energy Mater. (submitted).
[3] J. C. Haygarth, Thin Solid Films 72 (1980) 51.

[4] C. F. Powell, J. H. Oxley and J. M. Blocher, eds., Vapor Deposition (Wiley, New York, 1966).
[5] J. R. Peterson, J. Vac. Sci. Technol. 11 (1964) 715.
[6] H. E. Bennet, J. M. Bennet and E. J. Ashley, J. Opt. Soc. Am. 52 (1962) 1245.
[7] H. E. Bennet, M. Silver and E. J. Ashley, J. Opt. Soc. Am. 53 (1963) 1089.
[8] G. Hass and L. Hadley, American Inst. of Physics Handbook, 2nd ed. (McGraw-Hill, New York, 1963) p. 6–119.
[9] G. Böhm and H. Goretzki, J. Less-Common Metals 27 (1972) 311.
[10] A. Schlegel, P. Wachter, J. J. Nickl and H. Lingg, J. Phys. C 10 (1977) 4889.
[11] C. Politis, Th. Wolf and H. Schneider, Proc. 7th Intern. Conf. on Chemical Vapor Deposition, 1979, vol. 79-3 (The Electrochemical Society, Princeton, New Jersey, 1979) p. 289.
[12] B. Zega, M. Kornmann and J. Amiguet, Thin Solid Films 45 (1977) 577.
[13] G. Chassaing, J. C. François, P. Graner, M. Sigrist, L. Roux and J. Chevallier, Proc. 8th Intern. Vac. Congr., vol. 2, Cannes (1980) p. 389.
[14] J. Rivory, J. M. Behaghel, S. Berthier and J. Lafait, Thin Solid Films 78 (1981) 161.
[15] H. Knosp and H. Goretzki, Z. Metallkd. 60 (1969) 587.
[16] F.-W. Flück, Thesis, University of Karlsruhe (1977).
[17] F. Stern, in: Solid State Physics, vol. 15, eds. F. Seitz and D. Turnbull (Academic Press, New York, 1963) p. 300.
[18] H. Knosp and V. Gerold, Z. Metallkd. 60 (1969) 627.
[19] M. L. Théye, Phys. Rev. B 2 (1970) 3060.
[20] H. Ehrenreich and H. R. Philipp, Phys. Rev. 128 (1962) 1622.
[21] As in ref. [8] p. 6-124.
[22] F. Wooten, Optical Properties of Solids (Academic Press, New York, 1972).
[23] J. H. Weaver, Proc. Intern. Conf. on Transition Metals, Inst. of Phys. Conf. Series Number 39, eds. M. J. G. Lee, J. M. Perz and E. Fawcett, Toronto (1977) p. 115.
[24] D. W. Lynch, C. G. Olson and J. H. Weaver, Phys. Rev. B 11 (1975) 3617.
[25] D. W. Lynch, C. G. Olson and D. J. Peterman, Phys. Rev. B 22 (1980) 3991.
[26] J. E. Alward, C. Y. Fong, M.El.-Batanouny and F. Wooten, Phys. Rev. B 12 (1975) 1105.
[27] A. Neckel, P. Rastl, R. Eibler, P. Weinberger and K. Schwarz, J. Phys. C 9 (1976) 579.
[28] P. Weinberger, Phys. Stat. Sol. (b) 98 (1980) 207.

REFERENCES

Allred, D. D., Michael R. Jacobson, and Elizabeth E. Chain, Sol. En. Mat. 1287 (1985).

Baraket, N., and B. O. Seraphin, OSC Technical Report NSF INT No. 76-02664, University of Arizona (1976).

Beensch-Marchwinka, G., and T. Berlicki, Thin Solid Films 62, 255 (1979).

Bennett, H. E., J. M. Bennett, and E. J. Ashley, J. Opt. Soc. Am. 52, 1245 (1962).

Bennett, H. E., and D. K. Burge, J. Opt. Soc. Am. 70(3), 268 (1980).

Bennett, J. M., Optics News (July 17, 1985).

Boehm, G., and H. Goretzki, J. Less-Common Metals 27, (1972).

Eastman, J., and P. W. Baumeister, J. Opt. Soc. Am. 64, 1369A (1974).

Goldschmidt, J., Interstitial Alloys (Plenum Press, New York, 1967).

Hägg, G., Z. Phys. Chem. Abt. B12, 33 (1931).

Hahn, R. E., The Optical Properties of Chromium Oxide Films and the High Temperature Stabilization of Silver Films for Photothermal Solar Energy Conversion, Ph. D. Dissertation, University of Arizona (1976).

Hass, G., and L. Hadley, American Institute of Physics Handbook, 2nd ed. (McGraw-Hill, New York, 1963).

Hauser, E., R. J. Zirke, J. Tauc, J. J. Hauser, and S. R. Nagel, Phys. Rev. Lett. 40, 1733 (1978).

Haygarth, J. C., private communication (1979).

Hunter, W., Handbook of Optical Properties of Solids, E. D. Palik, ed. (Academic Press, New York, 1985).

Jacobson, M. R., R. D. Lamoreaux, R. P. Shimshock, N. Rauof, and B. O. Seraphin, Proc. Soc. Photo-Opt. Instrum. Eng. 161(4) (1978).

Karlsson, B., R. P. Shimshock, B. O. Seraphin, and J. C. Haygarth, Sol. Energy Mater. 7, 401 (1983).

Karlsson, B., J. E. Sundgren, and B. O. Johansson, Thin Solid Films 87, 181 (1982).

Karlsson, B., and C. G. Ribbing, Proc. Soc. Photo-Opt. Instrum. Eng. 324, 52 (1982).

Karlsson, T., and B. Karlsson, "A Band Structure Based Rule for Selection of Transparent Heat-Mirrors of Non-Conventional Materials," preprint submitted to Thin Solid Films, 1984.

Knosp, H., and H. Gerold, Z. Mettal Kd. 60, 627 (1969).

Kramers, H. A., Atti. Congr. Intern. Fis. Como. 2, 545 (1927).

Kronig, R. de L., J. Opt. Soc. Am. 12, 547 (1926).

Martin, P. J., R. P. Netterfield, and W. G. Sainty, Vacuum 32, 359 (1982).

Mitra, S. S., Handbook of Optical Constants of Solids, E. D. Palik, ed. (Academic Press, New York, 1985).

Murarka, S. P., J. Vac. Sci. Technol. 17(4), 775 (1980).

Nestell, J. E., Jr., and R. W. Christy, Appl. Opt. 11, 643 (1972).

Nilsson, P. O., Appl. Opt. 7, 435 (1968).

Parks, R. E., R. E. Sumner, and J. T. Appels, Opt. Eng. 16(4), 332 (1977).

Perry, A. J., M. Grossl, and B. Hammer, Thin Solid Films 129, 263 (1985).

Perry, A. J., M. Georgson, and C. G. Ribbing, J. Vac. Sci. Technol. A4(6) (1986).

Pfluger, J. P., J. Fink, W. Weber, and G. Crecelius K.-P. Bohnen, Phys. Rev. B 30, 1155 (1984).

Pfluger, J. P., J. Fink, W. Weber, and G. Crecelius K.-P. Bohnen, Phys. Rev. B 31, 1244 (1985).

Robinson, R. S., Proc. Phys. Soc. B 65, 910 (1952).

Rogers, J. E., "Scattering of Light from Defects in Optical Materials," Ph.D. Dissertation, University of California, Los Angeles (1980).

Roessler, D. M., Brit. J. Appl. Phys. 16, 1119 (1965).

Roux, L., J. Hanus, J. C. Francois, and M. Sigrist, Sol. Energy Mater. 7, 299 (1982).

Schlegel, A., P. Wachter, J. Nickl, and H. Lingg, J. Phys. C. Solid State Phys. 10, 4889 (1977).

Seraphin, B. O., and A. B. Meinel, Optical Properties of Solids--New Developments, B. O. Seraphin, ed. (North Holland, New York, 1975), p. 927.

Shack, R. V., and J. E. Harvey, "An Investigation of the Distribution of Radiation Scattered by Optical Surfaces," OSC Final Report for Space and Missile Systems Organization under contract FO4701-74-C-0083, University of Arizona (1975).

Stern, F., Solid State Physics, Vol. 15, F. Seitz and D. Turnbull, eds. (Academic Press, New York, 1963), p. 300.

Toth, L. E., Transition Metal Carbides and Nitrides in Refractory Materials, Vol. 7 (Academic Press, New York, 1971).

Valkonen, E., C. G. Ribbing, and J. E. Sundgren, Appl. Opt. 25, 3624 (1986).